MARMARA UNIVERSITY
INSTITUTE FOR GRADUATE STUDIES
IN PURE AND APPLIED SCIENCES

METABOLIC ENGINEERING OF *CORYNEBACTERIUM GLUTAMICUM* FOR L-DOPA PRODUCTION

ELDIN KURPEJOVIĆ

DOCTORATE THESIS
Department of Bioengineering

Thesis Supervisor
Prof. Dr. Berna Sarıyar AKBULUT

Thesis CO- Supervisor
Prof. Dr. Volker V. WENDISCH

ISTANBUL, 2022

MARMARA UNIVERSITY
INSTITUTE FOR GRADUATE STUDIES
IN PURE AND APPLIED SCIENCES

METABOLIC ENGINEERING OF *CORYNEBACTERIUM GLUTAMICUM* FOR L-DOPA PRODUCTION

ELDIN KURPEJOVIĆ

DOCTORATE THESIS
Department of Bioengineering

Thesis Supervisor
Prof. Dr. Berna Sarıyar AKBULUT

Thesis CO- Supervisor
Prof. Dr. Volker V. WENDISCH

ISTANBUL, 2022

ACKNOWLEDGEMENT

I would like to express my deepest gratitude towards my supervisor Prof. Berna Sarıyar Akbulut and Prof. Volker F. Wendisch for their immense support and encouragement. It was an honor to be their student and learn from them. Additionally, I would like to thank the thesis evaluation committee Prof. Zeynep Petek Çakar and Assoc. Prof. Nihat Alpagu Sayar for their valuable contributions and thesis jury Prof. Dilek Kazan and Prof. Işıl Aksan Kurnaz. The funding provided for this work by TÜBİTAK projects 117M961 and 120N728 is also gratefully acknowledged.

I am so grateful to my lab-partners Gülsüm Merve Bastem and Beril Pakalin. They have always been there throughout this incredible journey and have given me strength and support at every step of the way. It was such a joy and honor to be working by their side. I would like to thank Arthur Burgardt for his help during my stay at Bielefeld University.

Also, I would like to thank the entire laboratory group of Bioengineering Department, for accepting me as a member from day one.

Finally, I am especially and eternally thankful to my mother Munirka, dearly departed father Šefko, my sisters Mersiha and Meliha, my brother Ermin, my friend Abdussamed Uras and Cemile Selin Aksoy for their support and motivation. They have always believed in me, which kept me going through the path of my PhD studies. This accomplishment would not be possible without their support.

October, 2022 **Eldin KURPEJOVIĆ**

TABLE OF CONTENTS

ÖZET

L-DOPA ÜRETİMİ İÇİN *CORYNEBACTERIUM GLUTAMICUM* METABOLİK MÜHENDİSLİK

Mikrobiyal sistemler aracılığıyla aromatik amino asitlerden aromatik bileşiklerin üretimi ilgi çekici ve sürdürülebilir bir biyoteknolojik yaklaşımdır. Bu çalışmada, metabolizma mühendisliği stratejileri kullanılarak *Corynebacterium glutamicum*'da 3,4-dihidroksifenil-l-alanin (L-DOPA) üretimi amaçlanmıştır. L-DOPA, Parkinson hastalığının tedavisinde en sık kullanılan ilaçtır. Bu doğrultuda, *Ralstonia solanacearum*'dan alınan tirozinaz enzimi, *C. glutamicum* hücrelerinde heterolog olarak eksprese edilmiş ve fermentatif üretimde harici olarak eklenen L-tirozin ile birlikte 255 ± 20 mg/L L-DOPA elde edilmiştir. Ayrıca, tam hücre biyotransformasyonu ile tirozinaz enzimini eksprese eden hücrelerde 6.6 mgDCW ile 400 ± 10 mg/L L-DOPA üretimi sağlanmıştır. L-DOPA üretiminin sürdürülebilirliğini test etmek amacıyla fındık kabuğu hidrolizatı tek karbon kaynağı olarak ilk kez değerlendirilmiş ve 20 ± 1 mg/L L-DOPA üretilmiştir.

L-DOPA üretimi amacıyla yapılan ilk denemelerde, yabanıl tür hücrelerde harici L-tirozin kullanılmıştır. Harici L-tirozin kullanımının önüne geçmek amacıyla *C. glutamicum* rasyonel olarak tasarlanmıştır. L-tirozin aşırı üretimi şu şekilde sağlandı: (i) prefenat dehidrataz (*pheA*), antranilat sentaz (*trpE*) ve fenilalanin aminotransferaz (*pat*) genlerinde translasyonel başlangıç kodon değişimleri, (ii) shikimat dehidrojenaz ve 3-dehidrokinat dehidratazı kodlayan *aroE* ve *qsuC* genlerinin aşırı ekspresyonu, (iii) *ptsG* geninin silinmesi ve inositol permeaz (*iolT2*) ve glukokinazın (*glcK*) genlerinin aşırı ekspresyonu yoluyla glukoz alımını sağlayan PtsG sisteminin inaktivasyonu, (iv) *C. glutamicum* ARO02 suşunda L-tirozin sentezi için gereken öncü havuzunu artırmak için ksilozun kullanılması. Üretimi daha da arttırmak için, L-tirozin yolağındaki tanımlanamayan aminotransferaz tahmin edilmiş ve L-tirozin biyosentezindeki rolünden yararlanılmıştır. Ticari olarak temin edilebilen L-tirozini üreten *C. glutamicum* ATCC 21573 suşunun genomu dizilenmiş ve olası rasyonel tasarım modifikasyonları hakkında ipucu elde etmek için genom çapında analiz yapılmıştır. Son olarak, tasarlanan suşta en yüksek L-tirozin titresi 3.6 ± 0.10 g/L olarak bulunmuştur. Bu suş, L-DOPA üretimi için kullanıldığında, 185 ± 9 mg/L'lik bir titre elde edilmiştir.

Anahtar kelimeler: *Corynebacterium glutamicum,* L-DOPA, L-tirozin, metabolik mühendislik

Ekim, 2022 **Eldin KURPEJOVIĆ**

ABSTRACT

METABOLIC ENGINEERING OF *CORYNEBACTERIUM GLUTAMICUM* FOR L-DOPA PRODUCTION

Production of aromatic compounds derived from aromatic amino acids using microbial systems is an attractive and sustainable biotechnological approach. With this motivation, here metabolic engineering of *Corynebacterium glutamicum* for 3,4-dihydroxyphenyl-l-alanine (L-DOPA) production is described. L-DOPA is the most commonly used drug for the treatment of Parkinson's disease. In this work, *Ralstonia solanacearum* tyrosinase was heterologously expressed in *C. glutamicum* cells by fermentative production to get 255 ± 20 mg/L of L-DOPA with externally added L-tyrosine. Tyrosinase expressing cells were also used for whole-cell biotransformation to get 400 ± 10 mg/L of L-DOPA with 6.6 mgDCW. Furthermore, production with hazelnut husk hydrolysate as the sole carbon source was evaluated for sustainable L-DOPA production for the first time, and 20 ± 1 mg/L of L-DOPA was produced.

Initial L-DOPA production efforts used external L-tyrosine with wild-type cells. To circumvent external L-tyrosine addition, *C. glutamicum* was then rationally designed. L-tyrosine over-production was achieved by: (i) translational start codon exchanges of prephenate dehydratase (*pheA*), anthranilate synthase (*trpE*), and phenylalanine aminotransferase (*pat*) genes, (ii) overexpression of *aroE* and *qsuC*, encoding shikimate dehydrogenase and 3-dehydroquinate dehydratase, respectively, (iii) inactivation of PtsG system for glucose uptake by deletion of *ptsG* of glucose uptake and overexpression of inositol permease (*iolT2*) and glucokinase (*glcK*), and (iv) utilization of xylose to increase precursor pool for L-tyrosine synthesis in the chassis of *C. glutamicum*, ARO02. To further enhance production, the unidentified aminotransferase in L-tyrosine pathway was predicted and its role in L-tyrosine biosynthesis was exploited. The genome of the commercially available L-tyrosine producing strain *C. glutamicum* ATCC 21573 was sequenced and genome-wide analysis was performed to get clues on possible modifications for the rational design. Finally, the highest L-tyrosine titer was 3.6 ± 0.10 g/L in the designed strain. When this strain was used for L-DOPA production, a titer of 185 ± 9 mg/L was obtained.

Keywords: *Corynebacterium glutamicum*, L-DOPA, L-tyrosine, metabolic engineering

October, 2022 **Eldin KURPEJOVIĆ**

CLAIM OF ORIGINALITY

METABOLIC ENGINEERING OF *CORYNEBACTERIUM GLUTAMICUM* FOR L-DOPA PRODUCTION

In this study, *Corynebacterium glutamicum* was metabolically engineered for the production of L-tyrosine and L-DOPA, for the first time. Additionally, thymol was evaluated as a potential L-DOPA antioxidant, for the first time, along with the most commonly used antioxidant ascorbic acid. The production of L-DOPA was performed both fermentatively and via whole-cell transformation. As a renewable carbon source, hazelnut husk hydrolysate was evaluated and L-DOPA was produced. This is the first study which describes sustainable L-DOPA production. Furthermore, the unidentified aminotransferase of the L-tyrosine biosynthesis pathway was predicted and this enzyme was proved to be involved in its biosynthesis.

October, 2022 **Prof. Dr. Berna SARIYAR AKBULUT** **Eldin KURPEJOVIĆ**

SYMBOLS

%:	Percentage
°C:	Celcius
g:	Gram
h:	Hour
L:	Liter
M:	Molar
mg:	Milligram
min:	Minute
mL:	Milliliter
mM:	Millimolar
v/v:	Volume per volume
w/w:	Weight per weight
µg:	Microgram
µL:	Microliter

ABBREVIATIONS

BHI:	Brain Heart Infusion
DNS:	3,5-Dinitrosalicylic Acid
DCW:	Dry Cell Weight
Km:	Kanamycin
LB:	Lysogeny Broth medium
MOPS:	3-morpholinopropanesulfonic acid
PKS:	Protocatechuic Acid
Spec:	Spectinomycin

LIST OF FIGURES

LIST OF TABLES

1. INTRODUCTION

1.1. Metabolic engineering for microbial cell factories

Metabolic engineering approach that emerged in the early 1990s and allows the rational design of microbial systems with high production capacity with fully defined genetics has gained significant attention in white biotechnology. When considered within the scope of genetic engineering, metabolic engineering involves the cellular production of a wide range of metabolites and heterologous proteins, and relieving of regulatory nodes and deletion/addition of genes to increase this production. Initial strain developments focused on techniques such as random mutations and screening/selection techniques to get hyper-producing strains (Hagino & Nakayama, 1973b; Torres & Voit, 2002). However, the instability of these mutations was their major weakness. This led to the metabolic engineering approach.

Until today, metabolic engineering has been applied successfully to many different microbial systems, from *Escherichia coli* to *Penicillium chrysogenum* and even *Saccharomyces cerevisiae*. *Corynebacterium glutamicum* is among the subjects of metabolic engineering that has come to the fore in studies and brought great success on an industrial scale (Becker & Wittmann, 2015; M. Ikeda & Nakagawa, 2003). Although *C. glutamicum* is specifically known for its industrial-scale production of L-glutamate and L-lysine, the production range of this bacterium has been expanded to synthesize different bio-based products and recombinant proteins with high value using metabolic engineering (Lee et al., 2016).

1.2. *Corynebacterium glutamicum*

The Gram-positive soil bacterium *C. glutamicum* was found and isolated by employees of a Japanese company, Kyowa Hakko (Tokyo, Japan), as a natural producer of L-glutamate (Kinoshita et al., 1957). Following its isolation, the majority of research has focused on the improvement of *C. glutamicum* strains for industrial glutamate production in the presence of simple sugars and ammonia.

Its essential physiological properties that make *C. glutamicum* an industrially important producer can be summarized as: (i) safety for health (GRAS = generally considered as safe); (ii) rapid growth to reach high cell densities; (iii) genetic stability and lack of recombination repair systems; (iv) limited restriction-modification repair systems; (v) no autolysis in the growth-restricted condition which allows metabolic activity to continue; (vi) low protease

activity which makes recombinant protein production attractive; (vii) presence of metabolic plasticity and secondary metabolism properties; and (viii) ability to use many different carbon sources and stress tolerance to carbon sources (Lee et al., 2016).

Initially, basic tools for genome engineering of *C. glutamicum*, including gene integration, modification, and silencing, have been developed, and an *E. coli*-conjugated system using mobile vectors (mob-bearing) has also been established (Pühler & Schwarzer, 1991). Isolation of natural *C. glutamicum* plasmids and the development of the first DNA transfer technologies for *C. glutamicum* could be regarded as milestones in metabolic engineering with this strain (Becker, Rohles, et al., 2018). The introduction of inducible shuttle vectors along with natural and synthetic promoters for tunable gene expression was another key step in further progress (Baumgart et al., 2013; Becker, Rohles, et al., 2018; Eikmanns et al., 1991; Peters-Wendisch et al., 2001; Stansen et al., 2005; Zhang et al., 2013). In addition to search for natural promoters for production, studies to develop stronger promoters by mutation and selection also continued (Pátek et al. 2013). The majority of inducible plasmids have been developed based on *E. coli* systems. pEKEx2, pXMJ19, and pVWEx1 are among the IPTG-inducible (isopropyl β-D-1-thiogalactopyranoside) plasmids for recombinant protein expression (Eikmanns et al., 1991; Jakoby et al., 1999; Peters-Wendisch et al., 2001). Unfortunately, the low permeability of *C. glutamicum* for IPTG, has led to lower expression with IPTG-induced systems when compared to *E. coli* (Pátek et al., 2003). Later, Kortmann et al. (Kortmann et al., 2015) have reported well-controlled expression and a homogeneous population with IPTG in *C. glutamicum* engineered to carry the DE3 region of *E. coli* BL21.

After the publication of the *C. glutamicum* ATCC 13032 genome sequence, known as the wild-type strain, by two separate working groups in 2003, a new era began for *C. glutamicum* in terms of industrial microbiology and biotechnology (M. Ikeda & Nakagawa, 2003; Kalinowski et al., 2003) The presence of its genome sequence has allowed a better understanding of *C. glutamicum* (Becker & Wittmann, 2012; Wendisch et al., 2006).

A short history of *C. glutamicum* strains is shown in Figure 1.1.

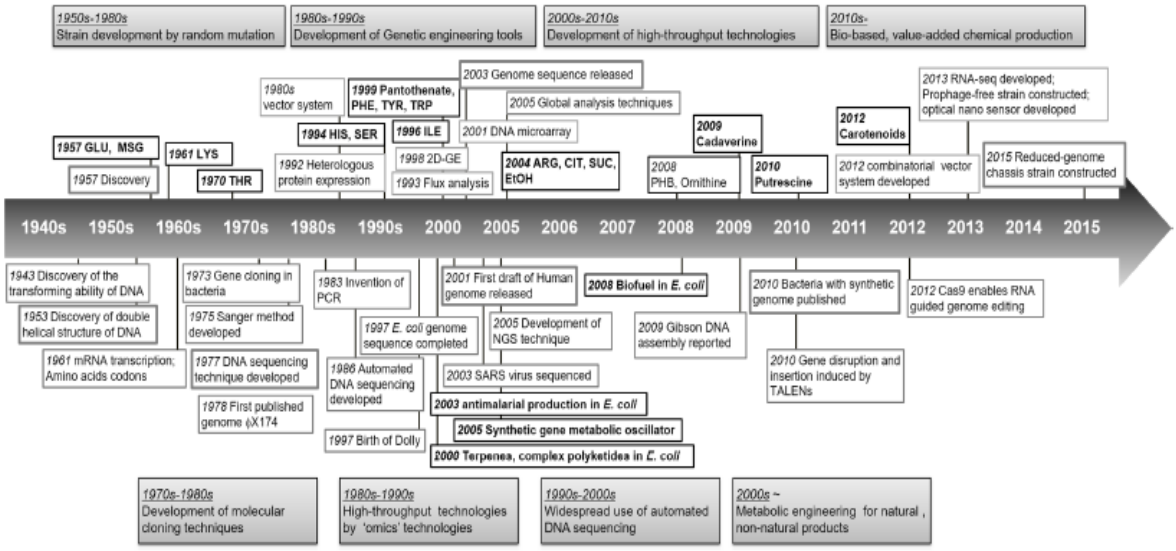

Figure 1.1: Short history of *C. glutamicum* (Lee et al., 2016).

With the availability to modify its metabolism, different rationally designed *C. glutamicum* strains were constructed for production of a wide range of different chemicals, fuels, materials and healthcare products (Wendisch et al. 2006; Becker and Wittmann 2012; Lee et al. 2016). Furthermore, its ability to naturally use a wide range of carbon sources from mono and disaccharides to organic and amino acids, have placed it at the top-used bacterial platforms in white biotechnology. Advances in metabolic engineering have enabled it to use other carbon sources such as cellobiose, lactose, galactose, glycerol and xylose, as well (Ikeda, 2012; Meiswinkel et al., 2013; Zahoor et al., 2012). In this regard, a major industrial advantage of *C. glutamicum* over most-commonly used microorganisms is its ability to co-utilize different carbon sources simultaneously (Kremling et al., 2009; Singh et al., 2008; Wendisch et al., 2000), which also allows effective utilization of mixed sugars, an in lignocellulosic wastes, as a carbon source. Possible utilization of lignocellulosic carbon sources also prevents competition with carbon sources derived from human feedstocks (Buschke et al., 2013; Mao et al., 2018).

1.3. L-DOPA

3,4-dihydroxyphenyl-L-alanine (L-DOPA), displayed in Figure 1.2, is an amino acid that is the most commonly used drug for the treatment of Parkinson's disease. Parkinson disease is a

central nervous system disorder usually occurring as the result of dopamine deficiency in brain.

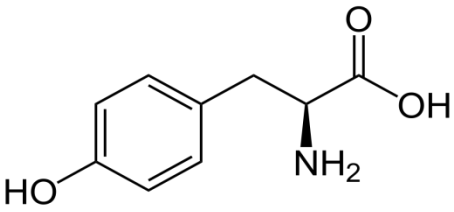

Figure 1.2: L-DOPA chemical structure.

As the number of elderly people suffering from the symptoms of Parkinson's disease is growing, the market size for L-DOPA is expanding rapidly (Koyanagi et al., 2005). The fact that L-DOPA can pass the blood-brain barrier, and dopamine cannot, makes it possible to increase dopamine levels in patients with Parkinson's disease symptoms with the administration of L-DOPA (Min et al., 2015). As presented in Figure 1.3, L-DOPA is one of the compounds that is derived from the aromatic amino acid L-tyrosine.

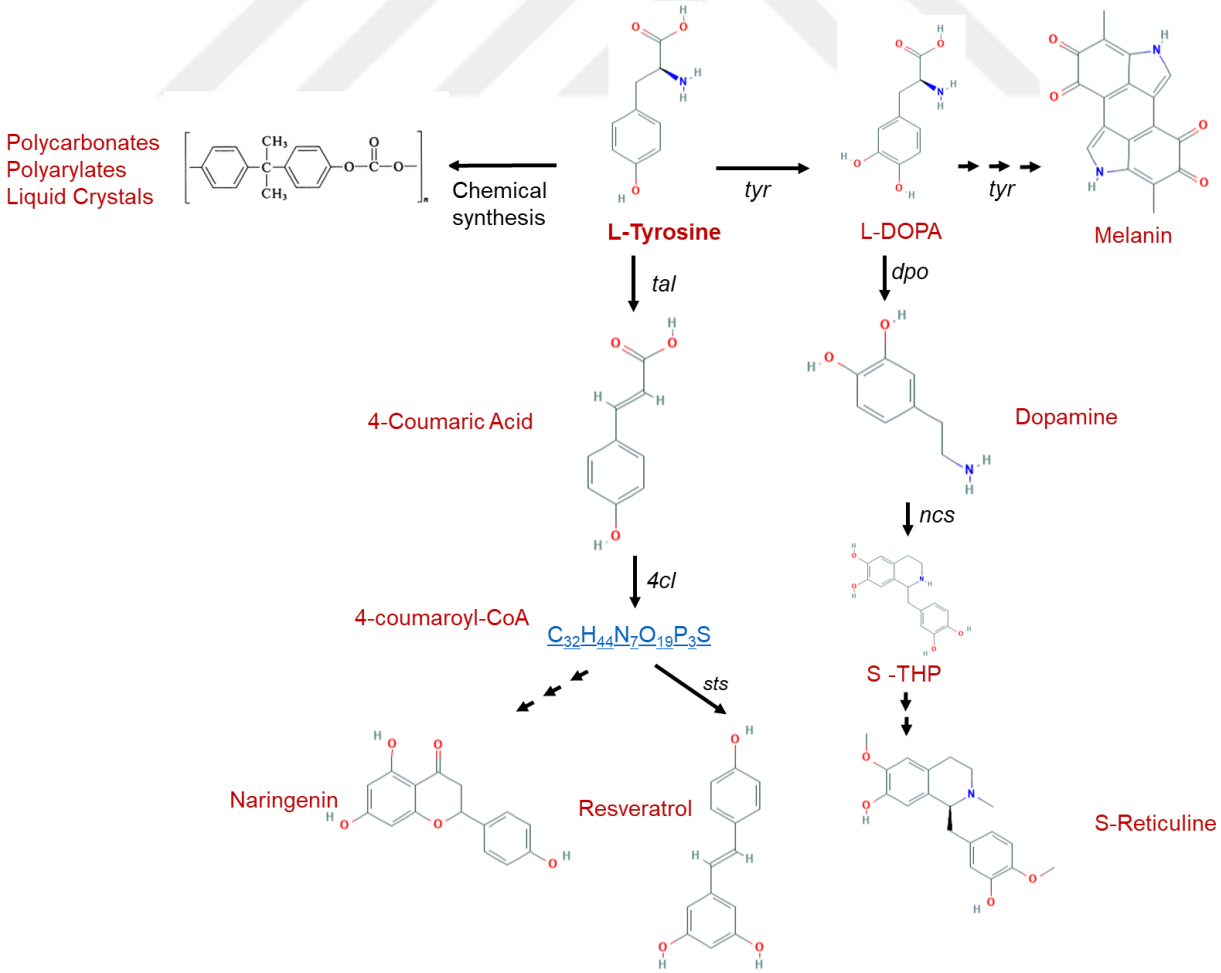

Figure 1.3: Compounds derived from L-tyrosine. *pal*: phenylalanine ammonia lyase; *tal*: tyrosine ammonia lyase; *4CL*: 4-coumaroyl:CoA ligase; *dpo*: dopa oxidase, *sts*: stilbene synthase, *tyr*: tyrosinase; *ncs*: norcoclaurine synthase; THP: tetrahydropapaveroline.

1.3.1 General overview of L-DOPA production

The current commercial production of L-DOPA largely depends on asymmetric hydrogenation. Unfortunately, asymmetric synthesis displays major disadvantages such as poor conversion rate and low enantioselectivity (Knowles, 2004). Thus, rationally designed microbial systems designated as the 'microbial cell factories' are attractive alternatives for the production of this valuable compound (Min et al., 2015).

Microbial production of L-DOPA may be based on microorganisms with at least one of the three enzymes: tyrosinase (EC 1.14.18.1), tyrosine phenol-lyase, TPL, (EC 4.1.99.2), or *p*-hydroxyphenylacetate 3-hydroxylase, PHAH, (EC 1.14.14.9). Production with TPL requires the toxic precursor, catechol, which complicates downstream processes and overall production and handling. Production with PHAH requires NADH as a cofactor, thus, continuous reducing power is required to regenerate NADH. For production with tyrosinases, unique cofactors or adaptor proteins may be required. Furthermore, these enzymes commonly possess both monophenolase (cresolase) and diphenolase (catecholase) activities, usually the latter being higher (Wei et al., 2016). As seen in Figure 1.4, cresolase activity catalyzes the *ortho*-hydroxylation of L-tyrosine to L-DOPA while catecholase activity catalyzes the oxidation of L-DOPA to L-dopaquinone. L-dopaquinone is non-enzymatically converted to dopachrome, which may be converted to melanine through further oxidation.

The only biotechnological approach used for commercial production is the enzymatic synthesis that uses the TPL enzyme of *Erwinia herbicola* (Koyanagi et al., 2005). This technology uses TPL enzyme for the *in-vitro* conversion of L-DOPA in the presence of pyruvate, ammonia, and catechol. High production costs together with the toxicity of catechol makes L-DOPA production using other bacterial routes more attractive and biofriendly alternatives. In this respect, the tyrosinase from the plant pathogen *Ralstonia solanacearum* which possesses a higher monophenolase to diphenolase activity (Hernández-Romero et al., 2006) may be an attractive enzyme for L-DOPA production. This is a feature that makes the tyrosinases favorable for L-DOPA production (Nakagawa et al., 2011). However, tyrosinase based microbial L-DOPA synthesis directly depends on L-tyrosine availability; therefore, hosts with high L-tyrosine production capacity will be preferred.

To date, there are no 'microbial cell factories' feasible to scale-up for industrial production of L-DOPA. Ease of growth and genetic modifications have placed particular emphasis on *Escherichia coli* as a producer of aromatic amino acids and aromatic compounds (Chávez-Béjar et al., 2012; Floras et al., 1996; Masato Ikeda, 2006; Zhou et al., 2011). Unfortunately, problem of phage contamination and the concern on food safety restricted its industrial scale applications (Tanji et al., 2008). Thus, the attractive properties of the workhorse *C. glutamicum* can make it a superior host for L-DOPA production. It has been used in the large-scale industrial production of different amino acids for more than 50 years since its discovery but despite of that, its potential for the production of the amino acids, L-tyrosine or L-DOPA, has not been exploited so far.

Table 1.1 summaries the L-DOPA production with different microbial platforms and enzyme used for its synthesis.

Table 1.1: L-DOPA production with different microorganisms (Wei et al., 2016).

Microorganism	**Substrate**	**Enzyme**	**Source**
Acremonium rutilum	L-Tyrosine	Tyrosinase	(Krishnaveni et al., 2009)
Aspergillus oryzae	L-Tyrosine	Tyrosinase	(Ali et al., 2005)
Yarrowia lipolytica NRRL-I43	L-Tyrosine	Tyrosinase	(Ali et al., 2007a)
Bacillus sp. JPJ	L-Tyrosine	Tyrosinase	(Surwase & Jadhav, 2011)
Brevundimonas sp. SGJ	L-Tyrosine	Tyrosinase	(Surwase et al., 2012)
E. coli	Glucose	Tyrosinase	(Nakagawa et al., 2011)
Erwinia herbicola	Catechol, Pyruvate	Tpl	(Koyanagi et al., 2005)
E. coli	Catechol, Pyruvate	Tpl	(Foor et al., 1993)
Pseudomonas aeruginosa	Catechol, Pyruvate	Tpl	(Park et al., 1998)
E. coli W (ATCC 11105)	L-Tyrosine	PHAH	(Jang Young Lee & Xun, 1998)
E. coli DOPA-30N	Glucose	PHAH	(Wei et al., 2016)

1.3.2 Challenges in L-DOPA production

A significant bottleneck in L-DOPA production and storage, is its ease of oxidation to undesired products (Min et al., 2015). L-DOPA is readily oxidized to a reactive dopaquinone, which is eventually converted to melanin components (Figure 1.4). The most commonly used way of dealing with this problem, is to prevent L-DOPA oxidation by adding molecules such as ascorbic acid or essential oils, that could prevent this reaction (Nikolova et al., 2019). To this end, one section of the thesis work was dedicated to the evaluation the effect of ascorbic acid, the most commonly used L-DOPA antioxidant, and thymol, which was reported to possess potential antioxidant properties (Satooka & Kubo, 2011; Zolghadri et al., 2019). Thymol was evaluated for the first time as an antioxidant in this work.

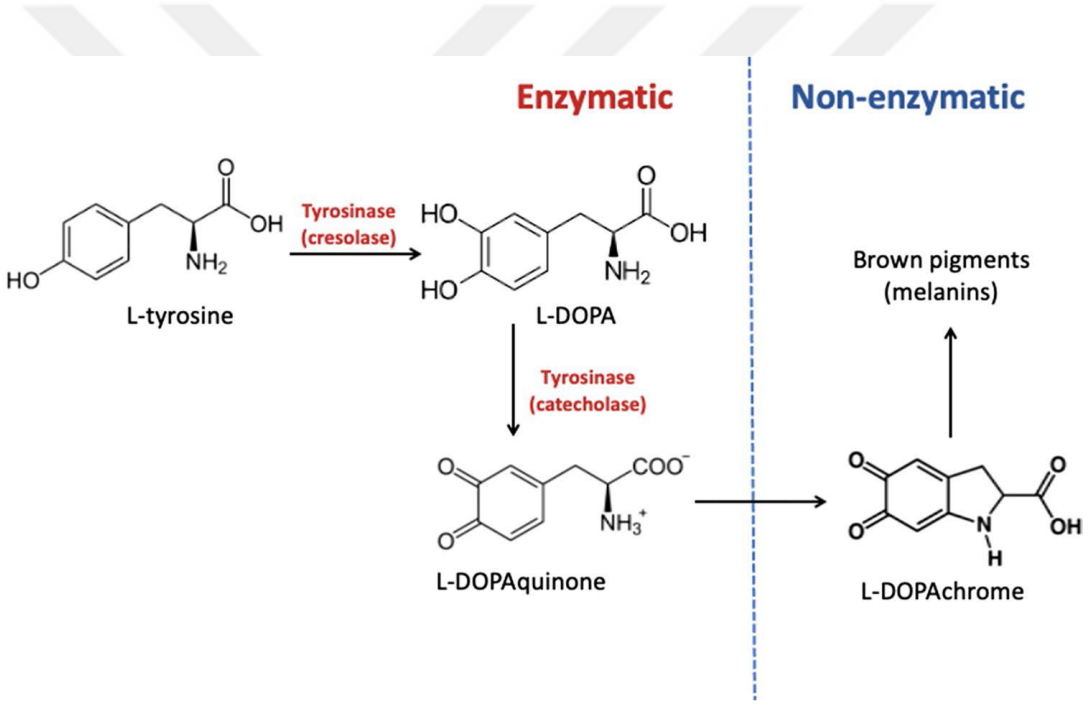

Figure 1.4: Conversion of L-tyrosine to L-DOPA and its downstream metabolites (Kurpejović et al., 2021).

1.4. L-tyrosine

Tyrosine (Figure 1.5) is one of the three aromatic amino acids which also serves as the precursor of numerous metabolites with defence, structural support, neurotransmitter, UV protectant, analgesic, and antioxidant functions that find applications in food, pharmaceutical, and cosmetic industries (Schenck & Maeda, 2018). Until recently, due to its relatively low

total market demand, its production has received less attention. With the realization of the different classes of specialized compounds derived from L-tyrosine (Figure 1.3), such as L-DOPA, melanin, naringenin, and resveratrol, its biotechnological synthesis has started to gain increasing interest (Chávez-Béjar et al., 2012).

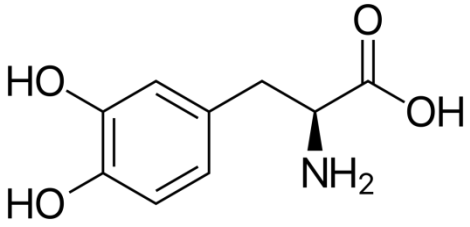

Figure 1.5: L-tyrosine chemical structure.

1.4.1 Biosynthetic route of L-tyrosine synthesis in *C. glutamicum*

Microbial L-tyrosine synthesis starts in the central carbon metabolism after the uptake of the carbon source, which is glucose for most bacteria. The first committed step towards L-tyrosine synthesis is the condensation of phosphoenolpyruvate (PEP), an intermediate of glycolysis, and erythrose 4-phosphate (E4P), an intermediate of pentose phosphate pathway, by the enzyme 3-deoxy-D-arabino-heptulosonate 7-phosphate synthase (DAHPS). The major glucose uptake and phosphorylation in *C. glutamicum* is mediated by phosphotransferase system (PTS) which uses PEP as the phosphate source. Since PEP is one of the two substrates for aromatic amino acids synthesis, its consumption by the PTS system is a significant disadvantage for aromatic amino acids synthesis. As reported by Lindner et al. (Lindner et al., 2011) *C. glutamicum* is able to grow in the absence of PTS system when grown on glucose; thus, this indicated the presence of an alternative glucose uptake system. This was explained by the glucose uptake through PEP-independent inositol permeases uptake system, which required at least one of the inositol permeases and a glucokinase. The main advantage of this route of glucose uptake for L-tyrosine biosynthesis is that PEP is not being consumed. This increases its availability for aromatic amino acids biosynthesis.

The condensation reaction of PEP and E4P then proceeds towards chorismate, which is the branching point between L-tryptophan on one side and L-tyrosine and L-phenylalanine on the other side (Figure 1.6). Aromatic amino acids synthesis is strictly regulated by the end products; both L-tyrosine and L-phenylalanine inhibit DAHPS and chorismate mutase (encoded by *csm*) while L-phenylalanine inhibits prephenate dehydratase (encoded by *pheA*) (Eggeling & Bott, 2005).

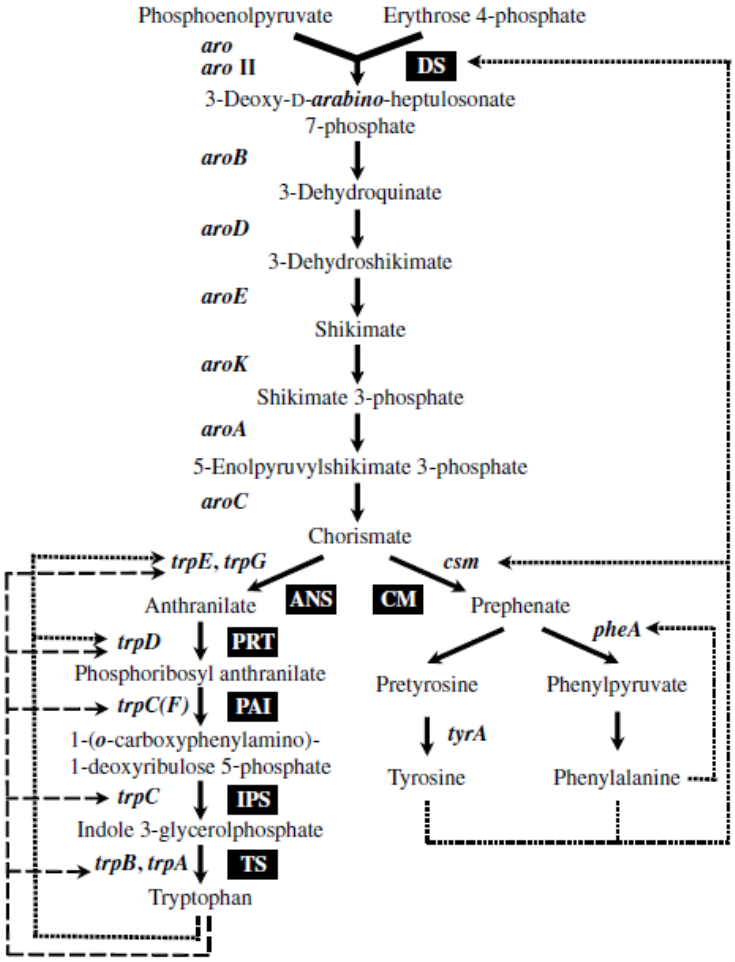

Figure 1.6: Regulation of aromatic amino acids biosynthesis in *C. glutamicum* (Eggeling & Bott, 2005).

1.4.2 The unidentified aminotransferase in L-tyrosine biosynthesis in *C. glutamicum*

There are two alternative routes in the post-chorismate node of microbial L-tyrosine biosynthesis (Fazel & Jensen, 1979). In the first route, prephenate is converted to L-tyrosine via hydroxyphenylpyruvate and in the second prephenate is converted to L-tyrosine via arogenate (pretyrosine). As documented by Fazel & Jensen (1979) *C. glutamicum* uses the arogenate route. In this route, the first required enzyme is an aminotransferase, which is responsible for the transamination of prephenate to arogenate. The second enzyme, prephenate dehydrogenase (*tyrA*), then converts the arogenate to L-tyrosine. The transaminase of this route is yet unknown in *C. glutamicum*. It is possible that among the 20

aminotransferases possessed by *C. glutamicum* (Marienhagen et al., 2005) one can be responsible for this aminotransferase activity.

Graindorge et al. (2014) has reported that the N-succinyldiaminopimelate aminotransferases in *Actinobacteria*, *Streptomyces avermitilis* and *Mycobacterium tuberculosis*, display prephenate aminotransferase activity. Furthermore, the fact that the 3-deoxy-7-phosphoheptulonate synthase and chorismate mutase of *M. tuberculosis* and *C. glutamicum* share significant structural similarities (Burschowsky et al., 2018), also may suggest a link between the transaminases of these two microorganisms. Thus, by screening the aminotransferases identified by Graindorge et al. (2014) for activity towards N-succinyldiaminopimelate, it may be possible to find an enzyme, which displays prephenate aminotransferase activity.

1.4.3 General overview of L-tyrosine production

Initial efforts for industrial production of L-tyrosine relied on its extraction from protein hydrolysates using a chemical approach. Later, an enzymatic approach utilizing tyrosine phenol-lyase has been established for a more economical price. Advances in metabolic engineering had shifted economically competitive L-tyrosine synthesis towards biotechnological methods that use engineered microbial cells. Those mostly included the integration of deregulated enzymes and overexpression of the genes encoding the rate-limiting enzymes. Incorporation of feed-back resistant DAHP synthase, along with the PEP synthase and transketolase in *E. coli* led to high L-tyrosine accumulation (Lütke-Eversloh & Stephanopoulos, 2007).

Production with *Pichia pastoris* via whole-cell transformation of pyruvate to L-tyrosine (Tang et al., 2021) and conversion of phenol, pyruvate, and ammonia via enzymatic conversion in immobilized *Escherichia intermedia* cells have been investigated, as well (Para et al., 1985). Its current production is majorly based on engineered *E. coli* strains (Chávez-Béjar et al., 2012).

L-tyrosine titers obtained with different microbial platforms are summarized in Table 1.2.

Table 1.2: The L-tyrosine titers with different microbial platforms (Lütke-Eversloh et al., 2007).

Microorganism	L-tyrosine (g/L)	Source
Pseudomonas aeruginosa	0.06	(Qi et al. 2002)
A. globiformis P46NTE	2.4	(Roy et al. 1997)
C. glutamicum ATCC 21562–ATCC 21573	4.3–12.3	(Hagino & Nakayama, 1974)
E. coli T2	9.7	(Lütke-Eversloh & Stephanopoulos, 2007)
E. coli	2	(Juminaga et al., 2012)
Erwinia herbicola ATCC 21434	53.5	(Enei et al., 1973)
C. intermedius ATCC 21073	10	(Para et al., 1985)

1.4.4 The L-tyrosine overproducer *C. glutamicum* ATCC 21573

L-tyrosine synthesis by *C. glutamicum* has received only very little attention. With classical strain breeding and screening/selection techniques, the *C. glutamicum* ATCC 21573 strain with an L-tyrosine titer of 12.3 g/L was constructed (Hagino et al., 1974; Hagino et al.,1973a, 1973b). The constructed strain was reported to be L-phenylalanine auxotroph and resistant to 3-aminotyrosine, *p*-fluorophenylalanine, and *m*-fluorophenylalanine. Using genetic engineering tools Ikeda and Katsumata (1992) were able to engineer a *C. glutamicum* strain for 26 g/L L-tyrosine production. However, both the host of production (Hagino & Nakayama, 1975) and the donors of regulation-insensitive enzymes (Hagino & Nakayama, 1974) were analog resistant mutants derived from wild-type cells using random mutagenesis. Because of their instability of these strains, engineering endeavors are required to get stable constructs for industrial applications.

Available L-tyrosine overproducer stains are products of random mutagenesis, therefore there is no exact information on how carbon flow was regulated towards L-tyrosine biosynthesis in these strains. Consequently, genome sequencing and genome-wide mutation analysis may be helpful to guide the construction of an L-tyrosine overproducer.

1.5. Renewable carbon sources

Advances in white biotechnology and increasing awareness of sustainability help to replace conventional sugars with renewable feedstocks as the carbon source for microbial production of both commodity and specialty chemicals (Heider & Wendisch, 2015; J. W. Lee et al., 2011; J. Liu et al., 2020; Pfeifenschneider et al., 2012; Wendisch et al., 2016). Biomass, especially wastes of agricultural activity is an attractive renewable feedstock with a steady and abundant supply as a result of rapid increase in volume and types of agricultural activities. Its use is carbon neutral and does not compromise the production of main food and even non-food crops. Microbial utilization of this huge quantity of biomass for industrial biotechnology may not only help its management towards climate change, water and soil contamination, and local air pollution and reduce waste disposal cost but may also generate revenue from the sale of the synthesized end product.

Lignocellulosic biomass is a material of primarily cellulose, hemicellulose and lignin polymers of different percentages with very small amounts of ash, pigment and protein (Harmsen et al., 2010). At the core are the organized cellulose macro-fibers, which are enveloped by the lignin. Hemicellulose molecules form a dispersed network between the lignin and cellulose portions. On average, lignocellulosic materials contain, 30-50 % cellulose and 15-35 % hemicellulose (Limayem & Ricke, 2012). Different sugars (e.g. glucose, mannose, galactose, xylose, arabinose, etc.) are the monomeric components of cellulose and hemicellulose; however, the quantity of the sugars that can be extracted from lignocellulosic biomass varies considerably depending on the biomass, on the type of crop species and the extraction method used (S. Singh et al., 2015). The presence of these sugars makes lignocellulosic biomass attractive for microbial bioprocesses.

1.5.1 Hazelnut husk as a renewable carbon course

Hazelnut husk is a lignocellulosic agro-waste that is commonly discarded through burning and not utilized for any other processes. Under normal weather conditions Turkey produces around 600,000 metric tons of hazelnut annually, which is approximately 75 % of the total production worldwide (Erdogan, 2018), yielding waste husk in approximately half that amount. Surek and Buyukkileci (2017) have made a more detailed analysis and given the composition of hazelnut husk as 15.4 % cellulose, 25.9 % klason lignin, 5.8 % xylan, 2.6 % galactan, 1.7 % arabinan, 10.6 % uronic acids, 5 % ash, 24.6 % extractives and 8 % protein. In total, this yielded ~ 35 % total carbohydrate content. However, when the fermentable

sugars of hazelnut husk were released using dilute acid treatment, a treatment technique, applicable on large scale, only ~ 12 % of the weight of hazelnut husk was released as reducing sugars (data not published). Dilute acid treatment reduces the recalcitrance due to the lignin, however it usually is not harsh enough to release the whole the sugar content. Nevertheless, hazelnut husk sugar hydrolysate can be used as a sole carbon source for microbial growth.

1.5.2 Cultivation of *C. glutamicum* on renewable carbon sources

Glucose is the major preferred carbon source of *C. glutamicum* wild-type strains. Unfortunately, these strains are unable to utilize the pentose sugar xylose, which is abundantly available in lignocellulosic biomass. This is a major drawback (Sasaki et al., 2019). The major advantageous property which sets *C. glutamicum* apart in utilizing lignocellulosic biomass is its ability to grow in the presence of different inhibitory by-products such as organic acids, phenolics, and furfurals present in lignocellulosic hydrolysates.

To this end, many studies engineered *C. glutamicum* strains capable of heterologous expression of xylose utilization genes, thus widening the plethora of the chemicals to be produced with this strain using renewable sources. Kawaguchi et al. (2006) showed that *C. glutamicum* expressing the xylose isomerase (*xylA*) and xylulokinase (*xylB*) genes was capable of using both glucose/xylose mixtures, and production of succinic and lactic acids. In another study *C. glutamicum* was shown to be capable of using glucose/xylose mixtures for riboflavin production (Pérez-García et al., 2021). Furthermore, *C. glutamicum* was reported to produce L-glutamate from rice straw and wheat bran hydrolysate (Gopinath et al., 2011). In another study, rice straw hydrolysate was utilized for the production of 260 mg/L of 5-amino valeric acid and 91 mg/L putrescine (Sasikumar et al., 2021). The engineered *C. glutamicum* GJ04, produced 61.7 mg/L of L-glutamate from acid pretreated wheat straw hydrolysate (Jin et al., 2020). *C. glutamicum* CGS5, was shown to grow on enzymatically hydrolyzed corn straw and produce 98.6 mg/L of succinate (Mao et al., 2018).

1.6. The objectives of the thesis:

The main objective of this work was to engineer L-DOPA production by *C. glutamicum* from a renewable carbon source, both fermentatively and via whole-cell biotransformation. The complete work could be catagorized in the following groups:

- Tyrosinase gene expression and L-DOPA synthesis from glucose, and glucose/xylose mixtures, fermentatively and via whole-cell biotransformation
- Evaluation of potential L-DOPA antioxidants and their optimization
- Evaluation of agrowaste hazelnut husk as a sole carbon source for L-DOPA production
- Metabolic engineering an L-tyrosine overproducer and its utilization for L-DOPA synthesis
- Hypothesis about the unidentified aminotransferase through the arogenate route of L-tyrosine biosynthesis in *C. glutamicum*
- Investigating the mutations in L-tyrosine overproducer *C. glutamicum* ATCC 21573

2. MATERIALS AND METHODS

2.1. Materials

2.1.1 Strains and plasmids

C. glutamicum ATCC 13032 and 21573 were purchased from American Type Culture Collection. Plasmid pEKEx2 was a kind gift from B.J. Eikmanns. The shuttle plasmids: pEKEx3, pEKEx3-*xylA*$_{Xc}$*xylB*$_{Cg}$, pSH1, and pSH1*xylA*$_{Xc}$*xylB*$_{Cg}$ were from Prof. Wendisch's laboratory.

The strains and plasmids used and constructed during this work are summarized in Table 2.1 and Table 2.2 respectively. Used oligonucleotides are presented in Table 2.3.

Table 2.1: List of strains used in this work.

Strain	Description	Reference/Source
Corynebacterium glutamicum		
C. glutamicum	Wild-type strain ATCC 13032	ATCC
CgEKV-I	Wild-type cells harboring pEKEx2-*tyr*$_{Rs}$	This work
CgEKV-II	CgEKV-I cells harboring pEKEx3-*xylA*$_{Xc}$-*xylB*$_{Cg}$	This work
C. glutamicum OP	L-tyrosine overproducing strain ATCC 21573	ATCC
ARO02	Genome-reduced chassis strain of *C. glutamicum* Δ*ldh* Δ*vdh*::P$_{ilvC}$-*aroG*^{D146N}	(Walter et al., 2020)
CgX	*C. glutamicum* carrying the plasmid pEKEx3-*xylA*$_{Xc}$*xylB*$_{Cg}$	This work
AROM1	*trpE*-TTG mutant of ARO02	This work
AROM2	*pheA*-TTG mutant of ARO02	This work
AROM3	*pheA*-TTG mutant of AROM1	This work
AROM4	*pat*-TTG mutant of ARO02	This work
AROM21	Δ*qsuABCD::P$_{tuf}$-qsuC* mutant of AROM2	This work
AROM22	Δ*iolR*:: *P$_{tuf}$-aroE* mutant of AROM21	This work
AROM23	Δ*ptsG*::P$_{tuf}$-iolTBest mutant of AROM2	This work
AROM3X	AROM3-pSH1-*xylA*$_{Xc}$*xylB*$_{Cg}$	This work

Strain	Description	Reference/Source
AROM3D	AROM3-pEKEx3-*tyr*$_{Rs}$	This work
C. glutamicum WDD	Δ*dapC* mutant of *C. glutamicum* 13032	This work
C. glutamicum EV	*C. glutamicum* WDD-pEKEx2	This work
C. glutamicum Dap	*C. glutamicum* WDD-pEKEx2-*dapC*$_{Cg}$	This work
AROM3EV	AROM3-pEKEx2	This work
AROM3Dap	AROM3-pEKEx2-*dapC*$_{Cg}$	This work
Escherichia coli		
E.coli TOP10	F- *mcrA* Δ(*mrr-hsd*RMS-*mcr*BC) Φ80*lacZ*ΔM15 Δ *lac*X74 *rec*A1 *ara*D139 Δ(*araleu*)7697 *gal*U *gal*K *rps*L (StrR) *end*A1 *nup*G	Invitrogen, USA
E. coli DH5α	*F-thi-1 endA1 hsdr17(r-, m-) supE44 1lacU169 (Φ80lacZ1M15) recA1 gyrA96*	(Hanahan, 1983)
E. coli S17-1	*recA pro hsdR* RP4-2-Tc::Mu-Km::Tn7	(Simon, 1983)

Table 2.2: List of plasmids used in this study.

Plasmid	Description	Reference/Source
pUC57-*tyr*$_{Rs}$	Amp^{R}; *E.coli* cloning vector with *Ralstonia solanacearum* tyrosinase gene	GenScript
pEKEx2	Km^{R}; *C. glutamicum/E. coli* shuttle vector for regulated gene expression; *Ptac*, *lacI*q pBL1 *oriVCg* pUC18 *oriVEc*	(Eikmanns et al., 1991)
pEKEx2-*tyr*$_{Rs}$	pEKEx2 harboring tyrosinase from *Ralstonia solanacearum*	This work
pEKEx3	Spec^{R}; *C. glutamicum/E. coli* shuttle vector; *Ptac*, *lacI*q; pBL1, *OriVCg*,*OriVEc*	(Stansen et al., 2005)
pEKEx3-*xylA*$_{Xc}$*xylB*$_{Cg}$	Spec^{R}; *C. glutamicum*/*E. coli*	(Meiswinkel et al.,

Plasmid	Description	Reference/Source
	shuttle vector with *xylA* gene from *Xanthomonas campestris* and *xylB* gene from *C. glutamicum*	2013)
pEKEx3-tyr_{Rs}	pEKEx3- harboring tyrosinase from *Ralstonia solanacearum*	This work
pSH1	Km^R; *C. glutamicum*/*E. coli* shuttle vector, constitutive expression	(Henke et al., 2016)
pSH1-$xylA_{Xc}B_{Cg}$	Km^R; *C. glutamicum*/*E. coli* shuttle plasmid carrying *xylA* gene from *Xanthomonas campestris* and *xylB* gene from *C. glutamicum*; constitutive expression	(Pérez-García et al., 2021)
pK19*mobsacB*	Km^R; *C. glutamicum/E. coli* shuttle vector for construction of insertion and deletion mutants in *C. glutamicum* (pK19 $oriV_{Ec}$ *sacB lacZ*)	(Schäfer et al., 1994)
pK19*mobsacB*-*trpE*-TTG	pK19*mobsacB* with a construct for replacement of *trpE* start codon, ATG to TTG	This work
pK19*mobsacB*-*pheA*-TTG	pK19*mobsacB* with a construct for replacement of *pheA* start codon, ATG to TTG	This work
pK19*mobsacB*-*pat*-TTG	pK19*mobsacB* with a construct for replacement of *pat* start codon, ATG to TTG	This work
pK19*mobsacB*-Δ*qsuABCD*::P_{tuf}-*qsuC*	pK19*mobsacB* with a construct for *qsuABCD* replacement (cg0501-cg0504) *by qsuC* (cg0503) with an artificial RBS under control of *C. glutamicum* promoter P_{tuf}	(Walter et al., 2020)
pK19*mobsacB*-Δ*iolR*::P_{tuf}-	pK19*mobsacB* with a construct for	(Walter et al., 2020)

Plasmid	Description	Reference/Source
aroE	*iolR* deletion (cg0196) *by aroE* (cg1835) integration with an artificial RBS under control of *C. glutamicum* promoter P_{tuf}	
pSH1-Δ*ptsG*::P_{tuf} iolTBest	Km^R; *C. glutamicum/E. coli* shuttle vector overexpressing *iolT2* gene from *C. glutamicum* and *glcK* gene from *Bacillus subtilis* subsp. *Subtilis* str. 168, constitutive expression	(Pérez-García et al., 2016)
pK19*mobsacB*-Δ*dapC*	pK19*mobsacB* with a construct for *dapC* (cg1253) deletion	This work
pEKEx2-$dapC_{Cg}$	pEKEx2 harboring *dapC* gene from *Corynebacterium glutamicum*	This work

Table 2.3: List of oligonucleotides used in this study. Overlapping regions for Gibson assembly are in bold, ribosome binding sites are underlined.

Name	Oligonucleotide sequence (5' to 3')
trpF1For	**GCATGCCTGCAGGTCGACTCTAGAG**GTTATTGCATCGCTAGTTGC
trpF1Rev	CATGGGGATTCGTGCTCAAGGGGCACCTACCGAGGAAATC
trpF2For	GATTTCCTCGGTAGGTGCCCCTTGAGCACGAATCCCCATG
trpF2Rev	**AATTCGAGCTCGGTACCCGGGGATC**CTTGTTGAGCTCGGCCTCGAG
ForTrpE	GTTATTGCATCGCTAGTTGC
RevTrpE	CGGGTTGGCTGCCAAAATGG
trpEseq1	CAGTGGTGGTGGCGCGCTAAC
trpEseq2	CATTGATCTGGGTGCGGAACTG
pheAF1For	**GCATGCCTGCAGGTCGACTCTAGAG**GGCTACCCAGGTTGGTTAGTC
pheAF1Rev	AACAGTTGGTGCGTCGCTCAAGGTTACACAGCTTAACCCGC
pheAF2For	GCGGGTTAAGCTGTGTAACCTTGAGCGACGCACCAACTGTT

Name	Oligonucleotide sequence (5’ to 3’)
pheAF2Rev	**AATTCGAGCTCGGTACCCGGGGAT**CGTTCTTCGGCTTGGAGGTGG
pheAfor	CCTTGGCTGGAATCACCATGC
pheArev	GTACACATGGGCGAGGCGCTC
pheAseq1	CCTTTTCCATCATGGTCC
pheAseq2	ACCTACCGCTTCCACCTG
pheAseq3	CAAGGCGTTCCAGTCCGAAG
patF1For	**GCATGCCTGCAGGTCGACTCTAGAG**CTTAATGCACGGGCTTTAGC
patF1Rev	GCCAAATCTGCTCTAATCAAGATTTACACAGTACTAGCCC
patF2For	GGGCTAGTACTGTGTAAATCTTGATTAGAGCAGATTTGGC
patF2Rev	**AATTCGAGCTCGGTACCCGGGGAT**CGTGGATTTCCTCAGTGGCAA
patFor	CAACTCATTAGCAGTGAGTCC
patRev	CTGACCGTCCTGATAGAGAGG
patSeq1	TGGCAGCCGCGATCACTG
patSeq2	GAATAGCCACCTTATTCATCG
qsuFor	CGACAATGAGCGAACAAC
qsuRev	ACGTCACCGTGAACTTAC
qsuSeq1for	GGATGCTGTGAAGGCGTC
qsuSeq2rev	CGCAACCGATGTGGGTGCC
qsuSeq3for	GGACACGACACCTTGGAAG
iolRfor	CATGACCACCGAAGCTCCCATTTG
iolRrev	CTTACCTGGCCACCAGAGTGGTTTC
aroE3forSeq1	TTGGGTTCTCACATCACTC
aroE3forSeq2	GGCACTCATCGAAGCCGG
aroE3revSeq3	GGCGAATTCAAGAGCTGC
aroErev	TTAGTGTTCTTCTGAGATGCC
forDapC	AATTCTGCAGAAGGAGAATCATATGACCTCTCGCACCCC
revDapC	CAGTGAATTCTTAGCTCAGGCGAGAAACAAAGGCGTCG
dapSeq1Rev	ACGACGGGGAGGAGGGAG
dapSeq2	GCCCTTCTTCCATTCGCG
dapSeq3	CTAAAACCTCAAACCTCG
dapSeq4	CTGAAGCGGGTCTGTACC
RstyrFor	AATTCTGCAG<u>AAGGAGA</u>ATCATATGGTCGTTCGTCGC

Name	Oligonucleotide sequence (5’ to 3’)
RstyrRev	CAGTGAATTCCTAAATAACCGCAACTTCAATAGATTCAGG
EFI-tyr	GTGTTCGTCAACCTGCC
ERI-tyr	GGAAGTACCAATCGCCG
ptsGiolTB-1	**GCATGCCTGCAGGTCGACTCTAGA**GCAACGCCGTCTAAGCGTGAA
ptsGiolTB-2	GTGGACATTCGCAGGGTAACGGCCAAATATGTTGCGATGTCGTCGTC AG
ptsGiolTB-3	ACTGACGACGACATCGCAACATATTTGGCCGTTACCCTGCGAATG
ptsGiolTB-4	TGCCGTTGACCTTGATCACAGTCGTTTAAGCCTTCTTGAAGATCTGG
ptsGiolTB-5	CGGCCAGATCTTCAAGAAGGCTTAAACGACTGTGATCAAGGTCAACG
ptsGiolTB-6	**AATTCGAGCTCGGTACCCGGGGAT**CCCTCTGTGAGGCCACGTTTTT C
BestSeq1	GGCCATATTTGCAGCATCCC
BestSeq2	AAGTACATCGGCCACTACAG
BestSeq3	TGATCAACGCGCTTATCG
BestSeq4	CCGCACCACCTTCATCATC
BestSeq5	CAGGTCAATGCCCGCAAAC
BestSeq6	AGCACACAGATCTAGCGCA
BestSeq7	GGGTATCGGCACCGGTATTT

2.1.2 Chemicals

D(+)-glucose, D(+)-xylose, D(-)-sorbitol, IPTG (Isopropyl β-D-1-thiogalactopyranoside), MOPS (3-morpholinopropanesulfonic acid), brain heart infusion (BHI) were from NeoFroxx GmbH. L-DOPA (3,4-Dihydroxy-L-phenylalanine) was from Carbosynth, L-tyrosine, L-tryptophan were from Neofroxx. Thymol was from Thermo Scientific. Sucrose and ammonium sulfate were from Isolab. Spectinomycin dihydrochloride 5-hydrate and L-phenylalanine were from PanReac AppliChem, kanamycin sulfate and ampicilin were from Roche. 3,4-Dihydroxybenzoic acid protocatechuic acid (PKS) was from Alfa Aesar. RedSafe DNA stain (20,000 X) was from ChemBio. Ascorbic acid was from Balmumcu Kimya.

Agar, urea, manganese (II) sulfate monohydrate, potassium phosphate monobasic, agarose, glycerol, biotin, and sodium chloride were from Sigma Aldrich. Iron (II) sulfate heptahydrate, calcium chloride, nickel (II) chloride hexahydrate, zinc sulfate heptahydrate,

magnesium sulfate heptahydrate, copper (II) sulfate pentahydrate, and di-potassium hydrogen phosphate were from Merck.

2.1.3 Buffers and media

BHI medium: In 1 liter of distilled water 37 g of BHI was dissolved and autoclaved at 121 °C for 15 minutes. To prepare solid medium for routine growth experiments, 15 g/L agar was also added prior to autoclave. For conjugation experiments, solid BHI medium contained 16 g/L agar.

LB medium: In 1 liter distilled water, 10 g of peptone, 5 g of yeast extract, and 10 g of NaCl were dissolved and autoclaved at 121 °C for 15 minutes. To prepare solid medium for routine growth experiments, 15 g/L agar was also added prior to autoclave. For conjugation experiments solid LB medium contained 16 g/L agar.

CGXII defined medium: CGXII medium was prepared by mixing 900 mL basic medium with 100 mL of the solution containing the carbon source. The basic medium contained 20 g/L $(NH2)_2SO_4$, 5 g/L urea, 1 g/L KH_2PO_4, 1 g/L K_2HPO_4 and 42 g/L 3-morpholinopropanesulfonic acid (MOPS). Its pH was adjusted to 7 with 4 M NaOH. For routine experiments, 40 % glucose was used to prepare CGXII medium containing 4 % glucose. Both components were autoclaved separately at 121 °C for 15 minutes.

Trace element concentrations in 1 liter of CGXII medium were as follows: 0.25 g/L $MgSO_4 \cdot 7H_2O$, 10 mg/L $CaCl_2$, 10 mg/L $FeSO_4 \cdot 7H_2O$, 10 mg/L $MnSO_4 \cdot H_2O$, 1 mg/L $ZnSO_4 \cdot 7H2O$, 0.2 mg/L $CuSO_4 \cdot 5H_2O$, 0.02 mg/L NiCl2·6H2O, 0.2 mg/L biotin, and 30 mg/L protocatechuic acid. All trace elements solutions were sterilized separately with 0.22 μm filters and stored at – 20 ^oC, and mixed with other two components before use.

CGXII medium with hazelnut husk hydrolysate as the sole carbon source: When husk hydrolysate was used as the sole carbon source in defined CGXII medium, a concentrated (5X) basic medium was prepared. This contained 100 g/L $(NH_2)_2SO_4$, 25 g/L urea, 5 g/L KH_2PO_4, 5 g/L K_2HPO_4 and 210 g/L MOPS in 1 L distilled water. Its pH was not adjusted. It was autoclaved at 121 °C for 15 minutes. The pH of husk hydrolysate was adjusted to 7 with 10 M NaOH. 50 mL of CGXII medium with husk hydrolysate had 80 % hydrolysate and 20 % concentrated basic medium. Trace element concentrations were identical to that of CGXII with glucose as the carbon source.

All media and buffers are summarized in Table 2.4.

Table 2.4: List of media and buffers.

Media and buffers	**Composition**
Brain heart infusion (BHI)	37 g/L BHI
Solid brain heart infusion	15 g/L agar
	37 g/L BHI
Brain heart infusion sorbitol (BHIS)	37 g/L BHI
	91 g/L Sorbitol
Lysogeny broth (LB)	10 g/L Peptone
	5 g/L Yeast extract
	10 g/L Sodium chloride
Solid Lysogeny broth (LB)	10 g/L Peptone
	5 g/L Yeast extract
	10 g/L Sodium chloride
	15 g/L Agar
CGXII medium	20 g/L $(NH_2)_2SO4$,
	5 g/L urea,
	1 g/L KH_2PO_4
	1 g/L K_2HPO_4
	42 g/L MOPS
	4% (w/v) glucose
	0.25 g/L $MgSO_4 \cdot 7H_2O$
	10 mg/L $CaCl_2$
	10 mg/L $FeSO_4 \cdot 7H_2O$
	10 mg/L $MnSO_4 \cdot H_2O$
	1 mg/L $ZnSO_4 \cdot 7H2O$
	0.2 mg/L $CuSO_4 \cdot 5H_2O$
	0.02 mg/L $NiCl_2 \cdot 6H_2O$
	0.2 mg/L biotin
	30 mg/L protocatechuic acid (PKS)
TG buffer	90 % :1 mM Tris HCl
	10 % :10 % Glycerol
Nitrate molybadate reagent (NMR)	10 % $NaNo_3$

Media and buffers	Composition
	10 % Na_2 MoO_4
Mercury sulfate reagent (MSR)	15 % $HgSO_4$ in 5 N sulfuric acid.
Nitrate reagent (SN)	0.2 % $NaNO_3$
Isothermal reaction buffer (IRB) 5X	250 µL/mL 2 M Tris-HCl
	25 µL/mL 2 M $MgCl_2$
	50 µL/mL 1 M DTT
	50 µL/mL 100 mM NAD
	100 µL/mL 10 mM dNTPs
	500 µL/mL 50% PEG-8000
	25 µL/mL ddH_2O
DNS reagent	10 g/L DNS
	300 g/L potassium-sodium tartrate
	2 M NaOH solution
TAE buffer (50X)	242 g/L Tris base
	18.61 g/L Disodium EDTA
	59.955 g/L Acetic acid

2.2. Methods

2.2.1 Molecular biology techniques

2.2.1.1. Polymerase chain reaction (PCR) and colony PCR

DreamTaq DNA Polymerase (Thermo Fisher) was used for routine and colony PCR reactions to amplify PCR products not larger than 5 kb. Phusion High-Fidelity DNA Polymerase (Thermo Fisher) was used to amplify PCR products larger than 5 kb. The reaction mixtures used are given in Tables 2.5 and 2.6.

Table 2.5: Reaction mixtures for DreamTaq DNA polymerase.

Component (µl)	Volume (µl)
Template DNA	1-2
10x DreamTaq buffer	2.5
Forward primer (10 mM)	2.5
Reverse primer (10 mM)	2.5

Component (µl)	Volume (µl)
dNTP mix (10 mM)	0.5
$MgSO_4$ (50 mM)	0.5
DreamTaq DNA Polymerase	0.125
ddH_2O	*
Total volume	**25**

* The final volume of the reaction was adjusted by changing ddH_2O volume.

Table 2.6: Reaction mixtures for Phusion High-Fidelity DNA Polymerase.

Component (µl)	Volume (µl)
Template DNA	1-2
5X Phusion HF Buffer	10
Forward primer (10 mM)	5
Reverse primer (10 mM)	5
dNTP mix (10 mM)	1
Phusion DNA Polymerase	0.5
ddH_2O	*
Total volume	**50**

* The final volume of the reaction was adjusted by changing ddH_2O volume.

For routine PCR with plasmid or genomic DNA, 10-100 ng template DNA was used. For colony PCR, the template DNA was provided by dipping a small amount of cells with a sterile toothpick into the reaction mixture.

The conditions used to amplify genes using DreamTaq polymerase and Phusion™ High-Fidelity DNA Polymerase are given in Tables 2.7 and Table 2.8, respectively.

Table 2.7: PCR conditions in the thermocycler using DreamTaq DNA polymerase.

Step	Temperature	Time
Initial denaturation	95°C	5-10 minutes
Denaturation	95°C	30 seconds
Annealing	55-68°C	30 seconds
Extention	68°C	1 min/kbp
Final extention	68°C	10 minutes

Storage	4°C	∞

Table 2.8: PCR conditions in the thermocycler using Phusion DNA polymerase.

Step	**Temperature**	**Time**
Initial denaturation	98°C	30 seconds
Denaturation	98°C	10 seconds
Annealing	55-68°C	30 seconds
Extention	72°C	30 sec/kbp
Final extention	72°C	5 minutes
Storage	4°C	∞

2.2.1.2. Plasmid DNA isolation

Plasmid isolation from *E. coli* DH5α or *E. coli* TOP10 cells was achieved using the PureLink™ Quick Plasmid Miniprep Kit. 10 mL of overnight preculture was used. The plasmids were eluted in 50 µL of elution buffer.

2.2.1.3. Digestion PCR products and plasmid DNA with restriction enzymes

Approximately 1 µg of DNA (plasmid or PCR product) was digested in a reaction volume of 10-50 µL under the optimal conditions specified for the enzyme. In case of double digestion, a common buffer, in which both enzymes display high activity, was used. The restriction enzymes were heat-deactivated at 65 °C for 15 minutes.

2.2.1.4. Dephosphorylation of digested plasmid DNA

Dephosphorylation of double-digested plasmid DNA was achieved with Antartic Phosphatase (NEB) for 30 minutes at 37 °C. The reaction was stopped by incubating the reaction mixture at 80 °C for 2 minutes.

2.2.1.5. Cleaning of genes and plasmid DNA

In order to remove residuals from the reaction mixtures of genes and plasmid DNAs, purification was achieved with the PureLink™ PCR Purification Kit following the instructions given in the manual.

2.2.1.6. Ligation of genes and plasmid DNA

Ligation reaction was achieved with T4 ligase (Fermentas) by incubating the digested gene and the digested plasmid at 16 ^{o}C for 15 hours. For each 1 µg of plasmid DNA 1.5 µg of gene was used for ligation reactions. The final reaction volume was adjusted to 15 µL. The reaction was inactivated by incubation at 65 ^{o}C for 10 minutes.

2.2.1.7. Protocol for Gibson assembly

In Gibson assembly, multiple DNA fragments can be joined by overlapping sequences and the simultanoues action of three enzymes: 5′ exonuclease, DNA polymerase and DNA ligase (Gibson et al., 2009). The single-digested backbone, plasmid pK19*mobsacB*, was mixed with 3-fold of the DNA insert (which contain flanking regions for upstream and downstream of a gene to be modified, along with the desired modification itself) 15 µL of DNA Gibson Assembly mixture (Table 2.9), and completed to a final volume of 20 µL with ddH_2O. DNA inserts amplified using Gibson-specific primers contain 20-40 bp homology with the adjacent DNA fragments to be joined.

Table 2.9: The composition for 1 mL of DNA Gibson Assembly mixture.

Component	**Quantity (µL)**
5X IRB	267
T5 Exonuclease (NEB; 10 U/ µL)	0.53
Phusion High-Fidelity DNA Polymerase (NEB; 2U/µL)	17
Taq DNA Ligase (NEB; 40 U/µL)	133
ddH_2O	583

The mixture was incubated at 50 ^{o}C for one hour. The obtained reaction mixture was transferred to chemocompetent *E. coli* DH5α cells. Resulting colonies were used for screening with colony PCR. The clones with the correct sizes of PCR products were verified by sequencing.

2.2.1.8. Agarose gel electropohoresis

All DNA samples at all stages have been analyzed on 1 % agarose gels. Before solidification, 2.5 µL of RedSafe (20000x) DNA staining dye was added to the 50 mL of gel solution (1x RedSafe). Gene ladders were from Thermo Fisher and NEB (Appendix E).

1-5 µL of DNA samples were mixed with 0.2-1 µL of 6x loading dye respectively, and then loaded to the gels and run at 100 V for 30-45 minutes in 1xTAE buffer using PowerPac Basic (BioRad) device for separation. For gel imaging, ChemiDoc XRS+ System (Biorad) device was used.

2.2.2 Standard cultivation and transformation protocols for *E. coli*

2.2.2.1. Cultivation conditions

All strains were stored in 25 % glycerol solution at - 80 ^{o}C. *E. coli* strains were routinely grown in 10 and 50 mL LB medium in 50 and 250 mL flasks, respectively, at 37 ^{o}C and 180 rpm. When needed antibiotics were used with the concentrations given in Table 2.10.

Table 2.10: Antibiotic concentrations used for growing *E. coli* in selective media.

Antibiotic	**Concentration (µg/mL)**
Kanamycin	50
Spectinomycin	100
Ampicilin	50

2.2.2.2. Transformation of *E. coli* cells via heat shock

50 µL of stock *E. coli* cells was used to inoculate 5 mL of LB medium which was incubated overnight at 37 ^{o}C and 180 rpm. Then 5 mL of fresh LB medium was inoculated with a preculture when OD_{600} reached 0.4-0.6. Cells were collected at 5000 rpm for 10 minutes at 4 ^{o}C. The supernatant was removed completely, and the cells were resuspended in 100 µL of ice-cold 0.1 M $CaCl_2$ and incubated on ice for one hour. The cells were mixed with ~ 1 µg of plasmid DNA, and further incubated on ice for one hour. Then mixtures were incubated at 42 ^{o}C for 1 minute and immediately placed on ice for 10 minutes. To the mixtures, 800 µL of fresh LB without antibiotics was added and the mixtures were incubated at 37 ^{o}C and 180 rpm for one hour. Then, cells were collected at 5000 rpm for 10 minutes at 4 ^{o}C and after resuspension they were plated on solid LB containing the proper antibiotic.

2.2.3 Standard cultivation and transformation protocols for *C. glutamicum*

2.2.3.1. Cultivation conditions

All strains were stored in 25 % glycerol solution at - 80 ^{o}C. *C. glutamicum* strains were grown in 25 and 50 mL CGXII medium in 250 mL and 500 mL baffled flasks, respectively.

Strains were activated and grown as follows:

- Glycerol stocks were streaked on BHI agar plates, and incubated for two days at 30 ^{o}C.
- Colonies on plates were used to inoculate the overday preculture in 5 mL BHI medium. This was incubated for 6 hours, at 30 ^{o}C and 200 rpm.
- 50 mL of fresh CGXII medium, with glucose as the carbon source, was inoculated with 2 mL of overday preculture and incubated overnight at 30 ^{o}C and 150 rpm.
- Main culture was inoculated with the overnight preculture to a starting OD_{600} ~ 1. Strains were grown at 30 ^{o}C and 150 rpm.

When needed, antibiotics were used with the concentrations given in Table 2.11.

Table 2.11: Antibiotic concentrations used for growing *C. glutamicum* in selective media.

Antibiotic	**Concentration (µg/mL)**
Kanamycin	25
Spectinomycin	100
Ampicilin	50

2.2.3.2. Growth in 96-well plates

To investigate growth profiles of constructed strains and effects of different supplements on bacterial behavior, growth was performed in 96-well U-bottom plates. 10-mL CGXII medium was prepared and deposited into 96-well U-bottom plate wells. Into each well, 0.22 mL of medium was added and OD_{600} was adjusted to ~ 1 by adding 5-10 µL of overnight preculture. Growth was performed for 24-72 hours in BIOTEK-ELx808 microplate reader, in fast continuous shaking mode at 30 °C. OD_{600} was monitored continuously.

2.2.3.3. Growth in PreSens Shake Flask Reader (SFR) vario

In 500-mL baffled flasks equipped with biomass, relative dissolved oxygen saturation (rDOS), and pH sensors, 50 mL of CGXII medium was inoculated with overnight preculture to a starting OD_{600} ~ 1. Growth was achieved at 30 ^{o}C and 150 rpm. All three parameters were measured simultaneously and recorded on a bluetooth-linked laptop.

2.2.3.4. Electrocompetent *C. glutamicum* cells preparation

50 µL of stock *C. glutamicum* cells was used to inoculate 5 mL of BHIS and the culture was grown overnight at 30 ^{o}C and 200 rpm. Then 600 µL of the preculture was used to inoculate 60 mL of BHIS medium. Cells were grown until OD_{600} reached 0.5. Grown cells were cooled on ice for 5 minutes and then collected at 5500 g, 4 ^{o}C for 20 minutes. Cells were washed three times with ice-cold TG buffer and two times with ice-cold 10 % glycerol, at 5000 g, 4 ^{o}C for 10 minutes. After final wash, cells were resuspended in 240 µL of ice-cold 10 % glycerol, aliquoted in 80 µL in pre-chilled eppendorf tubes, and stored at - 80 ^{o}C until used.

2.2.3.5. Electroporation of *C. glutamicum* cells

80 µL of electrocompetent cells were thawed on ice and mixed with ~ 1 µg of plasmid DNA of interest. The mixture was then immediately transferred into a pre-chilled electroporation cuvette and overlaid with 400 µL of ice-cold 10 % glycerol. The mixture was electroporated at 4 ms and 2.5 kV. After electroporation, the mixture was immediately transferred into 2 mL BHIS preheated to 46 ^{o}C and then incubated at 46 ^{o}C for 6 minutes. Then, mixtures were transferred into a shaking incubator and incubated at 170 rpm and 30 ^{o}C for one hour. Cells were collected by centrifugation for 3 minutes at 3000 rpm and 4 ^{o}C. The supernatant was removed and the cells are resuspended in the rest and plated onto BHIS containing proper antibiotic. Plates were incubated at 30 ^{o}C for two days.

2.2.3.6. Conjugation protocol for chromosomal alterations in *C. glutamicum*

Chromosomal modifications and gene deletion in *C. glutamicum* were done with two-step homologous recombination (Eggeling & Bott, 2005) by using the suicide vector pK19*mobsacB* (Schäfer et al., 1994). The transfer of constructed plasmids was performed via conjugation using *E. coli* S17 as donor strain (Walter et al., 2020).

The protocol for conjugation was performed as follows:

The recipient *C. glutamicum* cells preparation: 25 mL of BHI was inoculated with a single colony and incubated overnight at 30 ^{o}C and 150 rpm. 50 mL of BHI was inoculated with 1 mL of overnight preculture and grown to an OD_{600} of 1- 1.5. Cells were collected by centrifugation at 4,000 rpm for 7 minutes and then resuspended in 5 mL BHI. 800 µL aliquots of resuspended cells in were placed in 6 eppendorf tubes, and incubated at 50 ^{o}C for 9 minutes. Then they were stored at room temperature until further use.

The donor *E. coli* S17-1 cells preparation: 25 mL of BHI was inoculated with a single colony and incubated overnight at 37 ^{o}C and 180 rpm. 50 mL BHI with 50 µg/mL kanamycin was

inoculated with 1 mL preculture and grown to an OD_{600} of 1-1.5. In the same manner, cells were collected by centrifugation at 4,000 rpm for 7 minutes and then resuspended in 5 mL BHI.

Preparing the cell mixture: 800 µL of the recipient *C. glutamicum* cells was mixed very carefully with 200 µL of the donor *E. coli* S17-1 cells. The conjugation mixtures were then centrifuged at 3,000 rpm for 3 minutes. The supernatant was removed with a pipette and the remaining pellet was stirred very carefully with a sterile pipette tip. The pellet was poured onto a sterile 0.45 µm cellulose nitrate filter placed on an LB plate. After 10 minutes, plates were placed at 30 ^{o}C and incubated for 20 hours.

Screening for the conjugation clones: Filters were placed in 500 µL BHI and vortexed until the cell pellets were completely resuspended. The filters were removed and cell resuspension was centrifuged at 3,000 rpm for 2 minutes. The cells were resuspended and plated onto LB plates with 50 µg/mL nalidixin and 15 µg/mL kanamycin. Plates were incubated for two days. In this step *E. coli* cells were removed since they are sensitive to nalidixin, however *C. glutamicum* cells possess resistance towards this antibiotic. Then each colony was transferred onto an LB plate with 25 µg/mL kanamycin and an LB plate with 25 µg/mL kanamycin and 10 % sucrose. The plates were incubated overnight. The colonies resistant to kanamycin (grown on an LB plate with 25 µg/mL kanamycin) but sensitive to sucrose (no growth on LB plate with 25 µg/mL kanamycin and 10% sucrose) were selected and transferred onto LB plates with 10 % sucrose and incubated for two days. The colonies from these plates were transferred onto LB plates with 25 µg/mL kanamycin and LB plates with 10 % sucrose and incubated overnight. The colonies sensitive to kanamycin but capable of growing on LB plates with 10 % sucrose were selected for further analysis with colony PCR in order to screen for mutants with the desired chromosomal modification.

2.2.4 Fermentative L-DOPA production

Fermentative L-DOPA production from glucose and glucose/xylose mixtures

CgEKV-I strain was used for L-DOPA production from glucose and CgEKV-II strain was used was used for production from glucose/xylose mixtures. Precultures were prepared as explained in section 2.2.3. The main production medium was inoculated with an overnight preculture to a starting OD_{600} ~ 4. Medium was supplemented with 1 g/L L-tyrosine and copper sulfate pentahydrate (0–1.2 mM). Thymol (0.1-1 mM) and ascorbic acid (0.1-4 mM) were added as oxidation inhibitors. Stock solutions of thymol (100 mM), ascorbic acid (500 mM) and copper sulfate pentahydrate (40 mM) were filter-sterilized and stored at room

temperature. Thymol was dissolved in DMSO while ascorbic acid and copper sulfate pentahydrate were dissolved in ddH_2O. Tyrosinase expression was induced with 1 mM IPTG, 90 minutes after inoculation. The cells were grown for 24 hours and cell-free supernatants were analyzed for L-DOPA presence.

Fermentative L-DOPA production from hazelnut husk

For L-DOPA production from hazelnut husk, the CgEKV-II strain was used. Here, the medium was inoculated with overnight preculture volume to a starting OD_{600} ~ 1. Medium was supplemented with 0.4 mM copper sulfate pentahydrate, 0.2 mM thymol, and 1 g/L L-tyrosine. Tyrosinase expression was induced with 1 mM IPTG, 90 minutes after inoculation. The cells were grown for 120 hours and cell-free supernatants were analyzed for L-DOPA presence every 24 hours.

Fermentative L-DOPA production with AROM3D strain

The medium was inoculated with overnight preculture to a starting OD_{600} ~ 1 and supplemented with 0.5 mM L-phenylalanine. Tyrosinase expression was induced with 1 mM IPTG, 90 minutes after inoculation. 0.4 mM copper sulfate pentahydrate and 0.4 mM thymol were added 24 hours after the inoculation. Cells were grown for additional 24 hours and cell-free supernatants were analyzed for L-DOPA presence.

2.2.5 L-DOPA production via whole-cell biotransformation

Whole-cell biotransformation with cells obtained from glucose:

CgEKV-I cells, that had been used for fermentative L-DOPA production from glucose, were collected by centrifugation for 10 minutes at 10,000 rpm and 4 °C. Collected pellets were washed twice and resuspended in 10 mL distilled sterile water. To 15-mL falcon tubes with 10 mL of water and 1 g/L L-tyrosine, 25-50-100 μL of resuspended cells (equivalent to 3.3-6.6-13.2 mg of DCW) were added. Reactions were with w/o copper sulfate pentahydrate (0, 0.4 mM), thymol (0.1-0.4 mM) and ascorbic acid (1-4 mM). Thymol and ascorbic acid stock solutions prepared for fermentative L-DOPA production were used.

In order to preserve tyrosinase activity in the mixtures, to each falcon with reaction mixture couple of drops of chloroform was added (Kermasha & Tse, 2000). Tubes were incubated at 30 °C for 48 hours and cell-free supernatants were analyzed for L-DOPA presence.

Whole-cell biotransformation with cells obtained from hazelnut husk:

CgEKV-II were grown on hazelnut husk for 48 hours and collected by centrifugation for 10 minutes at 10,000 rpm and 4 °C. Collected pellets were washed twice and resuspended in 2 mL distilled sterile water. To 15-mL falcon tubes with 10 mL of water and 1 g/L L-tyrosine,

50-100-400-600 μL of resuspended cells (equivalent to 2-4-16-24 mg of DCW) were added. The reactions were supplemented with 4 mM ascorbic acid. In order to preserve tyrosinase activity in the mixtures, to each falcon with reaction mixture a couple of drops of chloroform was added. The tubes were incubated at 30 °C for 144 hours and cell-free supernatants were analyzed for L-DOPA presence every 24 hours.

2.2.6 L-DOPA and L-tyrosine detection and quantification methods

2.2.6.1. Arnow's method for L-DOPA detection

Arnow's test for L-DOPA detection is a colorimetric method that is based on the fact that it gives a dark yellow color when mixed with nitrous acid, and dark orange when mixed with a strong base e.g. sodium hydroxide (Arnow, 1937). The composition of the reaction mixture for Arnow's test is given in Table 2.12. For this cell-free supernatants were used. After the addition of each component, the mixture was vortexed briefly and the absorbance at OD_{530} was recorded. Titer was calculated using to the L-DOPA standard curve (Appendix B). In this work, Arnow's method was used only for detection of L-DOPA presence, since L-DOPA oxidation products interfere with the test.

Table 2.12: Composition for Arnow's test for L-DOPA detection.

Blank	**Sample**	**Standard L-DOPA (0.1mg/mL)**
1 mL dH_2O	1 mL supernatant	1 mL standard
1 mL 0.5 M HCl	1 mL 0.5 M HCl	1 mL 0.5 M HCl
1 mL NMR reagent	1 mL NMR reagent	1 mL NMR reagent
1 mL 1 M NaOH	1 mL 1 M NaOH	1 mL 1 M NaOH
1 mL dH_2O	1 mL dH_2O	1 mL dH_2O

2.2.6.2. Arnow's method for L-tyrosine detection

Initial L-tyrosine detection was perfomed by using Arnow's method (Arnow, 1937). 1 mL of cell-free supernatants were mixed with 1 mL of MSR reagent, boiled for 10 minutes, cooled and then mixed with 1 mL of nitrate reagent. Final volume of the reaction was adjusted 5 mL with distilled water. The presence of L-tyrosine was detected by measuring absorbance at OD_{530} and the titer was calculated using to the L-tyrosine standard curve (Appendix B). The composition of the test is given in Table 2.13.

Table 2.13: Composition for Arnow's test for L-tyrosine detection.

Blank	Sample	Standard L-Tyr (1mg/mL)
1 mL dH_2O	1 mL supernatant	1 mL standard
1 mL MSR reagent	1 mL MSR reagent	1 mL MSR reagent
1 mL SN reagent	1 mL SN reagent	1 mL SN reagent
2 mL dH_2O	2 mL dH_2O	2 mL dH_2O

2.2.6.3. High‑performance liquid chromatography (HPLC) for L-DOPA and L-Tyrosine detection and quantification

High-performance liquid chromatography (HPLC) analysis was performed by using an Agilent 1100 system equipped with an UV detector at 280 nm and C18 Zorbax column (250×4.6 mm, 5 μm). As the mobile phase, 0.1 N acetic acid–methanol (10:1) mixture was used (Yang et al., 2001). The mobile phase was subjected to degassing for 10 minutes in order to remove bubbles within the mixture. Fow rate was adjusted to 1.2 mL/minute and running time was 10 minutes. Analysis were performed at 30 °C (Surwase et al., 2012). Injection volume was 20 μL. Standard L-DOPA (0.01–1.5 mg/ mL) and L-tyrosine (0.02–1.0 mg/mL) were prepared in HPLC-grade water. Cell-free supernatants were used for analysis. Before injection the samples were filtered with sterile 0.45 μm filters. The retention time obtained was ~ 2.7 min for the standard L-DOPA and ~ 3.5 min for the standard L-tyrosine.

2.2.7 DNS method for quantification of reducing sugars

5 g of DNS was dissolved in 100 mL of 2 M NaOH solution. 150 g of potassium-sodium tartrate was added and mixed overnight. The final volume was adjusted to 500 mL with distilled water (Harisha, 2007). 500 μL of a sample was mixed with 3 mL of DNS reagent and boiled for 10 minutes. The reaction was stopped by incubation of the reaction mixture on ice for 5 minutes. OD_{540} values of the samples were recorded and the sugar concentration was calculated from the standard curve given in Appendix D.

2.2.8 Genome-wide analysis of L-tyrosine overproducer *C. glutamicum* ATCC 21573

A single colony from a fresh plate was inoculated into 10 mL of BHI and incubated overnight. The preculture was used to isolate the genomic DNA using NucleoSpin Microbial DNA Mini according to the manufacturer's instructions.

Illumina library preparation & MiSeq sequencing and assembly was performed at Bielefeld

University, CEBITEC, by Dr. Daniel Wibberg as explained in Wibberg et al. (Wibberg et al., 2016). The genome comparison of *C. glutamicum* wild-type and *C. glutamicum* OP was performed using Mauve alignment program (Darling et al., 2004) with default settings.

3. RESULTS

3.1. Development of a method for HPLC detection of L-DOPA and L-tyrosine

This thesis aims to produce L-DOPA from L-Tyrosine using the tyrosinase enzyme. Therefore, initial effort was directed to development of an analytical technique to detect and quantify these two molecules using HPLC. To this end, different conditions compiled from literature have been evaluated.

The first mobile phase tested was methanol (Surwase et al., 2012). When this mobile phase was used with measurement at 280 nm, a single peak could not be obtained for L-DOPA (Figure 3.4).

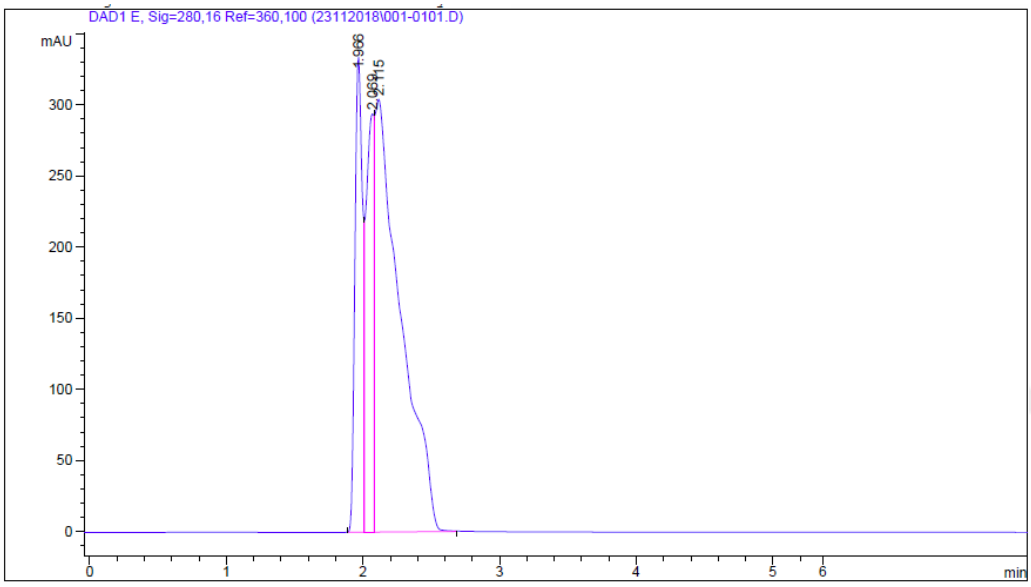

Figure 3.1: L-DOPA elution with methanol as the mobile phase.

The second mobile phase tested was methanol: 0.5% acetic acid (70:30) (V. Singh et al., 2017). Under this condition, measurements were taken at 210, 280 and 284 nm. Although chromatograms showed significant improvement with this mobile phase in both L-DOPA and L-tyrosine peaks (Figures 3.5-3.8), retention times of these two amino acids were too close to make quantitative measurements. Retention time was 2.09 for L-DOPA, while it was 2.10 for L-tyrosine. Thus, it was not possible to separate the mixture of these two amino acids under these conditions.

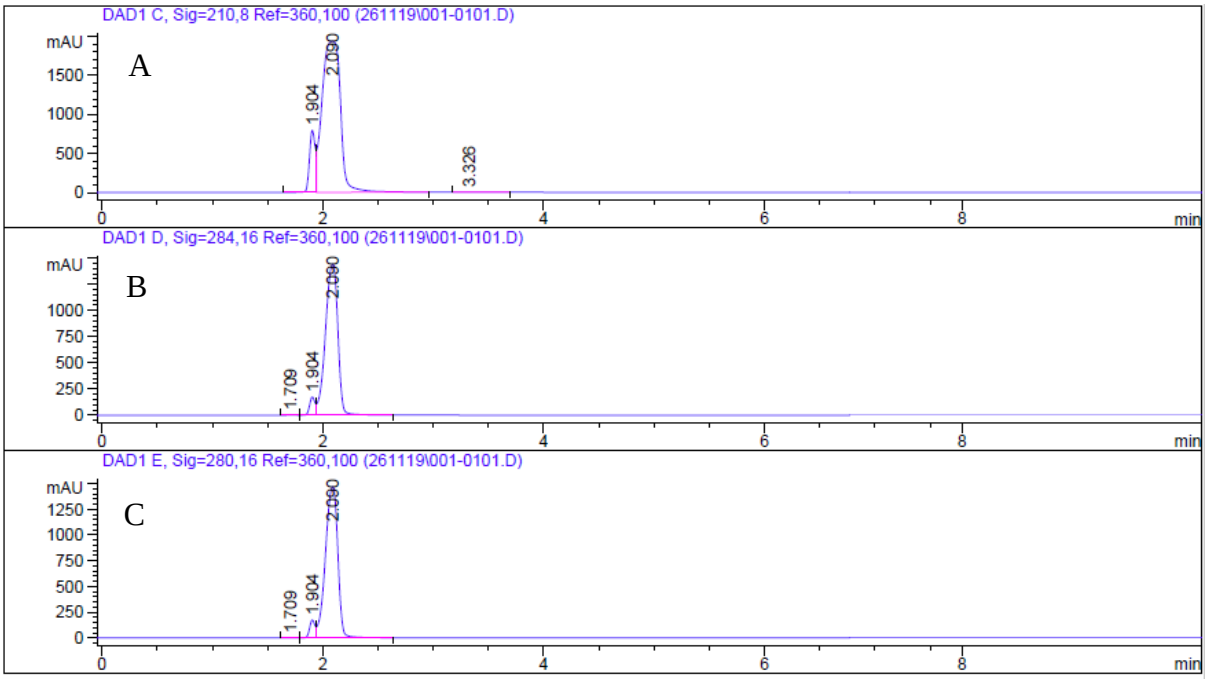

Figure 3.2: L-DOPA elution with methanol: 0.5% acetic acid (70:30) mobile phase. A) 210 nm, B) 284 nm, and C) 280 nm.

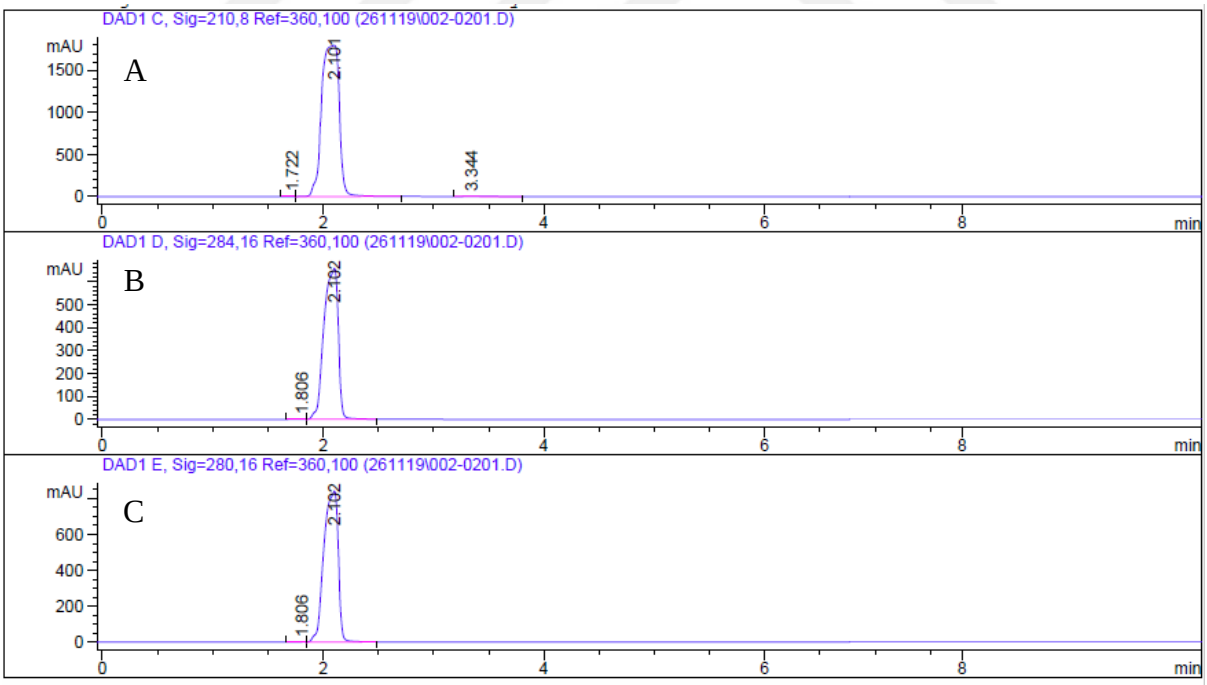

Figure 3.3: L-tyrosine elution with methanol: 0.5% acetic acid (70:30) as mobile phase. A) 210 nm, B) 284 nm, and C) 280 nm.

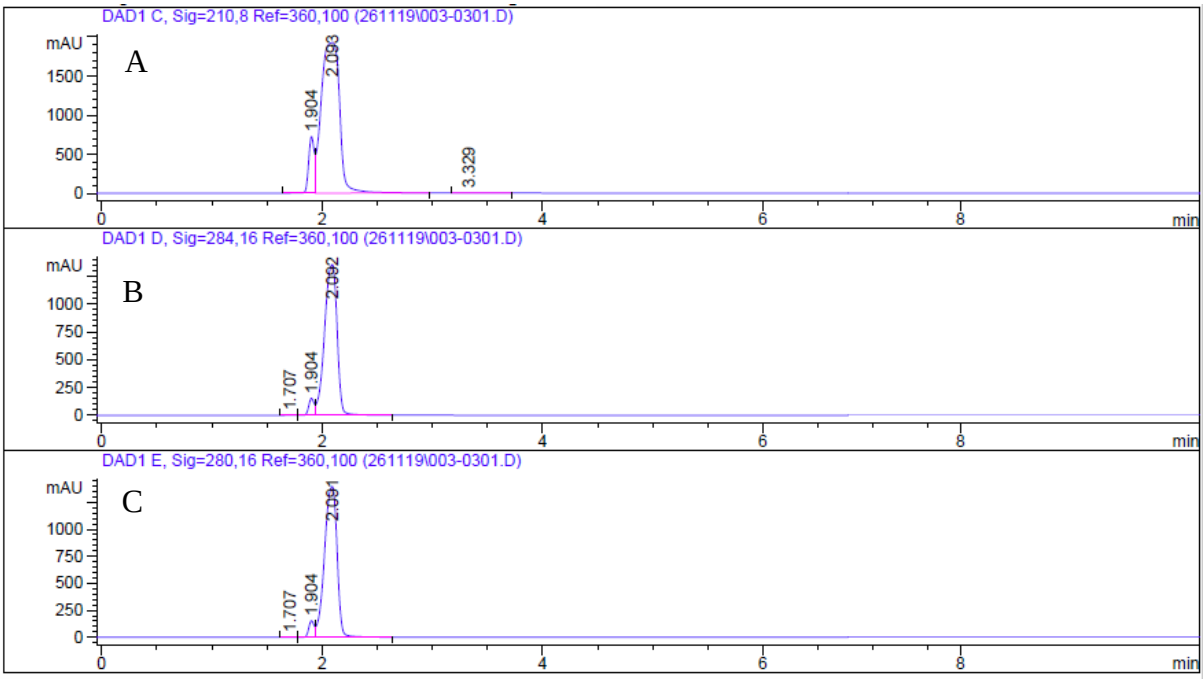

Figure 3.4: L-DOPA:L-tyrosine mixture elution (9:1) with methanol:0.5% acetic acid (70:30) as mobile phase. A) 210 nm, B) 284 nm, and C) 280 nm.

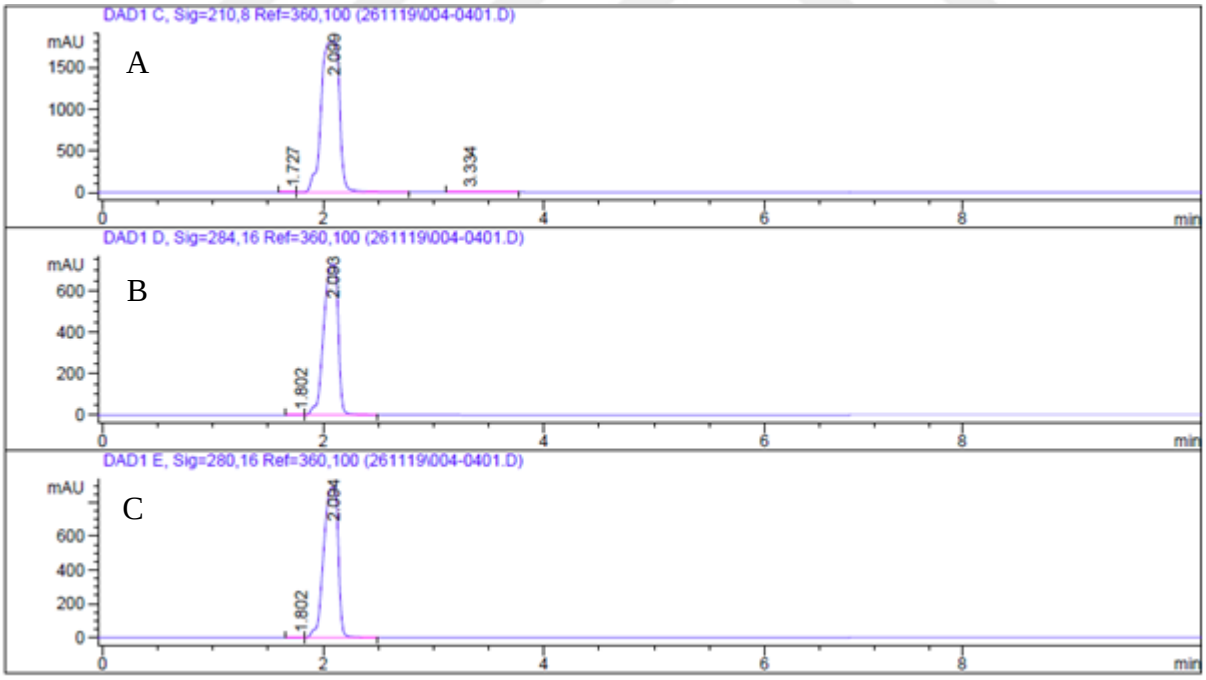

Figure 3.5: L-DOPA:L-tyrosine mixture elution (1:9) with methanol:0.5% acetic acid (70:30) as mobile phase. A) 210 nm, B) 284 nm, and C) 280 nm.

To further improve separation and detection by HPLC, methanol:0.1N acetic acid (1:10) was used as the mobile phase (Yang et al., 2001). Again under this condition, measurements were taken at 210, 280 and 284 nm. With this mobile phase, separation of L-DOPA and L-tyrosine improved significantly with retention different enough to enable quantification. The retention times obtained were 2.700 for L-DOPA and 3.297 for L-tyrosine (Figure 3.9 and Figure 3.10). Additionally, when different mixtures of these two molecules were analyzed using this same mobile phase, it was possible to get two distinct peaks for L-DOPA and L-tyrosine (Figure 3.11 and Figure 3.12).

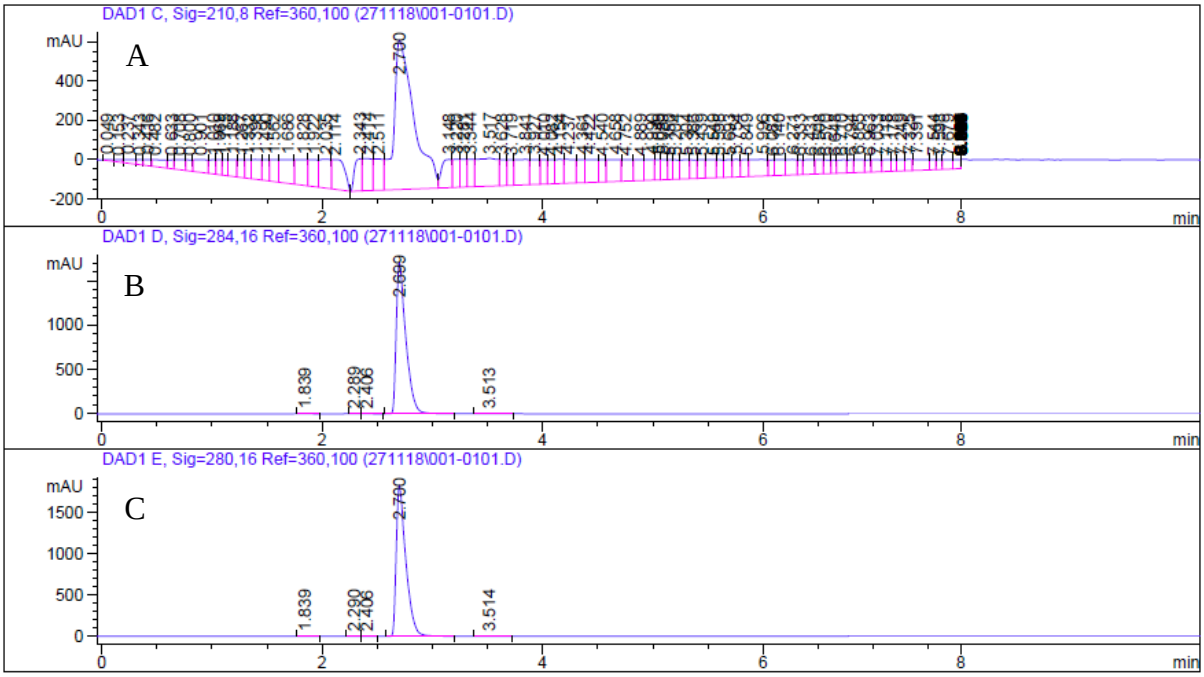

Figure 3.6: L-DOPA elution with methanol:0.1 N acetic acid (1:10) as the mobile phase. A) 210 nm, B) 284 nm, and C) 280 nm.

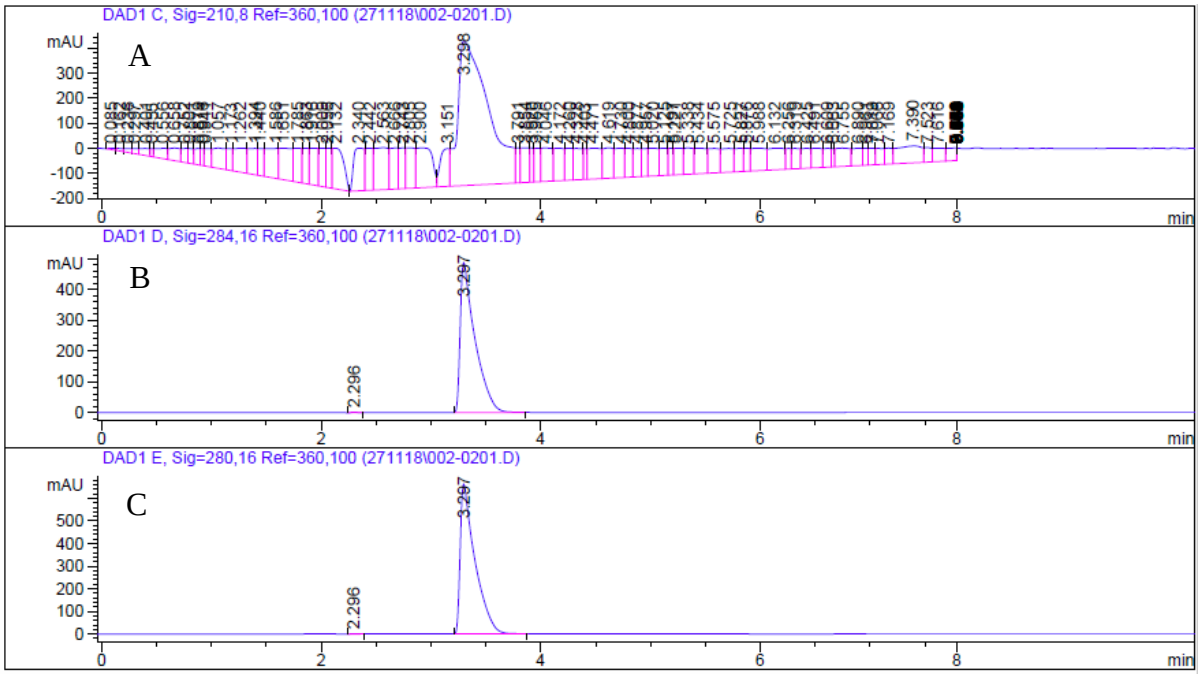

Figure 3.7: L-tyrosine elution with methanol:0.1 N acetic acid (1:10) as the mobile phase. A) 210 nm, B) 284 nm, and C) 280 nm.

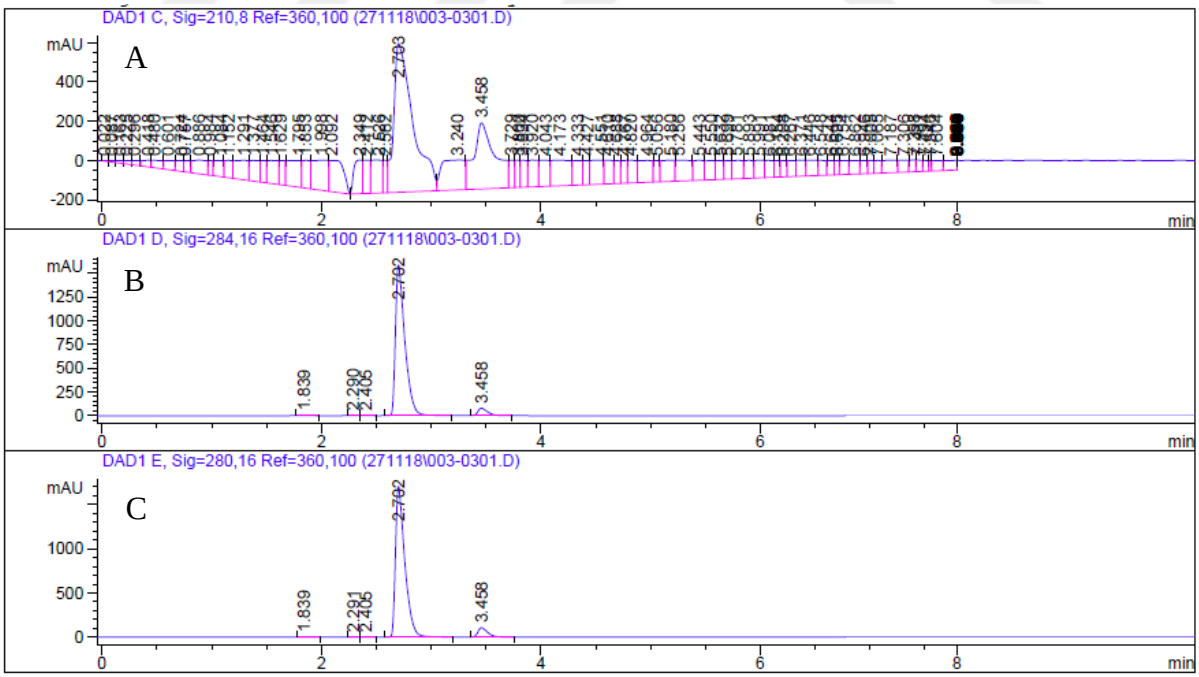

Figure 3.8: L-DOPA:L-tyrosine mixture elution (9:1) with methanol:0.1 N acetic acid (1:10) as the mobile phase. A) 210 nm, B) 284 nm, and C) 280 nm.

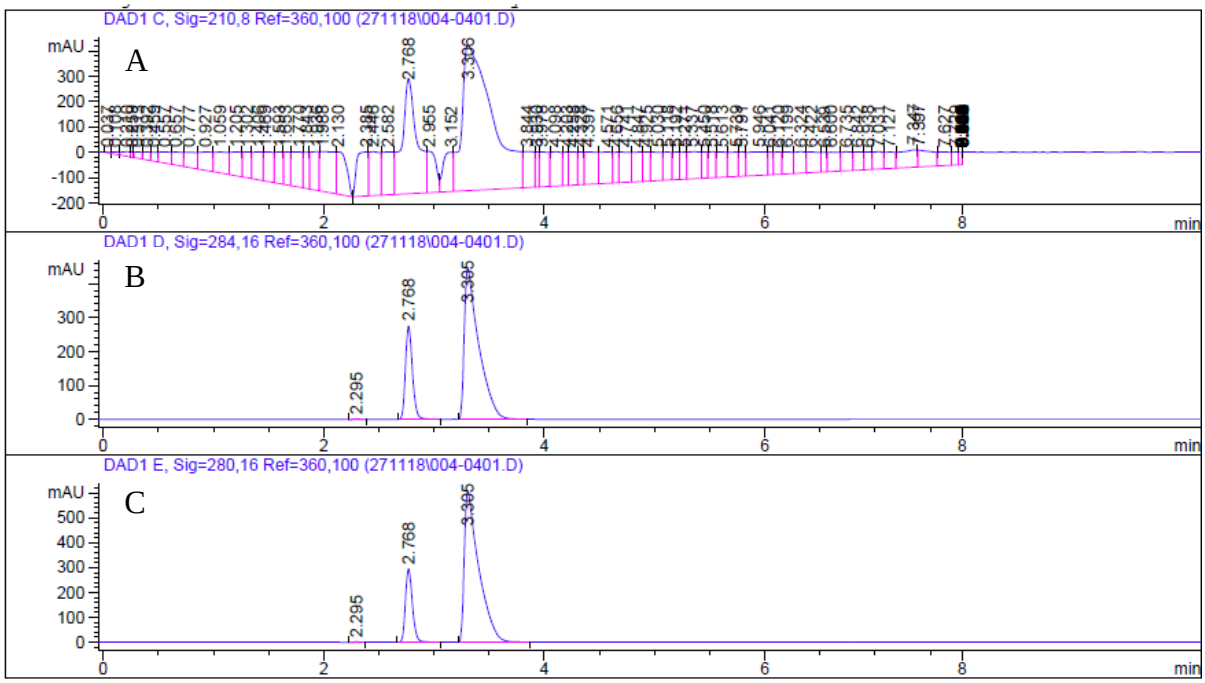

Figure 3.9: L-DOPA:L-tyrosine mixture elution (1:9) with methanol:0.1 N acetic acid (1:10) as the mobile phase. A) 210 nm, B) 284 nm, and C) 280 nm.

With these results, methanol:0.1 N acetic acid (1:10) was selected as the mobile phase and 280 nm as the detection wavelength.

3.2. The cloning of *Ralstonia solanacearum* tyrosinase gene (tyr_{Rs}) into pEKEx2 plasmid

The manually codon optimized tyrosinase gene delivered on pUC57 plasmid by GenScript was transformed and stored in *E. coli* TOP10 for further work. The sequences of the gene and the codon preference chart are provided in Appendix A. The tyrosinase gene of 1491 bp was amplified by polymerase chain reaction (PCR) using pUC57-tyr_{Rs} as the DNA template. The amplified gene is given in Figure 3.1.

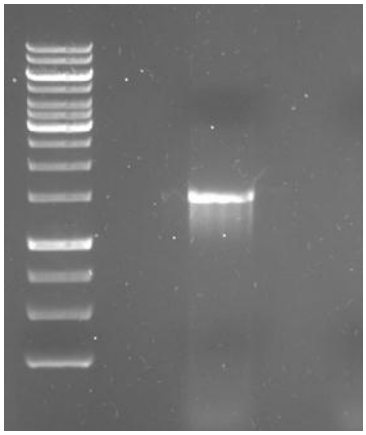

Figure 3.10: Tyrosinase gene on the agarose gel. Gene ruler: Thermo Fisher 1 Kb**.**

This PCR product and the pEKEx2 plasmid were both double-digested with PstI and XhoI enzymes and then they were ligated to obtain the tyrosinase expressing plasmid, as described in section 2.2.1. The ligation mixture was transformed into *E. coli* TOP10 cells and formed colonies were screened for the tyrosinase gene. To this end, plasmids isolated from colonies formed were digested with the PstI restriction enzyme and analyzed on agarose gels. The results obtained from 6 colonies are seen in Figure 3.2.

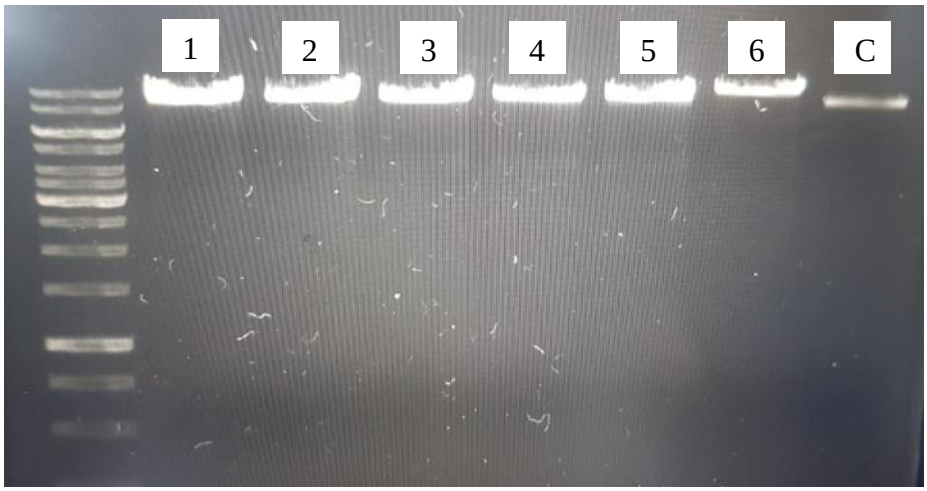

Figure 3.11: The agarose gel image of PstI-digested ligation products (1st to 6th) and (C) empty pEKEx2 plasmid. Gene ruler: Thermo Fisher 1 Kb.

Among the plasmids obtained from 6 different colonies, only the plasmids isolated from colony number 6 had a size slightly greater than the size of the control plasmid, pEKEx2. This indicated the presence of the tyrosinase gene. In order to confirm this, PCR was performed using the isolated plasmids from colonies 4, 5, and 6 as templates. The obtained results are presented in Figure 3.3. The tyrosinase gene was amplified only in the PCR containing the plasmid obtained from colony 6. This gene was sequenced for further confirmation. The obtained plasmids was named as pEKEx2-*tyr*$_{Rs}$.

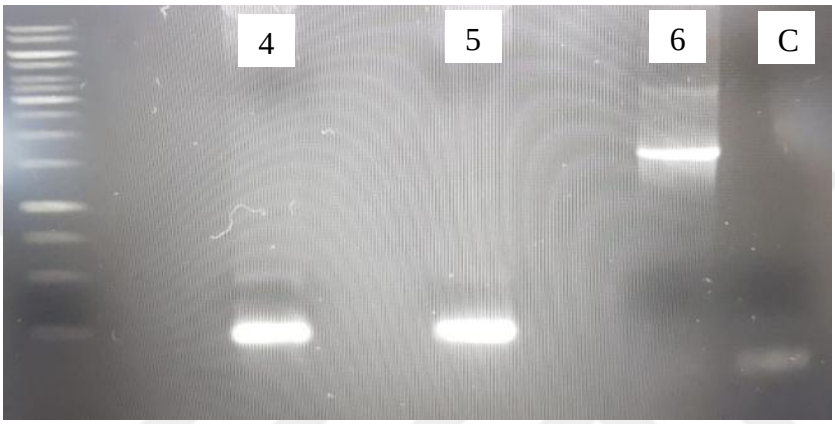

Figure 3.12: The products of PCR reaction with plasmids from colonies 4, 5, and 6. In the last line negative control from the reaction is seen. Gene ruler: Thermo Fisher 1 Kb.

For L-DOPA production, this plasmid was transformed to *C. glutamicum* via electroporation, as explained in 2.2.3.5 section.

3.3. Tyrosinase expression and L-DOPA detection

The pEKEx2-*tyr*$_{Rs}$ harboring cells, namely CgEKV-I, were grown for 24 hours for L-DOPA production w/o IPTG. The obtained fermentation broth and supernatants are shown in Figure 3.13. The culture containing the cells induced for tyrosinase production were dark while culture with cells without IPTG induction were light. This dark color was primarily from the supernatants, as seem in 3.13B.

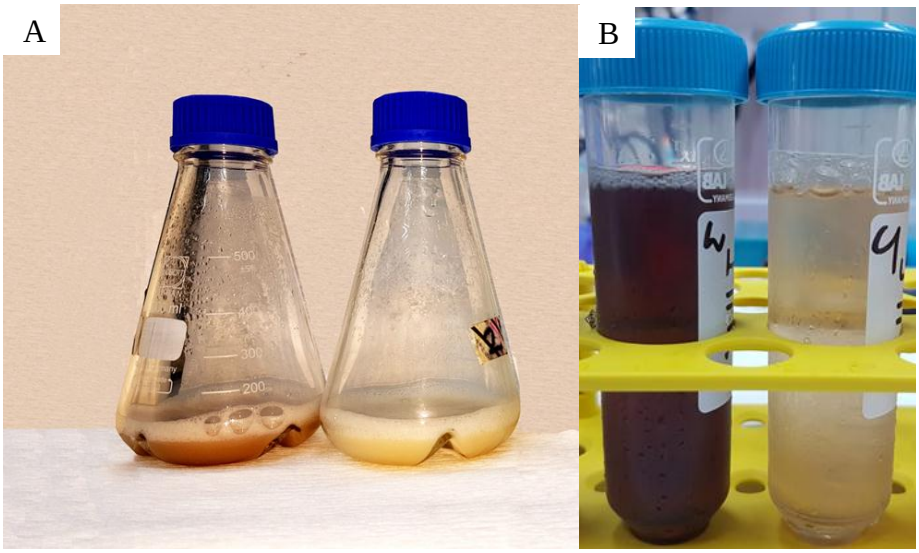

Figure 3.13: A) IPTG-induced (left flask) and uninduced CgEKV-I cells (right flask) and B) supernatants of IPTG-induced (left falcon) and uninduced CgEKV-I cells (right falcon).

Additionally, it was possible to detect the activity of the tyrosinase by the precipitation of dark pellets, presumably melanin, the oxidation product of L-DOPA (Figure 3.14B).

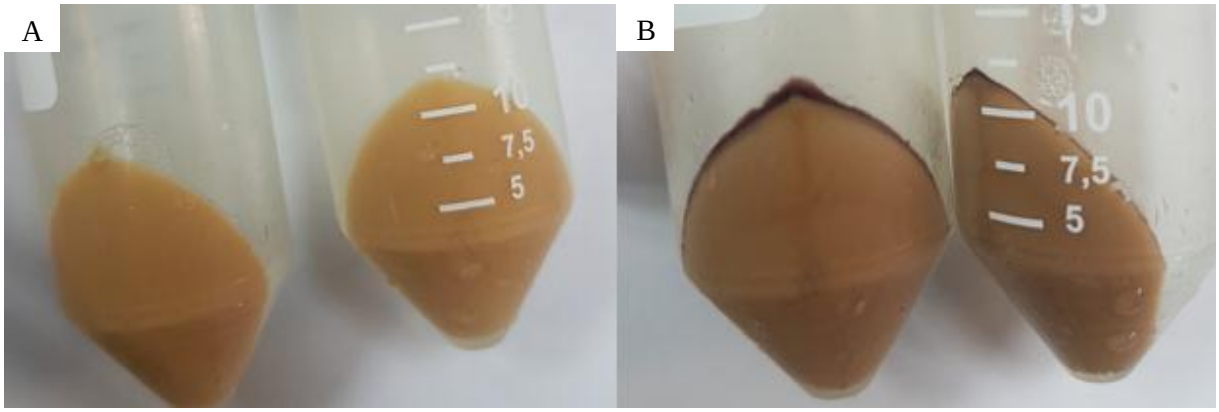

Figure 3.14: Harvested CgEKV-I cells A) uninduced and B) IPTG-induced.

Supernatants from the cultures (Figure 3.13B) were used for L-DOPA detection with Arnow's test and the results are shown in Figure 3.15. The standard curve used in Arnow's test for L-DOPA detection is given in Appendix B.

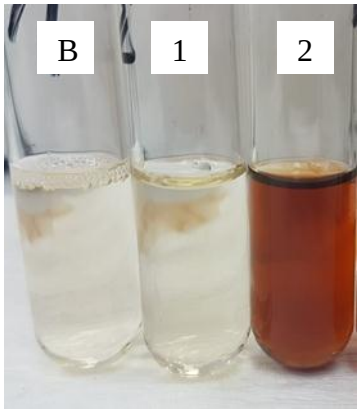

Figure 3.15: The results of Arnow's test: B) blank, 1) sample from uninduced CgEKV-I strain. 2) sample from induced CgEKV-I strain.

After verification of the presence of L-DOPA with Arnow's test, same supernatant samples were analysed with HPLC. The obtained chromatograms are presented in Figures 3.16 and 3.17.

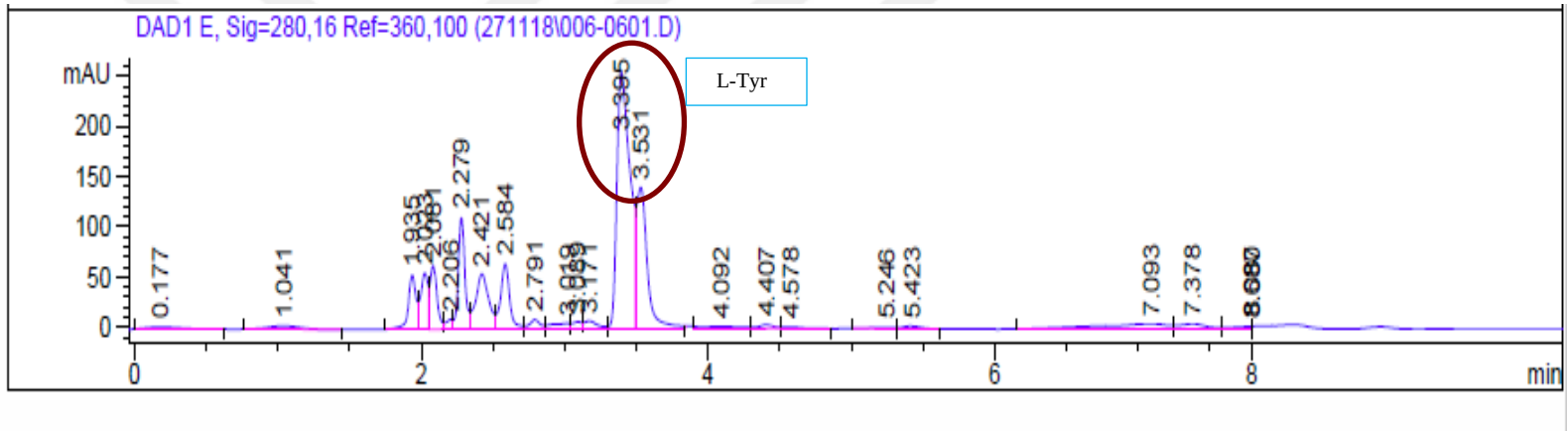

Figure 3.16: HPLC chromatogram of the sample from uninduced CgEKV-I strain.

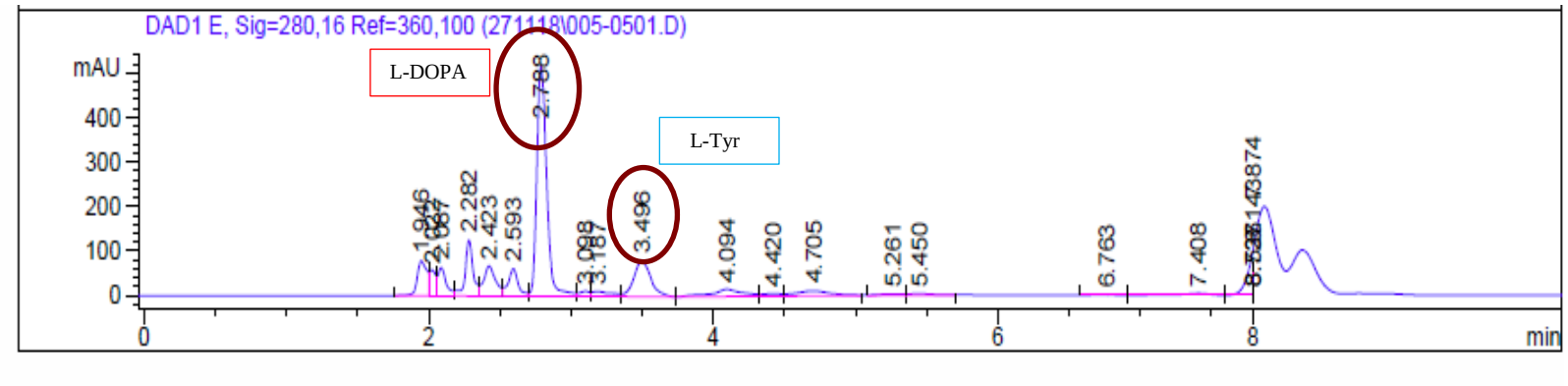

Figure 3.17: HPLC chromatogram of the sample from IPTG-induced CgEKV-I strain.

In Figure 3.16, it was seen that in the supernatant obtained from the uninduced sample, there was only the L-tyrosine peak (retention time of ~ 2.7 minutes) but there was no peak that corresponded to L-DOPA. On the other hand, in the supernatant obtained from the IPTG-induced sample, there was a peak that corresponded to L-tyrosine (retention time of 3.496 minutes) and there was a peak that corresponded to L-DOPA (retention time of 3.496 minutes) (Figure 3.17).

3.4. The effect of copper ions on bacterial growth

Copper is a cofactor that is required for the activity of the *R. solanacearum* tyrosinase. Unfortunately, copper is a heavy metal, therefore it may have unfavorable effects on bacterial growth during fermentative L-DOPA production. To this end, CgEKV-I cells were grown in the presence of different copper ion concentrations to find the optimal copper ion concentration. While lower concentrations (0.2 and 0.4 mM) had no adverse effect on growth, the presence of 0.8 mM significantly retarded growth. With 1.2 mM copper growth was almost completely inhibited (Figure 3.18A).

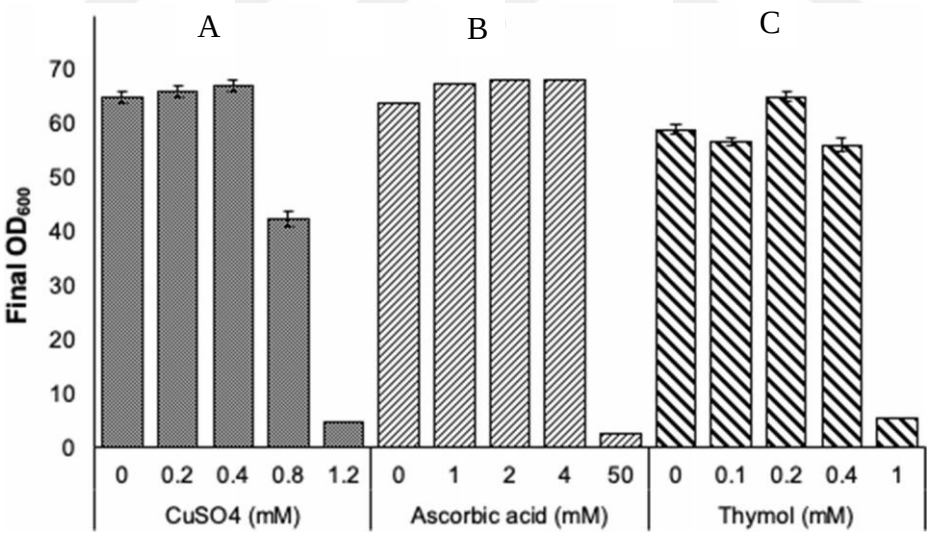

Figure 3.18: The effect of: copper ions, ascorbic acid, and thymol on the final OD_{600} of CgEKV-I cells.

3.5. The effect of L-DOPA antioxidants on bacterial growth

L-DOPA is readily oxidized in the presence of excess oxygen. In order to prevent L-DOPA oxidation, thus the loss in its concentration, two different antioxidants were evaluated in this

study. One of these antioxidants was the most commonly used ascorbic acid and the other one was thymol, which was only *in silico*-tested.

When CgEKV-I cells were grown in presence of low concentrations of ascorbic acid (1, 2 and 4 mM), no significant adverse effect on bacterial growth was observed. However, when the concentration was increased to 50 mM, this inhibited the growth completely, as seen in Figure 3.18B.

The second tested antioxidant was thymol which was dissolved in DMSO. Therefore, control cells were treated with an equal amount of DMSO. The highest tested DMSO concentration in this work was 1 %, which had no negative effect on the growth. Therefore, final concentration of DMSO in cultures supplemented with thymol were kept below this value. With low thymol concentrations (0.1, 0.2, and 0.4 mM) there was no negative effect on bacterial growth. When thymol concentration was raised to 1 mM, growth was retarded significantly (Figure 3.18C).

3.6. L-DOPA production from commercial sugars glucose and xylose

3.6.1 The effect of copper ions on L-DOPA production

As expected, there was no detectable L-DOPA production in the absence of the copper ions. To this end, copper ion concentration was gradually increased in order to find its optimal amount for production. Maximum L-DOPA titer was detected with 0.4 mM copper ions (0.036 ± 0.002 g/L L-DOPA). The titer with 0.2 mM copper ions was approximately 60 % lower than that obtained with 0.4 mM. Since the higher copper ion concentrations (0.8 and 1.2 mM) inhibited growth therefore decreased L-DOPA synthesis, 0.4 mM copper ions was selected as the optimal concentration for further experiments.

3.6.2 The effect of ascorbic acid on L-DOPA production

The presence of low concentrations of ascorbic acid e.g. 0.1, 1, 2, and 4 mM had no impact on L-DOPA titers. On the other hand, high concentrations, such as 50 mM, completely inhibited bacterial growth; thus prevented L-DOPA production. To this end, the concentration of ascorbic acid was not further optimized for fermentative L-DOPA production.

3.6.3 The effect of thymol on L-DOPA production

The results obtained for fermentative L-DOPA production with CgEKV-I and CgEKV-II grown on glucose and glucose/xylose respectively, are presented in Figure 3.19 and summarized in Table 3.1. All cultures were supplemented with 0.4 mM copper ions. When CgEKV-I strain was grown on glucose with the addition of 0.1 mM thymol, no change in L-DOPA titer was observed. As the thymol concentration was increased to 0.2 and 0.4 mM, L-DOPA titer increased 2 and 3.7-fold, respectively, when compared to the condition without thymol supplement. No L-DOPA accumulated with 0.6 mM thymol and 1 mM thymol completely inhibited growth thus there was no L-DOPA synthesis (Table 3.1).

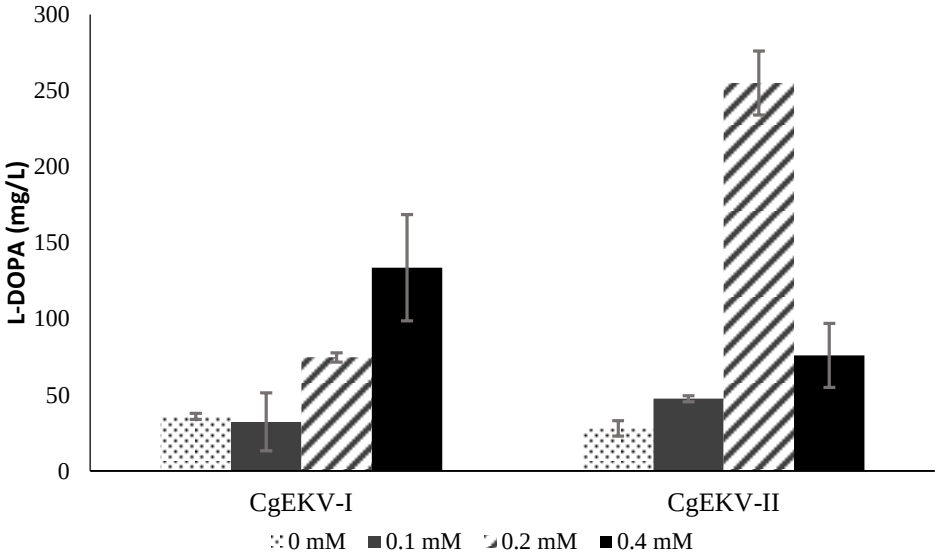

Figure 3.19: L-DOPA titers obtained with CgEKV-I and CgEKV-II strains with different thymol concentrations.

When the CgEKV-II strain was grown on a glucose/xylose mixture of 3:1 ratio, the addition of 0.1 mM thymol led to 1.7-fold increase in L-DOPA titer. With 0.2 mM thymol the titer increased almost 9-fold leading to 0.255 ± 0.020 g/L L-DOPA (Table 3.1). This was the highest titer under the tested conditions. Further increase in thymol concentration to 0.4 mM led to decreased titer, even though growth of CgEKV-II was not affected.

Table 3.1: L-DOPA production during microbial growth. G stands for glucose, and X for xylose.

Strain	C-sourse	Thymol (mM)	Titer ($g \cdot L^{-1}$)
CgEKV-I	4% G	0	0.036 ± 0.002

Strain	C-sourse	Thymol (mM)	Titer ($g \cdot L^{-1}$)
	4% G	0.1	0.032 ± 0.019
	4% G	0.2	0.074 ± 0.030
	4% G	0.4	0.133 ± 0.035
CgEKV-II	4% G	0	0.035 ± 0.004
	3% G + 1% X	0	0.028 ± 0.005
	3% G + 1% X	0.1	0.047 ± 0.002
	3% G + 1% X	0.2	0.255 ± 0.020
	3% G + 1% X	0.4	0.076 ± 0.021
	2% G + 2% X	0	< 0.004
	1% G + 3% X	0	< 0.004

3.7. L-DOPA production via whole-cell biotransformation

The CgEKV-I cells used for fermentative L-DOPA production were re-used for whole-cell biotransformation of L-tyrosine to L-DOPA (Figure 3.20). The effect of 0.4 mM copper ions, different ascorbic acid and thymol concentrations on L-DOPA were evaluated. Additionally, the effect of different cell concentrations was also evaluated as well.

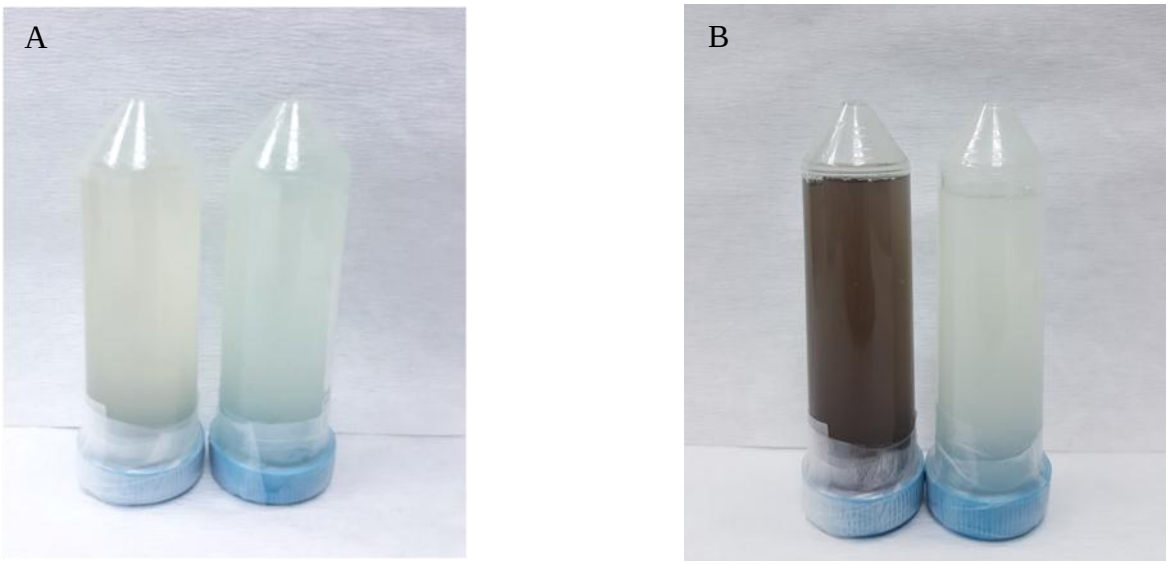

Figure 3.20: The whole-cell biotransformation samples with induced (left falcon) and uninduced (right falcon) CgEKV-I cells: A) at the start of whole-cell catalysis, and B) after 48 hours of incubation.

The effect of cell amount was tested by adding 25-50-100 µL of resuspended cells (equivalent to 3.3-6.6-13.2 mg DCW, respectively) to the reactions. With 25 µL and 100 µL cells, L-DOPA titer slightly lower. Therefore, in further whole-cell biotransformation reactions, 50 µL resuspended cells (6.6 mg DCW) were used.

Obtained results with different ascorbic acid, thymol, and copper ions concentrations, are summarized in Figure 3.21 and Table 3.2.

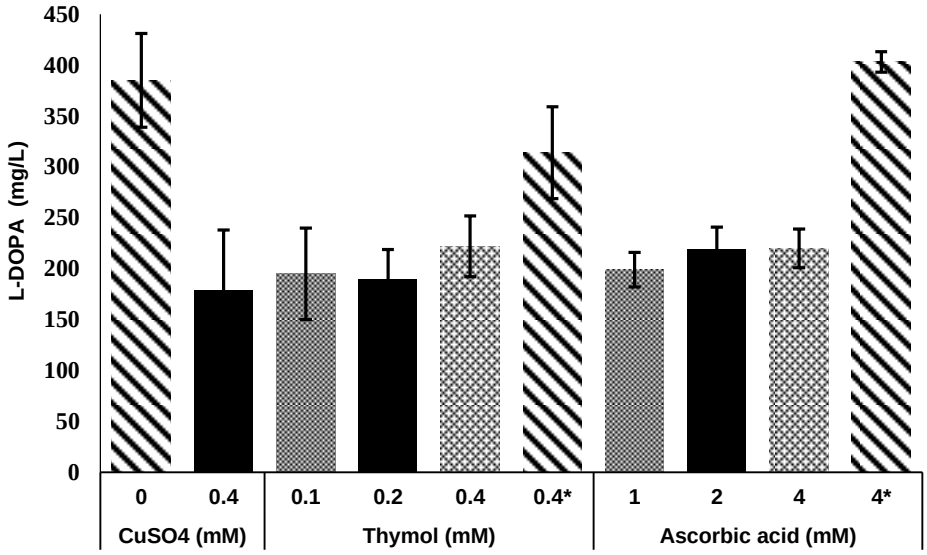

Figure 3.21: L-DOPA titers obtained via whole-cell biotransformation.

Table 3.2: Summary of whole-cell biotransformation to L-DOPA using CgEKV-I cells.

$CuSO_4$ (mM)	Thymol (mM)	Ascorbic acid (mM)	Titer (g/L)	g/gDCW*
0	0	0	0.39 ± 0.05	0.58 ± 0.07
0.4	0	0	0.18 ± 0.06	0.27 ± 0.09
0.4	0.1	0	0.20 ± 0.05	0.30 ± 0.07
0.4	0.2	0	0.19 ± 0.03	0.29 ± 0.05
0.4	0.4	0	0.22 ± 0.03	0.34 ± 0.03
0	0.4	0	0.31 ± 0.05	0.48 ± 0.07
0.4	0	1	0.20 ± 0.02	0.30 ± 0.03
0.4	0	2	0.22 ± 0.02	0.33 ± 0.04
0.4	0	4	0.22 ± 0.02	0.33 ± 0.05
0	0	4	0.40 ± 0.01	0.61 ± 0.02

* Per liter of L-tyrosine solution containing 0.66 mg DCW/mL CgEKV-I. 26.4 g DCW was obtained from 1 liter of cultivation using CGXII defined medium with glucose as carbon source.

In the samples without antioxidants, the formation of L-DOPA oxidation product, presumably melanine, was clearly visible (Figure 3.20B, left falcon). HPLC chromatograms of the supernatant form the reaction mixture at time zero and after 48 hours of incubation are seen in Figure 3.22. A clear decrease in L-tyrosine concentration can be observed with the concomitant increase in L-DOPA concentration following whole-cell biotransformation.

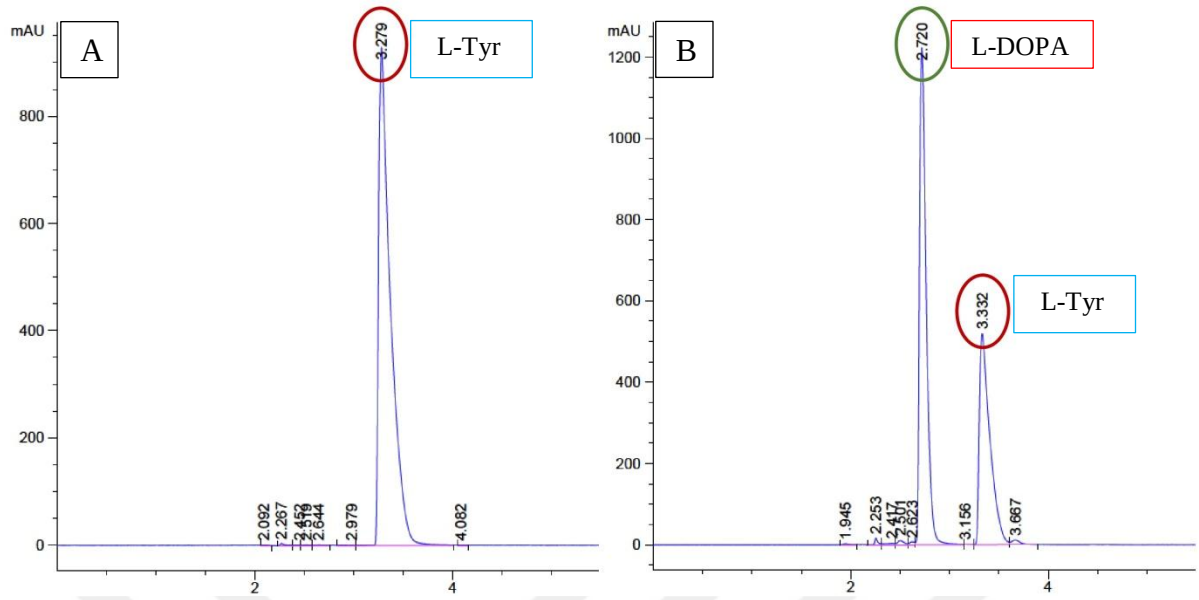

Figure 3.22: HPLC chromatograms of samples A) at the start of whole-cell biotransformation and B) after 48 hours of incubation.

The presence of additional copper ions in the reaction mixture somehow reduced L-DOPA titer to approximately half of that obtained without copper ions (Table 3.2), presumably by further increasing the activity of the tyrosinase thus converting L-DOPA to subsequent compounds e.g. dopachrome and dopaquinone. The addition of antioxidants to the mixture has not improved L-DOPA titer, however the final color of mixtures in the presence of antioxidants was light brown/transparent indicating reduced L-DOPA oxidation.

In the absence of copper ions, L-DOPA titer was 0.31 ± 0.05 g/L with 0.4 mM thymol and was 0.40 ± 0.01 g/L with 4 mM ascorbic acid. The later was the highest L-DOPA titer under the reaction conditions tested, which corresponded to 0.61 ± 0.02 g/gDCW.

The titer obtained with ascorbic acid was similar to that obtained in its absence but the major difference is the color of the resulting reaction mixtures; in its absence reaction mixtures were dark brown/black while in its presence light brown/transparent, i.e. it prevented the formation of dopachrome and dopaquinone and their subsequent non-enzymatic conversion to melanin through further oxidation.

3.8. L-DOPA production from hazelnut husk

3.8.1 *C. glutamicum* growth on hazelnut husk

In this part of the work, *C. glutamicum* strains with and without xylose utilization genes were tested for their ability to grow on husk as the sole carbon source. Cell growth with husk hydrolysate is shown in Figure 3.23.

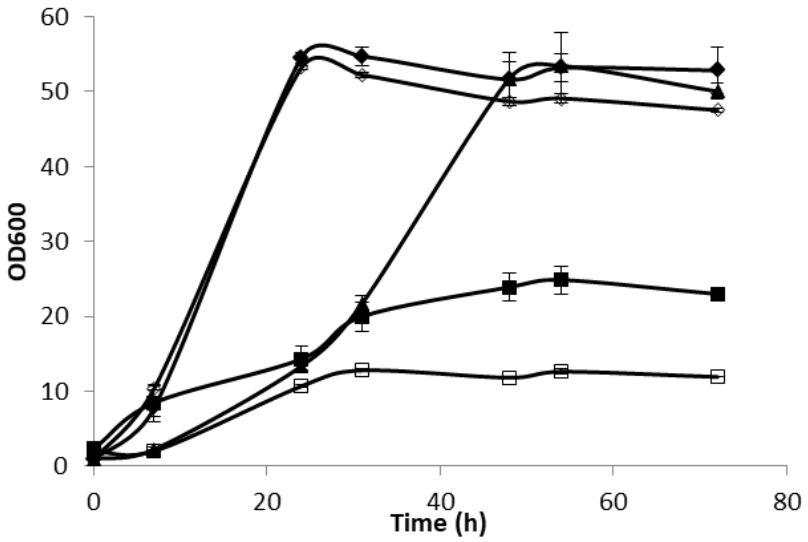

Figure 3.23: Bacterial growth on glucose, xylose, and husk. *C. glutamicum* wild-type on glucose (empty diamonds), *C. glutamicum* wild-type on husk (empty squares), CgX on glucose (black diamonds), CgX on xylose (black triangles), CgX on husk (black squares).

In this section, it was shown that CgX strain can grow on CGXII medium with pretreated hazelnut husk as the sole carbon source, and that presence of xylose genes, improved the growth as seen in Figure 3.23. However, with glucose, the most preferred carbon source, growth started amost immediately and the cells reached stationary phase in approximately 24 hours. However, with xylose as the sole carbon source, growth was somewhat slower in the fisrt 24 hours and exponential growth started rather late. Stationary phase was reached after 48 hours. The amount of xylose was expected to be higher than that of glucose in the husk hydrolysate. In line with this information, growth continued for about 48 hours with this hydrolysate.

3.8.2 Fermentative L-DOPA production from hazelnut husk

The conditions found to be optimal for L-DOPA production on glucose/xylose mixture, e.g. 0.4 mM copper ions and 0.2 mM thymol, were used when hazelnut husk was used as the sole carbon source. In the first 24 hours of fermentation no L-DOPA accumulated in cell-free supernatants. With incubation for 48 hours, the final OD_{600} reached 11 ± 1 and while L-DOPA titer was 0.017 ± 0.001 g/L. Incubation for 72 hours led to final OD_{600} of 23 ± 1 and L-DOPA titer of 0.020 ± 0.001 g/L. Incubation for 120 hours improved growth only slightly, however there was no further improvement in L-DOPA titer. As presented above, for the production of 0.020 ± 0.001 g/L of L-DOPA 210 g of hazelnut husk must be used.

3.8.3 L- DOPA production via whole-cell biotransformation with cells grown on husk hydrolysate

CgEKV-II strain was grown on husk as the sole carbon source, and used to transform L-tyrosine to L-DOPA. Since copper ions in combination with husk as the carbon source slowed the growth of CgEKV-II down, copper was not added when the cells were grown for biotransformation. The final OD_{600} of the cells grown on husk in absence of copper ions was 17 ± 0.12 after 48h incubation.

For whole-cell biotransformation reactions with cells obtained from glucose, the optimum amounts of resuspended cells and ascorbic acid was 50 µL (6.6mg DCW) and 4 mM respectively. However, when CgEKV-II cells were grown on CGXII medium with husk as the carbon source, the final amount of obtained cells was much lower than that obtained when grown on glucose. To this end, different amounts of resuspended cells (2-4-16-24mg DCW) were tested for their effect on L-DOPA titer and yield. Results obtained are summarized in Table 3.3. Figure 3.24. presents the effect of copper ions on L-DOPA titer during 144 hours.

Table 3.3: Summary of whole-cell biotransformation with cells grown on husk. All samples were supplemented with 4 mM ascorbic acid.

Time (h)	DCW (mg)	Cu^+ (mM)	L-DOPA (mg/L)	Yield (g L-DOPA/g DCW)
72				
	2	0.4	82±1	0.42±0.01
	2	0	31±1	0.17±0.01
	4	0	25±0	0.06

Time (h)	DCW (mg)	Cu^{+} (mM)	L-DOPA (mg/L)	Yield (g L-DOPA/g DCW)
	16	0	67±1	0.04
	24	0	107±3	0.04
96				
	2	0.4	97±1	0.49±0.01
	2	0	56±1	0.29
	4	0	43±0	0.11
	16	0	97±1	0.06±0.01
	24	0	142±1	0.06±0.01
120				
	2	0.4	97±1	0.49±0.01
	2	0	77±0	0.39
	4	0	58±0	0.15
	16	0	115±4	0.07±0.02
	24	0	163±2	0.07±0.02
144				
	2	0.4	100±1	0.51±0.01
	2	0	98±2	0.49±0.01
	4	0	76±0	0.19
	16	0	135±4	0.08±0.02
	24	0	184±1	0.08±0.01

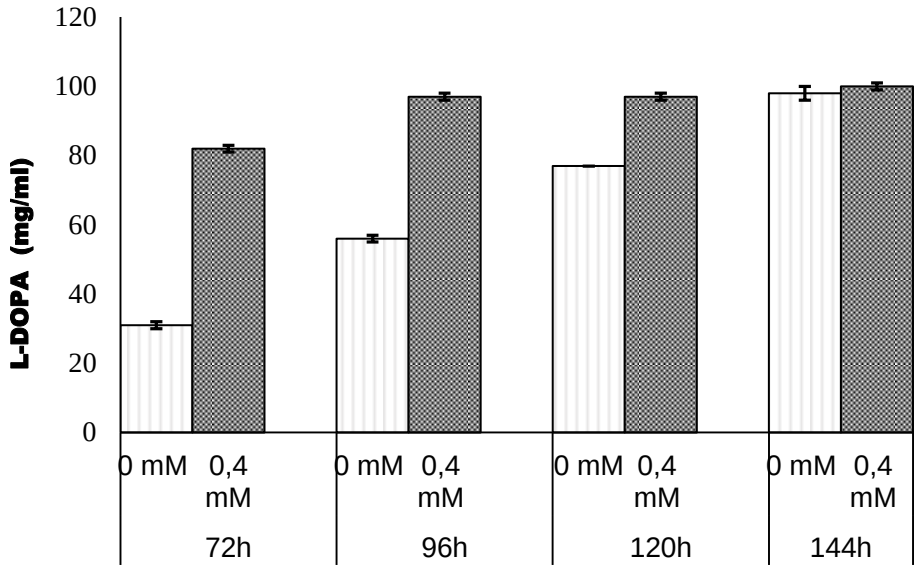

Figure 3.24: The summary of the copper ions effect on L-DOPA synthesis. In each reaction 2 mg of DCW was used.

Clearly, the time used for production of L-DOPA via whole-cell biotransformation also effected productivity of the process significantly. As an example, in the presence of copper ions, productivity was calculated as 1.14 mg/L·h after 72 hours, while it was 1.01 mg/L·h after 96 hours.

3.9. Metabolic engineering of *C. glutamicum* for L-tyrosine production

Tyrosinase based L-DOPA production relies on L-tyrosine. In the first part of the thesis, L-tyrosine was externally added for this production. Since this would increase cost of production, in the second part, an attempt was made to construct a rationally defined *C. glutamicum* L-tyrosine overproducer. As the parent strain a genome-reduced ARO02 strain (Walter et al., 2020) was selected. It was reported to be suitable for synthetic biology and industrial biotechnology applications. Furthermore, this strain contains the feedback-resistant form of 3-deoxy-D-arabinoheptulosonate 7-phosphate synthase from *E. coli*, along with inactivated vanilin dehydrogenase and lactate dehydrogenase genes, which disrupt carbon flow towards vanilin and lactate biosynthesis respectively. This would be expected to increase the available carbon for L-tyrosine synthesis.

For this attempt, the first the genes of shikimate pathway, the branching route from the shikimate pathway, the branched aromatic amino acid pathway, and the carbon uptake system, were targeted. For this, the following modifications were aimed:

1. Reducing the expression of genes leading to their synthesis, *pheA and pat,* and *trpE* respectively to decrease carbon flux towards L-phenylalanine and L-tryptophan,
2. Overexpression of genes in the shikimate pathway, *aroE* and *qsuC*, which encode shikimate dehydrogenase and 3-dehydroquinate dehydratase, respectively,
3. Deletion of gene cluster *qsuABD* to inactivate the pathway of shikimate degradation towards protocatechuate,
4. Inactivation of *ptsG* gene and overexpression of *iolT2* gene to channel glucose uptake to the non-PTS system,
5. Activate xylose utilization to assess the carbon source effect on L-tyrosine titer.
6. The missing aminotransferase *i*n the arogenate (pretyrosine) pathway of L-tyrosine biosynthesis predicted and its overexpression was evaluated.

The performed mutations are summarized in Figure 3.25.

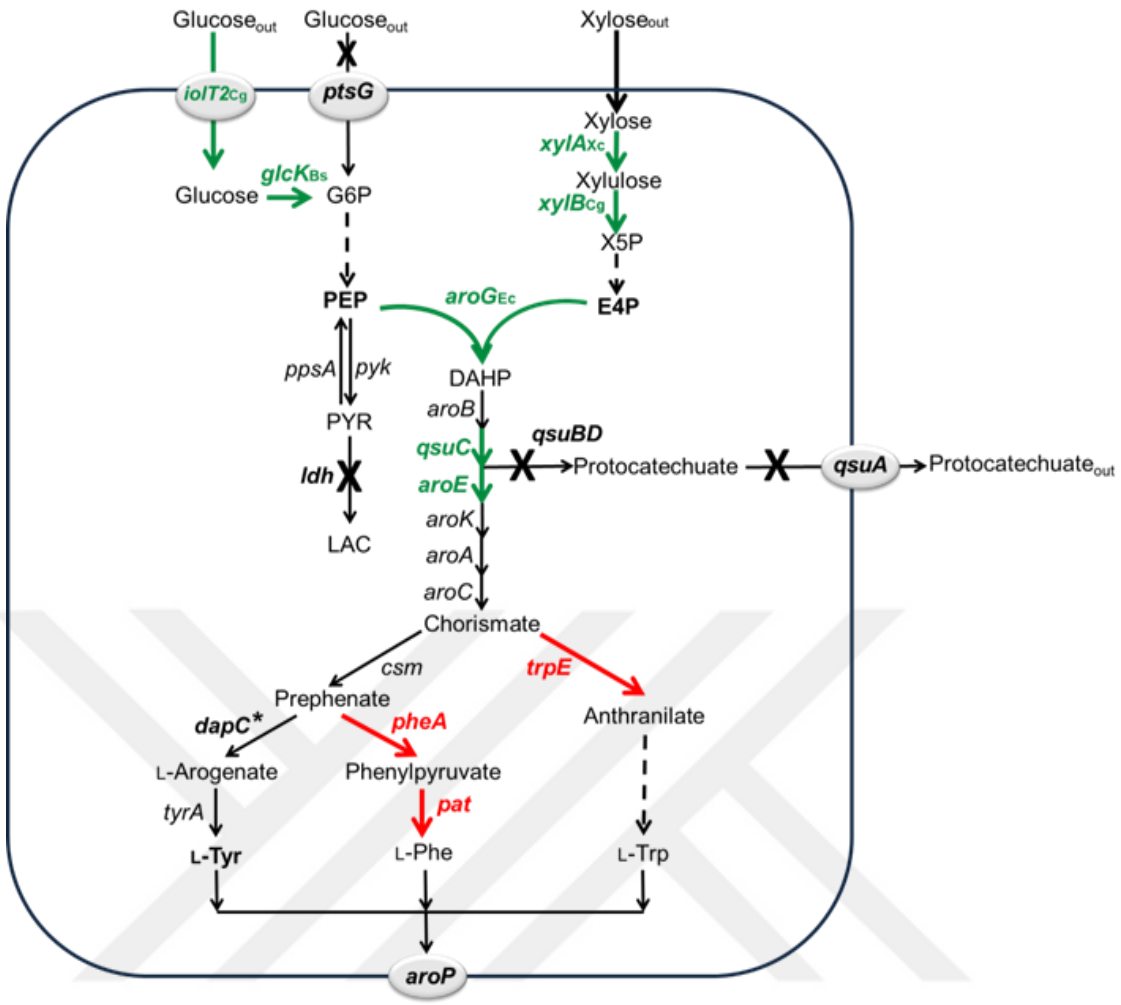

Figure 3.25: Schematic representation of L-tyrosine production. Green gene names and arrows represent chromosomal and plasmid overexpression, red gene names and arrows represent start codon replacement for reduced expression, **X** symbol on a pathway represent gene deletion, the gene with the asterisk has a predicted prephenate aminotransferase activity, and dashed arrows represent multiple reactions. *ptsG*: glucose-specific enzyme II component of PTS, *iolT2*$_{Cg}$: inositol transporter from *C. glutamicum*, *glcK*$_{Bs}$: glucose kinase from *Bacillus subtilis*, G6P: glucose-6-phosphate, PEP: phosphoenolpyruvate, *ppsA*: PEP synthase, *pyk*: pyruvate kinase, PYR: pyruvate, *ldh*: lactate dehydrogenase, LAC: lactate, *xylA*$_{Xc}$: xylose isomerase from *Xanthomonas campestris*, *xylB*$_{Cg}$: xylulokinase from *C. glutamicum*, X5P: xylulose-5-phosphate, E4P: erythrose 4-phosphate, *aroG*$_{Ec}$: 3-deoxy-7-phosphoheptulonate synthase from *Escherichia coli*, DAHP: 3-deoxy-7-phosphoheptulonate, *aroB*: 3-dehydroquinate synthase, *qsuC*: 3-dehydroquinate dehydratase, *qsuB*: 3-dehydroshikimate dehydratase, *qsuD*: shikimate dehydrogenase, *aroE*: shikimate dehydrogenase, *qsuA*: putative shikimate importer, *aroK*: shikimate kinase, *aroA*: 5-enolpyruvylshikimate-3-phosphate synthase, *aroC*: chorismate synthase, *trpE*: anthranilate synthase, L-Trp: L-tryptophan,

cg0975: chorismate mutase, *tyrA*: prephenate dehydrogenase, L-Tyr: L-tyrosine, *pheA*: prephenate dehydratase, *pat*: phenylalanine aminotransferase, L-Phe: L-phenylalanine, *aroP*: aromatic amino acid transporter.

The constructed strains and their properties are summarized in Table 2.1.

3.9.1 The effect of start codon exchanges on growth of constructed mutant strains

In order to construct a L-tyrosine overproducer, as the first module, the pathways downstream of chorismate were selected, so that the carbon flux was channeled primarily to towards L-tyrosine, rather than the other two aromatic amino acids.

To this end, the start codons of three genes leading to the biosynthesis of L-phenylalanine and L-tryptophan, *pheA and pat*, and *trpE* respectively, have been changed from ATG, which is the most preferred start codon leading to the highest gene expression, to the less preferred TTG codon, leading to the reduced gene expression. Since there was no change in the size of the PCR products with start codon exchange, agarose gel images are not shown. The start codon exchanges were confirmed by DNA sequencing. As an example, the change in the sequence of *trpE* gene is given in Figure 3.26.

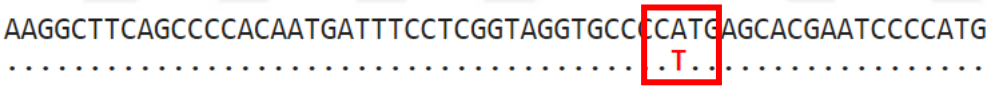

Figure 3.26: Start codon exchange *trpE* gene in AROM1 strain.

In order to evaluate the effect of start codon exchanges on the constructed strains, cells were grown in 96-well plates and the obtained results are presented in Figure 3.27. AROM1 and AROM4 strains with the start codon exchanges in *trpE* and *pat*, displayed no change in growth, and additional L-tryptophan or L-phenylalanine have not further improved their growth (Figure 3.27A and 3.27D). However, the start codon exchange of the *pheA* gene in both AROM2 and AROM3 strains led to L-phenylalanine bradytrophy, as seen in Figures 3.27B and 3.27C. The addition of 2 mM L-phenylalanine restored the growth of both strains.

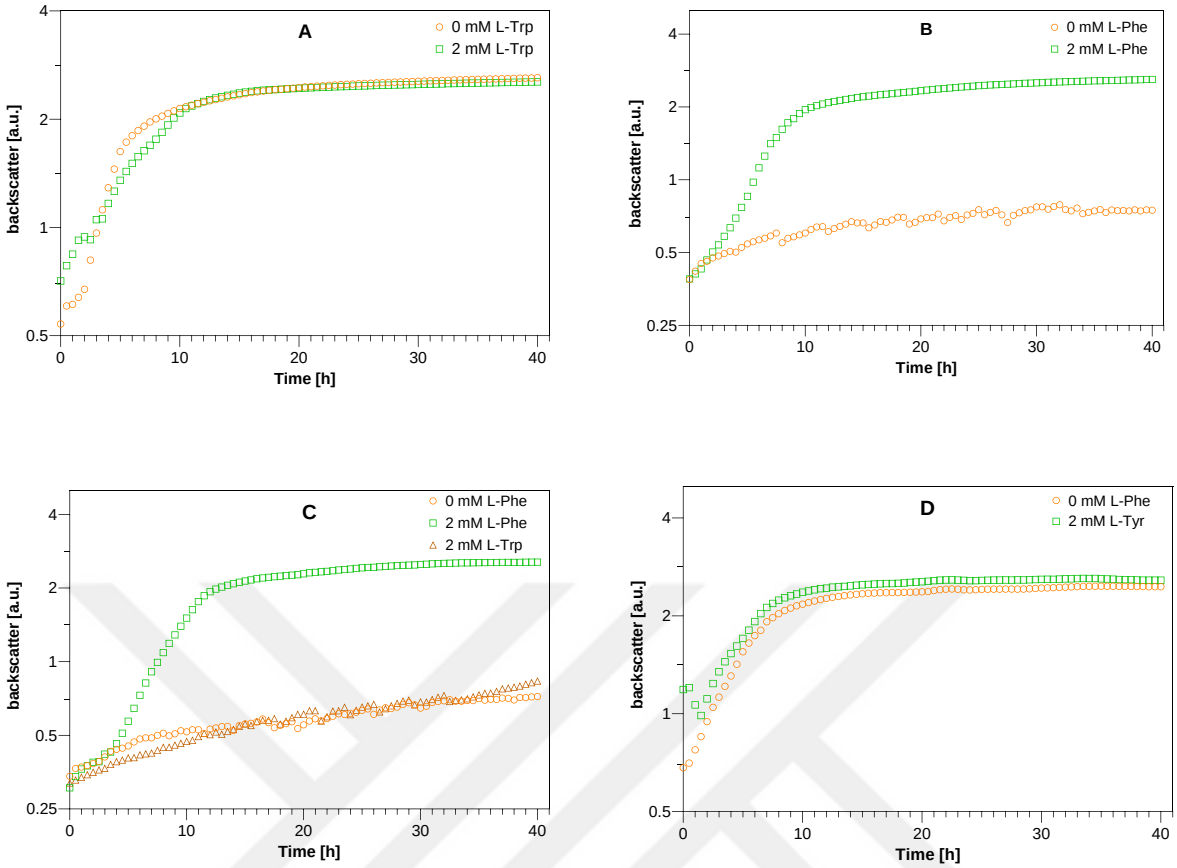

Figure 3.27: Growth of constructed mutants in 96-well plates. A) AROM1, B) AROM2, C) AROM3, D) AROM4. Backscatter signal is given in arbitrary units (a.u.).

3.9.2 L-phenylalanine supplementation optimization for growth and L-tyrosine production

Excess of L-phenylalanine can lead to feedback inhibition of enzymes involved in aromatic amino acids synthesis, while improving the growth; therefore, its concentration was adjusted in this section. As seen in Figure 3.28 a gradual increase in L-phenylalanine concentration from 0.01-0.2 mM improved growth, while 0.5 mM L-phenylalanine restored growth completely.

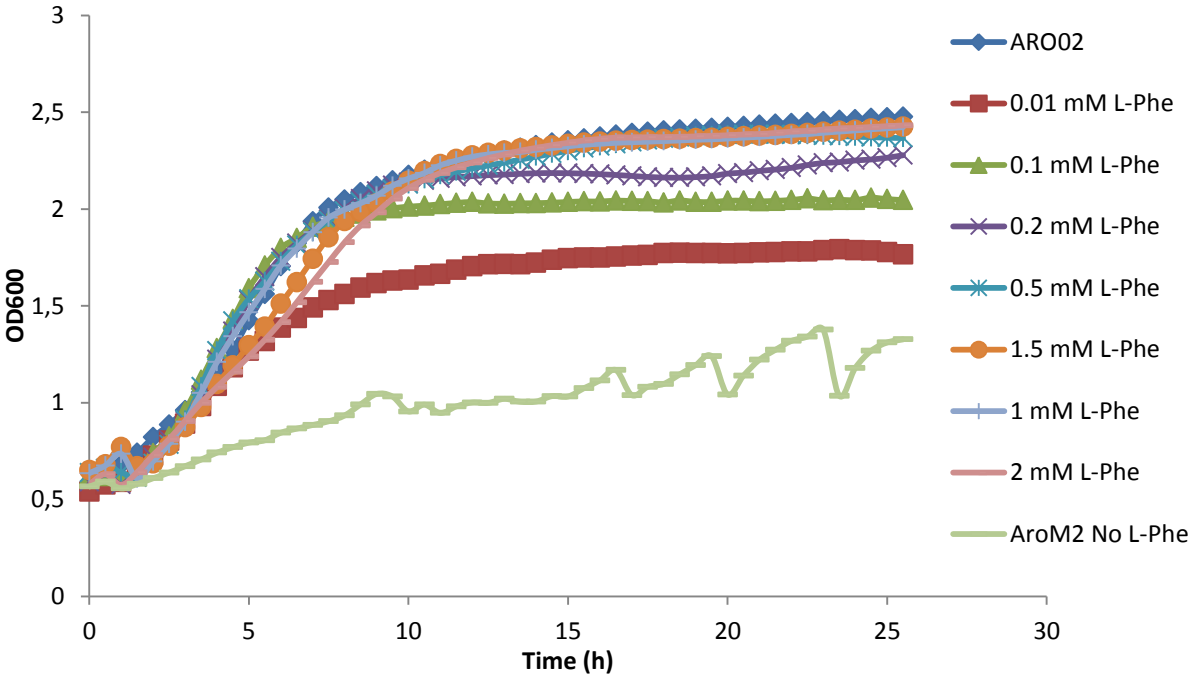

Figure 3.28: AROM2 strain grown in 96-well plates supplemented with different L-phenylalanine concentrations. ARO02 strain was grown as the control strain. Backscatter signal is given in arbitrary units (a.u.).

In order to find an L-phenylalanine concentration, which improves growth but at the same time does not inhibit L-tyrosine synthesis, AROM2 strain was selected as the reference strain and grown in 50 mL CGXII medium supplemented with 0.1, 0.5, and 1 mM L-phenylalanine. The obtained results are presented in Figure 3.29.

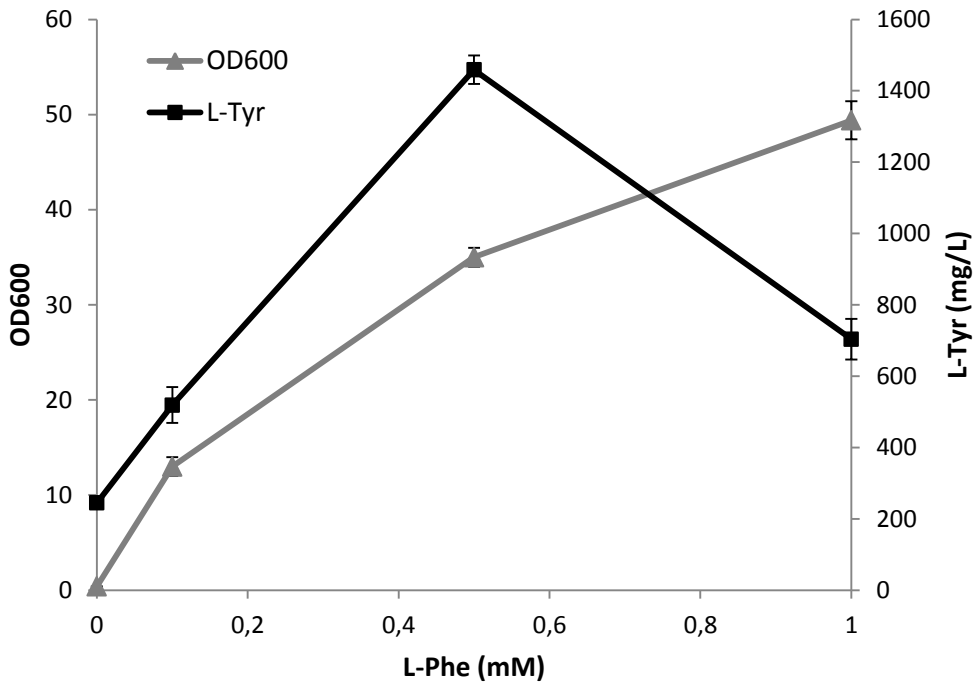

Figure 3.29: AROM2 strain grown in 500 mL flasks for 24 hours and supplemented with 0.1, 0.5, and 1 mM L-phenylalanine.

As seen in Figure 3.29, the increase in L-phenylalanine improved growth significantly, while reducing the L-tyrosine titer, as expected. However, when no L-phenylalanine was added to the medium, AROM2 strain produced 245 mg/L L-tyrosine, and the final OD_{600} barely reached 0.4. This meant that the strain is L-phenylalanine bradytroph, not auxotroph. The highest L-tyrosine titer was observed with 0.5 mM L-phenylalanine. Further increase in L-phenylalanine concentration improved growth but reduced L-tyrosine titer by ~ 50% (Figure 3.29).

Based on the results displayed in Figure 3.29, 0.5 mM L-phenylalanine was selected for further experiments with AROM2 strain and the strains derived from it.

3.9.3 The effect of start codon exchanges in *pat, trpE* and *pheA* genes on L-tyrosine titer

Both the parent strain ARO02 and the strains derived from it, were tested for their ability to produce L-tyrosine and the obtained results are summarized in Table 3.4. The only mutation that did not have effect on L-tyrosine titer was the start codon exchange on *pat* gene, which produced similar amount of L-tyrosine as the parent strain.

Change in the start codon of *trpE* doubled L-tyrosine titer in AROM1 strain when compared to the parent strain. To this end, this mutation was selected to be included in further work for L-tyrosine overproduction. The mutation that had the highest effect on L-tyrosine titer was the start codon exchange on *pheA* gene. This mutation in AROM2 strain led to 44-fold improved L-tyrosine production when compared to the parent strain, ARO02. Finally AROM3 strain with the start codons exchanges in both *trpE* and *pheA* was constructed, since both these mutations improved L-tyrosine production. With this strain 3.1 g/L of L-tyrosine was produced, which was about 10 % higher when compared to AROM2 but 50-fold higher than L-tyrosine obtained with the ARO02 parent strain.

Table 3.4: OD_{600} values and L-tyrosine titers of ARO02 and the constructed strains.

Strain	**OD_{600}**	**L-Tyr (g/L)**
ARO02	55 ± 1	0.06 ± 0.01
AROM1	42 ± 3	0.14 ± 0.01
AROM2	25 ± 7	2.70 ± 0.08
AROM3	24 ± 1	3.10 ± 0.14
AROM4	52 ± 3	0.07 ± 0.01
AROM21	22 ± 3	2.50 ± 0.08
AROM22	20 ± 1	2.50 ± 0.01
AROM3Dap	18 ± 1	3.01 ± 0.07

3.9.4 The effect of overexpression of shikimate pathway genes *aroE* and *qsuC* on L-tyrosine titer

In this section, first the effect of overexpression of shikimate pathwas genes, *aroE* and *qsuC,*on L-tyrosine production was evaluated. Then, the inhibition of carbon flux towards the shikimate degradation product, protocatechuate, was tested as well.

The L-tyrosine titer obtained with AROM21 strain, in which *qsuABD* genes were deleted as *qsuC* gene was integrated under the P_{tuf} promoter, was similar to that obtained with AROM2 strain as seen in Table 3.4. Similarly, the mutation in AROM22 strain, in which *iolR* gene was deleted by integration of *aroE* under the P_{tuf} promoter into its locus, has made no change on L-tyrosine titer.

3.9.5 The effect of channeling glucose uptake system from PTS to inositol permeases on growth and L-tyrosine titer

In order to increase PEP availability for L-tyrrosine synthesis, the PTS component for glucose uptake gene (*ptsG*) was inactivated by integration of both inositol transport gene (*iolT2*) from *C. glutamicum* and glucokinase (*glcK*) from *Bacillus subtilis* This change was expected to reroute glucose uptake from PTS, which consumes PEP, to inositol uptake system, which is independent of PEP. This change was first confirmed on an agarose gel (Figure 3.30) and then by DNA sequencing.

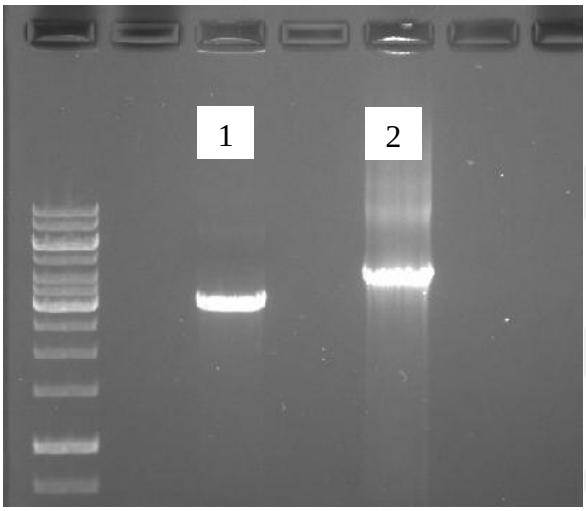

Figure 3.30: Gel electrophoresis image of 1) *ptsG* from *C. glutamicum* wild-type and 2) Δ*ptsG*::iolTBest from AROM23. Gene ruler: Thermo Fisher 1 Kb.

In the absence of inositol, which activates inositol uptake system, the growth of AROM23 was very low, as seen in Figure 3.31. Contrary to expectations, L-tyrosine titer with this strain was only 2.1 ± 0.074 g/L, even after 72 hours growth. The addition of 2 mM inositol, which stimulated glucose uptake by the inositol permease IolT2, the growth was improved, however the titer was only 0.48 ± 0.001 g/L L-tyrosine even after 72 hours growth.

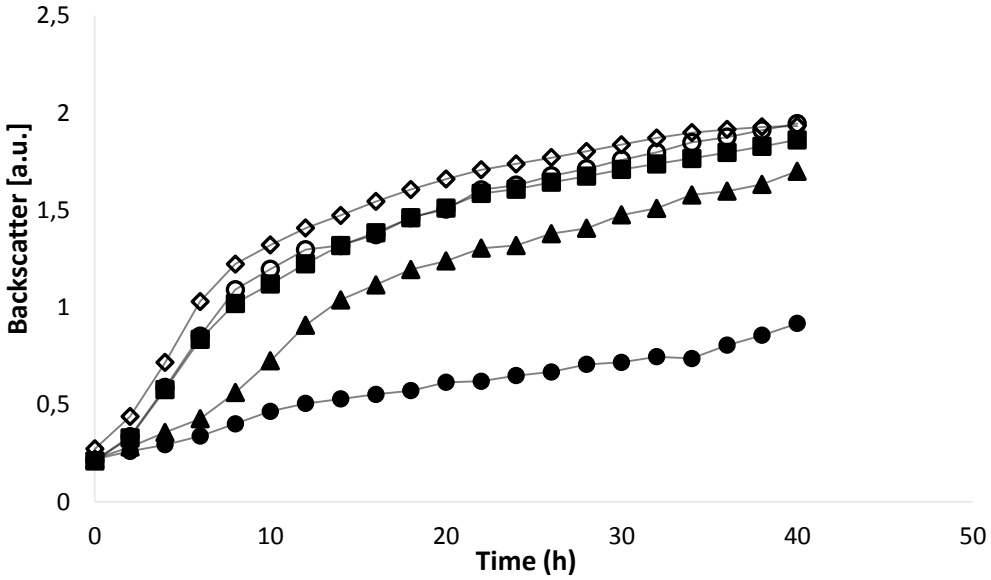

Figure 3.31: AROM23 growth in 96-well plate. O mM Inositol (black circles), 0.1 mM Inositol (black triangles), 0.5 mM Inositol (black squares), 1 mM Inositol (empty circles), 2 mM Inositol (empty diamonds). Backscatter signal is given in arbitrary units (a.u.).

3.9.6 L-tyrosine production from glucose/xylose mixtures

In order to examine L-tyrosine production with cells grown on glucose/xylose mixtures and xylose, the strain with the highest L-tyrosine titer, AROM3, was transformed with xylose utilization genes, and designated as AROM3X. In contrast to glucose, for xylose uptake and phosphorylation, PEP is not utilized. To this end, it was expected to observe increased L-tyrosine titer based on increased PEP and E4P. E4P is an intermediate of the pentose phosphate pathway, though which xylose is catabolized. Simultaneously, it is a building block for L-tyrosine synthesis.

The results obtained are summarized in Table 3.5.

Table 3.5: L-tyrosine titer obtained with AROM3X strain after 48 hours growth**.**

Carbon source	**OD_{600}**	**L-Tyr (g/L)**
Glu (40 g/L)	25	3.20
Glu (30 g/L) + Xyl (10 g/L)	24±1	3.20±0.07
Glu (10 g/L) + Xyl (30 g/L)	24±3	3.60±0.10
Xyl (40 g/L)	21±2	1.70±0.10

L-tyrosine titer using 4 % xylose as the carbon source was approximately half of that obtained with the same amount of glucose. When different mixtures of glucose and xylose were tested, titer increased with glucose:xylose in 1:3 (v/v) ratio to a titer of 3.60 ± 0.1 g/L of L-tyrosine.

3.9.7 The screening for unidentified aminotransferase in L-tyrosine biosynthesis in *C. glutamicum*

As the final attempt to engineer *C. glutamicum* for L-tyrosine overproduction, an aminotransferase catalyzing the reaction from prephenate to arogenate was targetted. Since it has not been identified yet, the initial step was to identify a gene encoding it.

The *Rv1178* gene from *M. tuberculosis*, which was reported to possess prephenate aminotransferase function (Graindorge et al., 2014), was taken as the reference for sequence comparison against 20 aminotransferases from *C. glutamicum* (Marienhagen et al., 2005). The *dapC* gene from *C. glutamicum* showed 63.23 % sequence identity to the *Rv1178* gene from *M. tuberculosis*, as seen in Figure 3.32. To this end, it was hypothesized that *dapC* gene could be the unidentified aminotransferase in L-tyrosine biosynthesis through arogenate route.

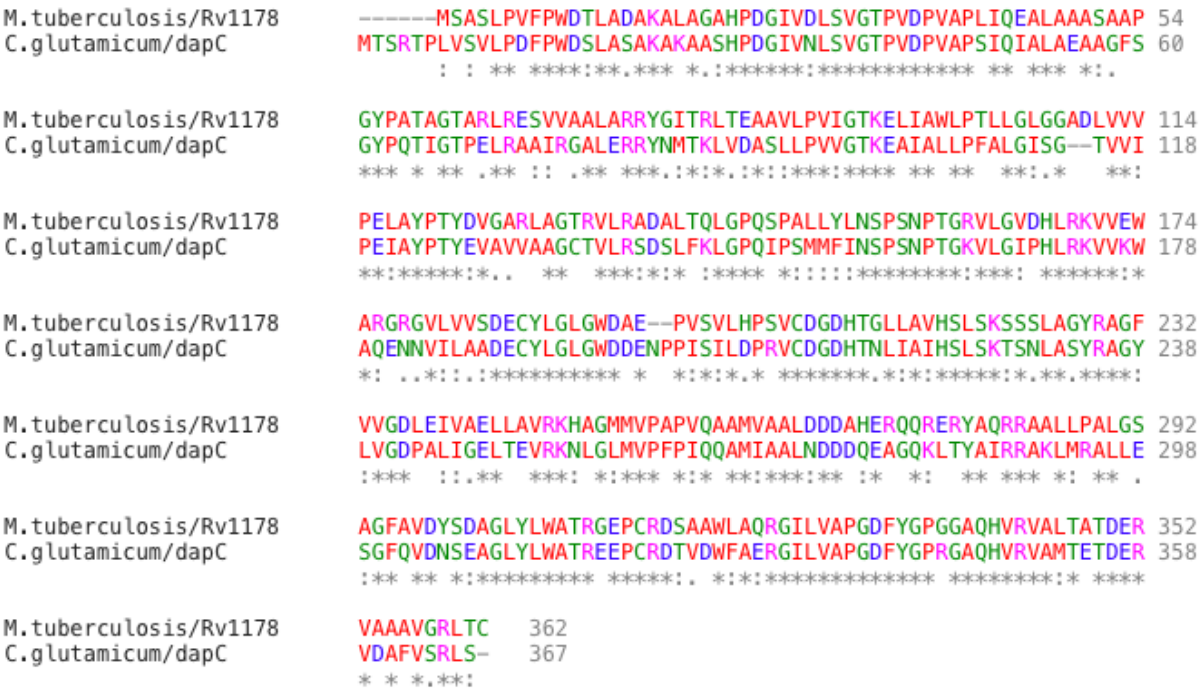

Figure 3.32: Sequence alignment of *M. tuberculosis* Rv1178 with *C. glutamicum* DapC (Cg1253) enzymes.

3.9.7.1. The effect of *dapC* gene deletion on *C. glutamicum* growth

In order to examine the role of *dapC* in L-tyrosine biosynthesis and bacterial growth, firstly this gene was deleted from the *C. glutamicum* wild-type chromosome and the obtained strain was designated as *C. glutamicum* WDD. This deletion was first confirmed on an agarose gel (Figure 3.33) and then by DNA sequencing.

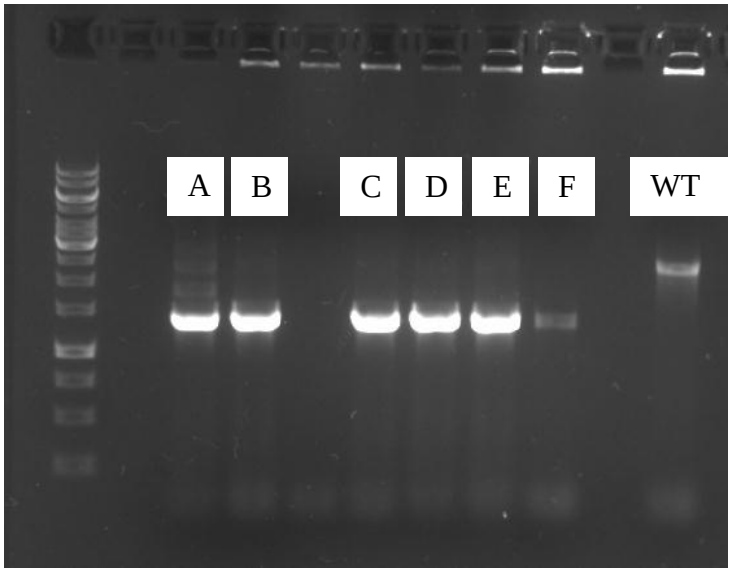

Figure 3.33: The electrophoresis gel image of colony PCR of deleted *dapC* gene in colonies A-F, and *dapC* from *C. glutamicum* wild-type (WT). Gene ruler: NEB 1 Kb.

This strain grew well in complex medium BHI, however, it grew very slowly in minimal CGXII medium. This was a hint of possible L-tyrosine bradytrophy; to this end, *C. glutamicum* WDD was grown in 96-well plates in CGXII medium with different L-tyrosine concentrations, and the results are presented in Figure 3.34.

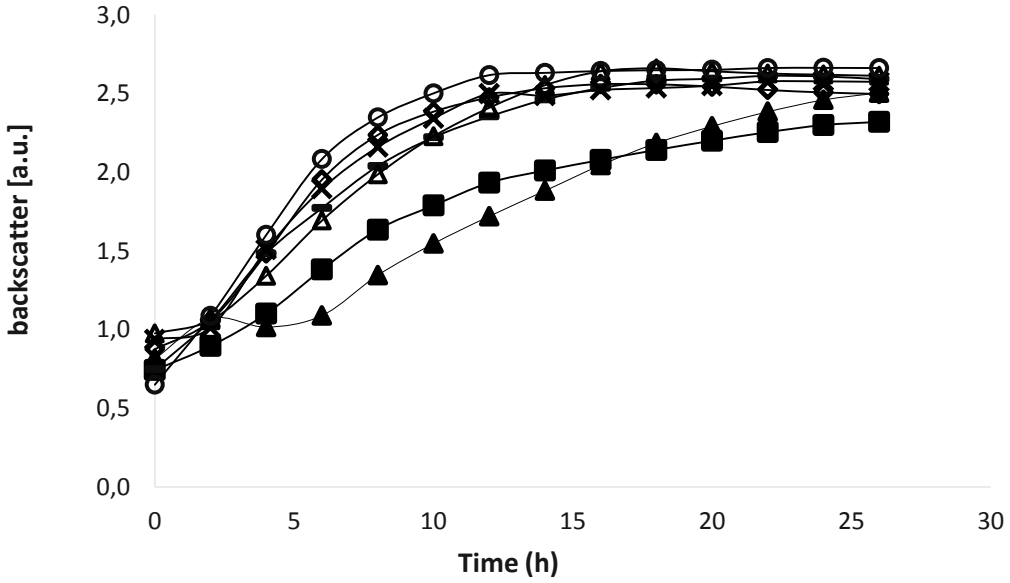

Figure 3.34: Growth of three *C. glutamicum* WDD strain in CGXII with different L-tyrosine concentrations: 0 mM (black squares), 0.01 mM (black triangles), 0.1 mM (empty triangles), 0.5 mM (short lines), 1 mM (symbol X), 1.5 mM (empty diamonds),

C. glutamicum wild-type (empty circles). Backscatter signal is given in arbitrary units (a.u.).

As seen in Figure 3.34 the absence of *dapC* made *C. glutamicum* L-tyrosine bradytroph while L-tyrosine addition improved the growth. These are strong indications of its involvement in L-tyrosine biosynthesis.

3.9.7.2. The effect of *dapC* overexpression on L-tyrosine titer

In order to evaluate the potential effect of *dapC* gene on L-tyrosine overproduction, it was overexpressed in AROM3, the strain with the highest L-tyrosine titer. The obtained strains, AROM3EV that carried the empty vector, and AROM3Dap that overexpressed the *dapC* gene, produced around 3 g/L of L-tyrosine (Table 3.5), which indicated that *dapC* has no effect on L-tyrosine overproduction. This result was not unexpected since *dapC* encodes an aminotransferase that operate in near equilibrium.

3.9.7.3. Genetic complementation of *C. glutamicum* WDD with *dapC*

In order to test the complimentary effect of plasmid-borne expression of *dapC* in *C. glutamicum* WDD, this strain was transformed with both empty vector and vector carrying *dapC* gene to obtain *C. glutamicum* EV and *C. glutamicum* Dap respectively.

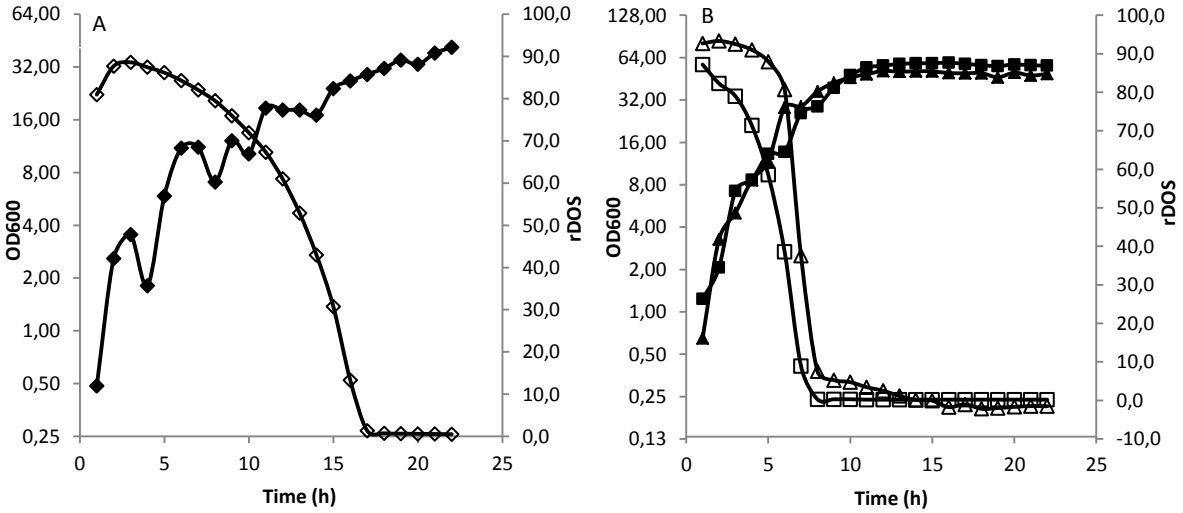

Figure 3.35: Measurements of cell growth with filled symbols showing OD_{600} and empty symbols showing rDOS measurements. A) *C. glutamicum* WDD EV (diamonds); B) *C. glutamicum* Dap (triangles) and *C. glutamicum* wild-type (squares).

As seen in Figure 3.35A, the absence of *dapC* in *C. glutamicum* resulted in retardation in growth, which was restored by *dapC* expression in the *C. glutamicum* Dap strain. As seen in Figure 3.35B, the growth behavior and oxygen consumption in both wild-type and *C. glutamicum* Dap strains were similar, which proved genetic complementation of *C. glutamicum* EV with *dapC* expression.

3.9.7.4. Evaluating the effect of L-lysine addition on *C. glutamicum* WDD growth

Since *dapC* gene encodes the N-succinyldiaminopimelate aminotransferase in the diaminopimelate dehydrogenase independent route for L-lysine biosynthesis in *C. glutamicum* (Hartmann et al., 2003), at this point it was hypothesized that supplementation of *C. glutamicum* WDD with L-lysine may restore its growth in the same way L-tyrosine supplementation did. To this end, *C. glutamicum* WDD was grown in 500 mL baffled flasks in PreSens Shake Flask Reader (SFR) vario device, in 50 mL of CGXII medium with 1.5 mM of L-tyrosine and 1.5 mM of L-lysine. The obtained results are seen in Figure 3.36.

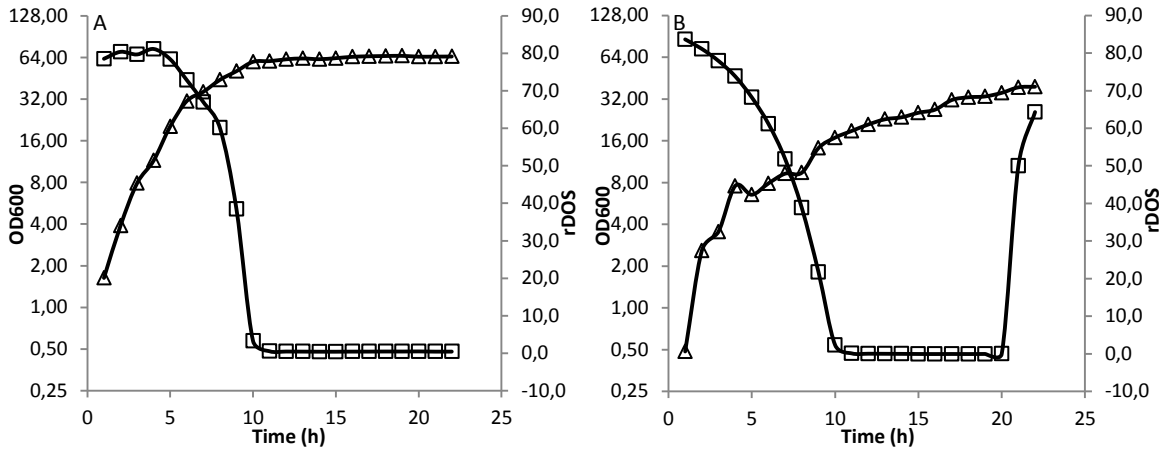

Figure 3.36: Growth of *C. glutamicum* WDD cells supplemented with A) 1.5 mM L-tyrosine and B) 1.5 mM L-lysine. Triangles: OD_{600}, squares: relative dissolved oxygen saturation (rDOS).

As seen in Figure 3.36B, addition of 1.5 mM of L-lysine did not restore the growth of *C. glutamicum* WDD. This can be concluded since growth stopped after 20 hours of incubation, as indicated by the rising in rDOS at that point, and the low final OD_{600}. On the other hand, as seen in Figure 3.36A, L-tyrosine supplementation has completely restored the growth which continued after 20 hours of incubation since there is no rising in rDOS.

3.10. L-DOPA production with L-tyrosine producing AROM3D strain

3.10.1 Fermentative L-DOPA production with AROM3D strain

The strain with the highest L-tyrosine titer on glucose, AROM3, was transformed with pEKEx3-tyr_{Rs} in order to evaluate L-DOPA production without external L-tyrosine addition. The strain was designated as AROM3D. The tyrosinase cofactor copper and the antioxidant thymol had adverse effects on the growth of AROM3D, here cells were allowed to grow for 24 hours for the expression of tyrosinase. Tyrosinase expression was induced at the time of inoculation. After this time, cofactor copper and the antioxidant thymol were added and after addition 24 hours of this additons, L-DOPA was detected in supernatants of cells. The results obtained with Arnow's method can be seen in Figure 3.37.

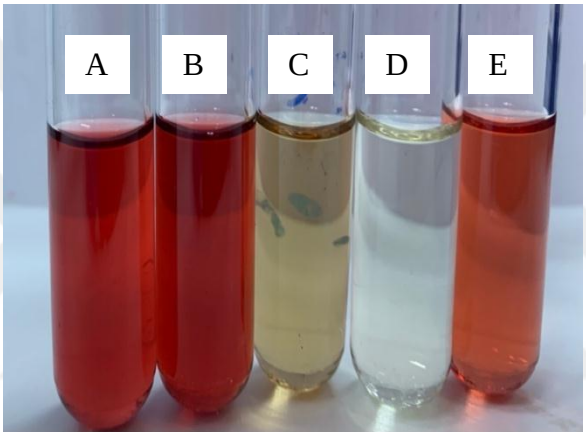

Figure 3.37: Results obtained with Arnow's method: A and B) when copper ions and thymol are added 24 hours after inoculation, C: when copper ions are added at the inoculation, D) copper ions and thymol are added at the inoculation and E) standard L-DOPA (0.1 mg/mL).

The L-DOPA titer and final OD_{600} obtained after 24 hours after copper ions and thymol addition was 185 ± 9 mg/L and 17 ± 1 respectively.

3.10.2 Whole-cell biotransformation of L-tyrosine from AROM3 strain with CgEKV-II cells grown on husk hydrolysate

In this section, the need for addition of L-tyrosine for L-DOPA production was circumvented. Supernatants obtained from AROM3 strain, containing ~ 3 g/L L-tyrosine, were used as the substrate for whole-cell biotransformation.

The obtained results are summarized in Table 3.6.

Table 3.6: L-DOPA obtained with CgEKV-II cells grown on husk hydrolysate.

Sample	Copper ions (mM)	Ascorbic acid (mM)	L-DOPA (mg/L)
1	0.4	0	155±23
2	0	4	202±43
3	0.4	4	165±21

3.11. Analysis of the L-tyrosine overproducer *C. glutamicum* ATCC 21573

In this part of the study a commercially available L-tyrosine overproducer's genome was sequenced in order to find potential mutations that could be integrated into rationally designed L-tyrosine producing *C. glutamicum* strains. To this end, a genome-wide variation analysis was performed in order to identify mutated genes involved in L-tyrosine production and the results are summarized in Table 3.7.

Table 3.7: Mutational statistics of *C. glutamicum* ATCC 21573 as compared to *C. glutamicum* wild-type.

Total number of SNPs	**28090**
SNP type statistics	
Total substitutions	27611
Total insertions	208
Total deletions	271
SNP effect statistics	
Intergenic SNPs	3503
Synonymous SNPs	18634
Chemically neutral SNPs	1817
Chemically different SNPs	4010
Stop Mutations	47
AA Insertions	50
AA Deletions	76

The distribution of the verified mutations that includes substitutions, insertions and deletions is shown in Figure 3.38. When compared to the wild-type strain *C. glutamicum* ATCC 13032, there were a total of 28090 mutations, of which 27611 were single nucleotide polymorphisms (SNPs) and 479 were insertion/deletion mutations (InDels). Among the identified SNPs, 20186 were in genes with known function (73.1%), 2983 were in hypothetical genes (10.8%), 1114 were in transcription factors (4%), and 171 were in transposase group of genes (0.62%). Of the insertion mutations, 35 were in genes with known functions (16.8%), 4 were in hypothetical genes (1,92%), 2 were in transcription factors (0.96%), and 8 were in transposases (3.84%). Of the deletion mutations, 54 were in genes with known functions (19.9%), 13 were in hypothetical genes (4.8%), 2 were in transcription factors (0.74%), and 7 in transposases (2.58%).

Figure 3.38: Graphical summary of SNPs and InDels in the genome of *C. glutamicum* OP as compared to type strain *C. glutamicum* wild-type**.**

Then, *C. glutamicum* ATCC 21573 was both grown and tested for L-tyrosine overproduction on different carbon sources.

Additionally, in order to get insight and understand the carbon flux redistribution for L-tyrosine overproduction in *C. glutamicum* ATCC 21573, detailed mutational analysis to the pathways of the central carbon and alternative carbon transport and metabolism, aromatic amino acids biosynthesis, and degradation pathways were performed (Appendix Tables C1-C6).

3.11.1 Growth and L-tyrosine biosynthesis of *C. glutamicum* ATCC 21573 on different carbon sources

Aromatic amino acid biosynthesis starts with the condensation of PEP and E4P and it is now well established that PTS independent routes increase PEP availability which in turn leads to increased flux towards aromatic compounds (Lindner et al., 2011). Accordingly, L-tyrosine overproducer cells were grown in the presence of carbon sources with different entry routes on 96-well plates, and then the profiles obtained were compared with those of the wild-type cells. Furthermore, the presence of the other two aromatic amino acids on growth has been investigated since (i) the overproducer had been reported to be L-phenylalanine auxotroph (H Hagino et al., 1974) and (ii) L-tyrosine shares the shikimate pathway with L-phenylalanine and L-tryptophan in the biosynthetic route.

In the presence of glucose, the most preferred carbon source for *C. glutamicum*, growth was significantly less and slower in the overproducer. However, both wild-type and overproducer cells reached stationary phase at the end of 18 hours. Addition of inositol to enhance glucose uptake by the inositol permease (Lindner et al., 2011) made no significant change (Figure 3.39A). When media contained a mixture of L-phenylalanine and L-tryptophan, growth of the mutant cells was only marginally better. The presence of L-phenylalanine and L-tryptophan in different wells has shown that L-phenylalanine was the major contributor to this change in growth (Figure 3.39B). Growth of the overproducer cells was similarly less and slow with the two other PTS-dependent sugars, fructose and sucrose (Figure 3.39C).

Next, the utilization of two groups of carbon sources with PTS-independent uptake routes was investigated. In the first group was the pentose sugar, ribose, and in the second group were the organic acids, acetate and citrate. With ribose as the sole carbon source, growth was again less and slower in the overproducer (Figure 3.39D). In the presence of the two organic acids as carbon and energy sources, rather different results were found. With acetate, L-phenylalanine was required for a slow steady growth and cells were still in exponential phase at the end of 18 hours. In the absence of L-phenylalanine, growth was fast and unsteady and ceased rapidly

(Figure 3.39E). Regarding citrate uptake, both citrate importers CitH and TctABC are activated by calcium ions, while magnesium only activates TctABC (Brocker et al., 2009). Here, during growth on citrate in CGXII medium, which contains ~10 mM in Mg^{2+}, the growth of the L-tyrosine overproducer was significantly slow. Uptake was probably achieved by the TctABC transporter only. With the presence of 2 mM calcium ions, there was a significant improvement in the growth of both cells but the difference was more pronounced in the overproducer. This shows the importance of CitH in citate uptake in the overproducer (Figure 3.39F).

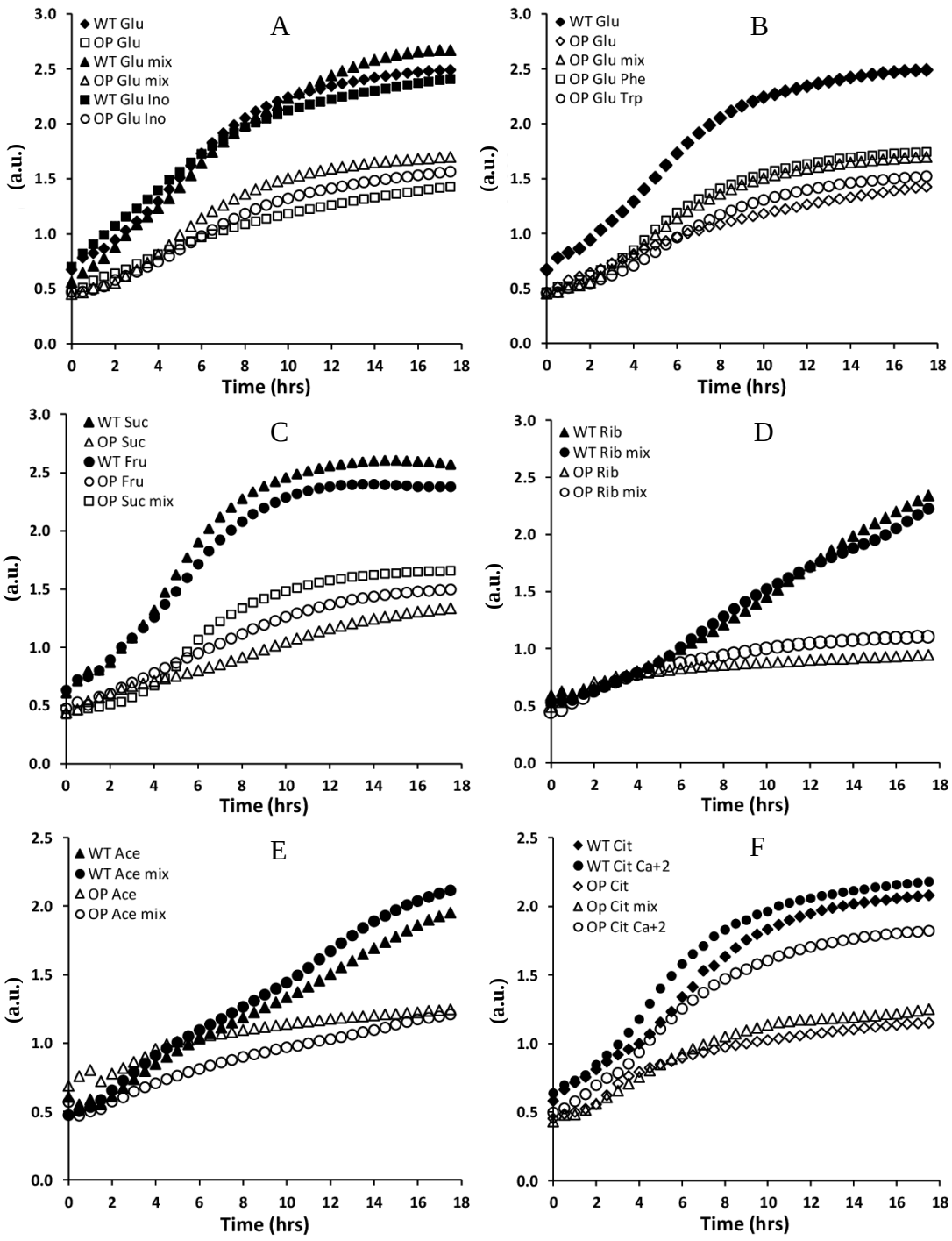

Figure 3.39: Growth of *C. glutamicum* wild-type (WT) and *C. glutamicum* ATCC 21573 (OP) in 96-well plates. Averages from triplicate experiments are presented. ([Ca^{+2}] was adjusted to 2 mM with $CaCl_2$). *Mix:2 mM L-phenylalanine + 2 mM L-tryptophan, Ino: 2 mM inositol. Backscatter signal is given in arbitrary units (a.u.).

With none of the tested carbon sources, addition of the aromatic amino acid mixture to growth media did help the growth rate and cell concentration to approach the values observed with the wild-type cells.

The results obtained in 96-well plates have shaped experiments for L-tyrosine synthesis in the overproducer cells. Since the variation in the utilization of PTS dependent sugars was negligible, only glucose along with the non-PTS carbon sources were used in further experiments. Regardless of the carbon source utilized, there was always measurable L-tyrosine synthesis in the overproducer cells. Maximum titer was obtained with glucose; however, the titer obtained with citrate was comparable. The presence of L-phenylalanine had a stimulatory effect on growth but, unfortunately, it decreased L-tyrosine synthesis. Results obtained from triplicate experiments are presented in Table 3.8.

Table 3.8: L-tyrosine titer obtained with *C. glutamicum* ATCC 21573 after 48 hours incubation.

Strain	**Carbon source**	**OD_{600}**	**L-Tyr titer ($mg \cdot L^{-1}$)**
Wild-type	Glucose	52.3±1.0	0
Overproducer	Glucose	3.5±0.1	222.5±5.5
Overproducer	Glucose*	5.6±0.3	64±11.5
Overproducer	Ribose	2.5±0.1	108.5±2.5
Overproducer	Acetate	1.9±0.1	159.0±3.0
Overproducer	Citrate	2.8±0.2	181.5±6.5

* supplemented with 2 mM L-phenylalanine.

3.11.2 Mutational analysis of *C. glutamicum* ATCC 21573 genome for L-tyrosine related genes

The major pathways considered in detail are displayed in Figure C1 in Appendix C. Detailed mutations in genes of selected pathways are given in Tables C1-C6 in Appendix C.

In both *E. coli* and *C. glutamicum*, PEP synthase of gluconeogenesis and transketolase of pentose phosphate pathway were the primary choices for altering flux towards PEP and E4P, respectively (Gu et al., 2013; Lütke-Eversloh & Stephanopoulos, 2007; Shen et al., 2012; Yakandawala et al., 2008). In *C. glutamicum*, the overexpression of transketolase alone has only barely enhanced aromatic amino acids yield (M. Ikeda et al., 1999). Nevertheless, in

many further studies, both transketolase (*tkt*) and PEP synthase (*ppsA*) were always among the targeted enzymes in aromatic compound synthesis (Masato Ikeda & Katsumata, 1999; Kogure et al., 2016; Zhang et al., 2015). In *C. glutamicum* ATCC 21573, transketolase was found to have a single conservative replacement, while PEP synthase has few, mostly conservative replacements. Their contribution L-tyrosine overproduction is unclear with current knowledge.

Among the enzymes that received attention for their contribution to the PEP pool were pyruvate kinase (*pyk*) and the enzymes of the anaplerotic reactions, phosphoenolpyruvate carboxykinase (*pck*), phosphoenolpyruvate carboxylase (*ppc)*, and pyruvate carboxylase (*pyc*), which are all under tight transcriptional regulation (Buchholz et al., 2013; Peters-Wendisch et al., 2001). Furthermore, enzymes that regulate pyruvate flux such as pyruvate dehydrogenase (*pqo*), *aceE* (pyruvate dehydrogenase E1 component), and *ldh* (L-lactate dehydrogenase) have also been in the focus of different studies to investigate their contribution to PEP and pyruvate availability, not only towards aromatics (Zhang et al., 2015), but also towards other amino acids (Buchholz et al., 2013). In *E. coli*, by weakening the acetate node, the Pta-AckA pathway, it was possible to improve L-tryptophan production (L. Liu et al., 2016). All above mentioned enzymes are important to direct flux from PEP and pyruvate derived molecules to and from the TCA cycle and to control flux within the cycle (Kallscheuer & Marienhagen, 2018). Except for anaplerotic reactions leading to oxaloacetate formation, the others have minor changes, which suggests that their contributions to carbon flux redirection could be marginally small. Interestingly, the dehydrogenase enzymes of pyruvate degradation encoded by the genes *adhC, betB,* and *dld*, which were critically affected in the *C. glutamicum* 21573, seemed not to attract much attention in the construction of aromatic compounds overproducer strains.

Apart from being an indispensable precursor for many biosynthetic reactions, due to its role in PTS, PEP has been a subject for improving production of aromatic compounds. In this context, re-routing glucose uptake to PTS-independent paths has been considered for increasing the PEP pool. In engineered *C. glutamicum* cells devoid of PTS, inositol permeases function as the alternative gates for glucose import (Brüsseler et al., 2018; Kallscheuer & Marienhagen, 2018; Klaffl et al., 2013; Zhang et al., 2015). The remarkable number of changes in the gene encoding PtsG, specific to glucose uptake, leads the way to postulate that the L-tyrosine overproducer could not use PTS for glucose uptake. There were only very few mutations in the genes encoding the inositol permease and the glucokinase that are required in

the alternative utilization path. However, growth profiles of the *C. glutamicum* 21573 in the presence of glucose indicated that glucose utilization was rather poor. PTS-mediated glucose uptake is critically affected, while the activity of the inositol permeases is not clear. Only if growth with glucose had been unaffected, it could have been proposed that the inositol permeases is fully functional. Under these circumstances, the problem might also be associated with glucose catabolism following uptake. Nevertheless, although the cells barely grew, the utilization of a PTS-independent route which prevented consumption of PEP might have contributed to the accumulation of 222.5 ± 5.5 mg/L L-tyrosine. The number of mutations in PTS components specific for fructose and sucrose uptake were not as high as in PtsG, but growth was still slower and less. This could again be correlated with pathways following their uptake.

In the majority of studies on aromatic amino acid overproduction in *C. glutamicum*, L-phenylalanine or L-tryptophan have been focal points. Generally, for L-phenylalanine overproduction, the feedback resistant form of prephenate dehydratase was used (Zhang et al., 2013, 2015), while L-tryptophan overproduction necessitated silencing of chorismate mutase in addition to overexpression of TrpD and utilization of the feedback resistant form of TrpE (Veldmann et al., 2019). In *C. glutamicum* 21573, the changes in *pat* and specifically in *pheA* probably lead to reduced flux towards L-phenylalanine. Since PheA is under tight feedback regulation (Zhang et al., 2013), even if its inhibitory mechanism is not altered by the replacements, its expression might be expected to be lower as a result of changes in its promoter region. Thus, it could be a modification target.

4. DISCUSSION

4.1. L-DOPA production using the wild-type strain, *C. glutamicum* ATCC 13032

L-DOPA is a precursor to valuable compounds such as catecholamine transmitters dopamine and norepinephrine (Nagatsua & Sawadab, 2009), polymers such as melanin (Pavan et al., 2020), benzylisoquinoline alkaloids such as (S)-reticuline (Nakagawa et al., 2011). (S)-reticuline is an intermediate of well-known alkaloids berberine, morphine and glaucine (Matsumura et al., 2017). To this end, having a low-cost platform which produces high amounts of L-DOPA would pave the way for the synthesis of other valuable compounds.

Commonly, for *in vitro* L-DOPA synthesis, different enzyme or cell immobilization techniques have been exploited. Among the first evaluated immobilization platforms were alginate (Wichers et al., 1983), magnetic beads (Tuncagil et al., 2009) and poly(ethyleneoxide) (Yildiz et al., 2013). Furthermore, electroenzymatic synthesis of L-DOPA was explained by Min et al. (2010). Even though high conversion percentages of L-tyrosine to L-DOPA were obtained with similar setups, their major disadvantages were the impractical system setup and the complexity of product recovery.

L-DOPA synthesis with tyrosinases has been generally restricted to biotransformation of L-tyrosine by natural tyrosinase producers that include fungi such as *Aspergillus oryzae* and *Yarrowia lipolytica* and bacteria such as *Brevundimonas* sp. SGJ and *Bacillus* sp. JPJ (Ali et al., 2007b; Ikram-ul-Haq et al., 2002; Surwase et al., 2012; Surwase & Jadhav, 2011). The major disadvantage of fungal strains for which the titer may reach up to 3 g/L with optimized strains and parameters (Ali et al., 2007b) was the long periods (~ 120 hours) required for fungal growth, which adversely affects productivity. This calls into question the suitability of fungal systems for scale-up. Bacterial platforms used for the same biotransformations gave ~ 0.4 g/L and ~ 0.5 g/L of L-DOPA with *Brevundimonas* sp. SGJ (Surwase et al., 2012) and *Bacillus* sp. JPJ (Surwase & Jadhav, 2011) respectively, in the absence of significant optimization. Only after substantial optimization and cell recycling, titer reached ~ 3.8 g/L with *Brevundimonas* sp. SGJ. In all the mentioned studies, various concentrations of ascorbic acid have been used as a reducing reagent to prevent oxidation to dopachrome.

Among the microbial systems used for *in vivo* L-DOPA production, *Acremonium rutilum* is a fungal strain with a titer of 0.9 g/L L-DOPA (Krishnaveni et al., 2009). With 72–120 hours cultivation periods, productivity was 7.4–12 mg/(L·h). The engineered *E. coli* cells with tyrosinase or only tyrosine hydroxylase activity were intended to produce plant alkaloids and L-DOPA was only an intermediate in production (Matsumura et al., 2018; Nakagawa et al.,

2011). With the *Streptomyces castaneoglobisporus* tyrosinase ~ 0.3 g/L L-DOPA was synthesized, while with *Drosophila melanogaster* tyrosine hydroxylase ~ 1 g/L L-DOPA was synthesized. Operating in fed-batch mode for 90 h, L-DOPA productivity was 3–11 mg/(L·h) with these *E. coli* cells. Both *E. coli* cells were obtained following substantial genetic modifications and were cultivated in media that possessed components of rich growth media, such as yeast extract, tryptone, and beef extract, which also render the bioprocess unsuitable for scale-up.

As clearly seen, microbial production of the Parkinson's disease drug L-DOPA has been a subject of interest in the last decade. Even though L-DOPA yields of designed processes were high, many of these processes required industrially unfavorable fungi and bacteria (Ali et al., 2005; Park et al., 1998) which are easily contaminated and prone to phage invasion, toxic substrates such as catechol (Koyanagi et al., 2005; S. G. Lee et al., 1996), and addition of expensive components for production medium, which challenged the economical feasibility and scale-up of the process (Fordjour et al., 2019; Wei et al., 2016).

Proposed here is sustainable L-DOPA production form both commercially available fermentable sugars and the renewable carbon source hazelnut husk hydrolysate using the GRAS bacterium *C. glutamicum*. Three *C. glutamicum* strains were constructed; (1) wild-type strain with heterologous expression of *R. solanacearum* tyrosinase gene, (2) wild-type expressing the *R. solanacearum* tyrosinase along with xylose utilization genes, and (3) L-tyrosine overproducing AROM3 strain with heterologous expression of *R. solanacearum* tyrosinase gene. Since lignocellulosic wastes contain significant amounts of xylose, overexpression of xylose utilization genes enables the use of lignocellulosic biomass as a carbon and energy source for sustainable L-DOPA production. *C. glutamicum*'s ability to tolerate inhibitory byproducts in lignocellulosic hydrolysates, such as phenolic compounds and furfurals, constitutes an extra advantage to make this strain an ideal candidate to be used for this production using hydrolyzed lignocellulosic biomass (Gopinath et al., 2011).

In the current study, the initial L-DOPA titer was ~ 0.04 g/L with fermentative production using *C. glutamicum* cells. The main reason for this relatively low titer compared to the engineered *E. coli* was the oxidation of L-DOPA. Unfortunately, the major challenge in tyrosinase based L-DOPA production is the dual nature of this enzyme and L-DOPA oxidation to subsequent metabolites, as well as their nonenzymatic conversion to melanin. To this end, different molecules have been tested for their ability to inhibit tyrosinase activity thus melanin formation (Da Silva et al., 2017; Kim & Uyama, 2005; Zolghadri et al., 2019). However, many of them were toxic and economically unfeasible, while ascorbic acid stood

out as a valuable alternative due to its availability and nontoxic nature (Kim & Uyama, 2005). Therefore, the antioxidant ascorbic acid was tested both *in vivo* (Fordjour et al., 2019; Ros et al., 1993) and *in vitro*. However, excess of ascorbic acid was reported to show inhibitory properties against the tyrosinase enzymes (Surwase & Jadhav, 2011). The results presented here are compatible with this information since there was no L-DOPA synthesis in this system with high ascobic acid concentrations. On the other hand, lower concentrations have not improved L-DOPA titer as well. Probable explanation for this might be the fact that ascorbic acid is quickly consumed in the process as reducing quinones formed by tyrosinase (Kim & Uyama, 2005).

Since tyrosinases, and more importantly their inhibitors, are of pharmaceutical significance based on their ability to prevent melanin overproduction, many studies have focused on finding efficient inhibitors of both natural and synthetic origin (Zolghadri et al., 2019). With this aim the essential oil, thymol, was proposed as an inhibitor (Da Silva et al., 2017). The superiority of thymol over other inhibitors is that it is a redox inhibitor rather than a substrate or an inhibitor of the tyrosinase enzymes (Satooka & Kubo, 2011). In other words, in contrast to ascorbic acid, thymol prevents L-DOPA oxidation by inhibiting the formation of undesired metabolites that will complicate downstream processes, but not by inhibiting enzyme activity. Thus, thymol was evaluated as a potential L-DOPA antioxidant in this study. In the presence of thymol, L-DOPA titer in *C. glutamicum* cells has improved to 0.13 ± 0.04 g/L with cells growing on glucose and to 0.26 ± 0.02 g/L with cells growing on a mixture of glucose and xylose. This titer obtained with a mixed carbon source was comparable to the value obtained with the same tyrosinase in *E. coli* cells. Furthermore, the shorter cultivation period also helped to keep the productivity at 12 mg/(L·h). Since L-DOPA is very sensitive to oxygen, the final L-DOPA titer will clearly benefit from further bioprocess optimization.

Unlike *E. coli*, *C. glutamicum* cells gave this titer in a medium devoid of rich media components not suitable for scale-up, which makes the bioprocess far from industrial feasibility. The ability to co-utilize glucose and xylose mixture to reach this titer places this organism in the center of sustainable L-DOPA production using renewable carbon sources.

4.2. L-DOPA production using rationally designed *C. glutamicum* L-tyrosine overproducer

L-tyrosine is the immediate precursor of L-DOPA. For this reason, as the next step, an endeavor has been made to circumvent the addition of L-tyrosine as the substrate for L-DOPA

production. For this purpose, an L-tyrosine overproducer *C. glutamicum* strain was rationally designed and used for L-DOPA synthesis.

4.2.1 Construction of the L-tyrosine overproducer *C. glutamicum*

In microbial cells, shikimate pathway is the committed route for aromatic amino acid synthesis, which starts with the condensation of the metabolic precursors PEP and E4P. Then diversion to L-tryptophan, L-phenylalanine, and L-tyrosine is at the chorismate branch point, downstream of the shikimate pathway. Therefore, studies targeting aromatic amino acid synthesis commonly focus on shikimate pathway and the branched aromatic amino acid pathway. These two pathways constituted the major routes of modification for aromatic amino acid overproduction also in *C. glutamicum* (Averesch and Krömer, 2018). Apart from central carbon metabolism, much research has focused on the regulated DAHP synthase, which catalyzes the first reaction of the shikimate pathway, the condensation between PEP and E4P. As the primary target of this pathway, various feedback resistant forms of this enzyme have been investigated for aromatics overproduction (Gu et al., 2013; Hernández-Chávez et al., 2019; M. Ikeda et al., 1999; Masato Ikeda & Katsumata, 1992; Lütke-Eversloh & Stephanopoulos, 2007; Zhang et al., 2013). To this end, strain ARO02 was selected as the base strain for rational design because it has integrated a feedback resistant form of DAHP synthase from *E. coli* in its chromosome (Walter et al., 2020).

The majority of studies for aromatic amino acid overproduction in *C. glutamicum* focus on either L-tryptophan or L-phenylalanine. Generally, for L-phenylalanine overproduction, the feedback resistant form of prephenate dehydratase, encoded by *pheA*, have been used (Zhang et al., 2013, 2015) while L-tryptophan overproduction necessitated silencing of chorismate mutase in addition to the overexpression of *trpD* and feedback resistant form of *trpE,* genes involved in L-tryptophan biosynthesis (Veldmann et al., 2019).

These data indicated that the activities of prephenate dehydratase and anthranilate synthase component 1 are important to channel flux from chorismate towards L-phenylalanine and L-tryptophan, respectively, their activities were genetically reduced via start codon exchanges in *pheA* and *trpE* in ARO02. This was expected to increase flux towards L-tyrosine. Indeed, lowering the expression of these two feed-back regulated enzymes were found be important for channeling carbon flow towards L-tyrosine. Clearly the impact of *pheA* was higher than that of *trpE*. On the other hand, the start codon replacement in phenylalanine aminotransferase, *pat,* the second enzyme specific for L-phenylalanine synthesis, was found to be futile for L-tyrosine overproduction.

As an additional attempt to increase L-tyrosine production, the unknown aminotransferase responsible for conversion of prephenate to pretyrosine (arogenate) was predicted.

The deletion of the gene encoding the predicted aminotransferase DapC transformed the wild-type *C. glutamicum* strain into an L-tyrosine bradytroph. This result supported the role of DapC in L-tyrosine biosynthesis but there should at least be one other aminotransferase involved in the conversion of prephenate to arogenate, since the deletion of *dapC* did not make *C. glutamicum* L-tyrosine auxotroph. However, its overexpression had no influence on L-tyrosine titer, as expected, since aminotransferases commonly operate near equilibrium (Taylor et al., 1998).

Downstream of the first committed step of the shikimate pathway, *qsuC* and *aroE* genes have been the focus of a number of studies towards shikimate synthesis (Averesch & Krömer, 2018; Kogure et al., 2016; Sato et al., 2020; Zhang et al., 2015). Different enzymes of this pathway have been targeted by various studies for achieving higher rates of flux through the shikimate pathway for shikimic acid, aromatic molecules or related compounds (Kogure et al., 2016; Purwanto et al., 2018; Zhang et al., 2015). To this end, it was reasonable to hypothesize that increasing flux through this pathway will improve L-tyrosine production. In this study, shikimate dehydrogenase, encoded by *aroE*, and dehydroquinate dehydratase encoded by *qsuC* (*aroD*) were integrated into the genome under the strong P_{tuf} promoter to increase flux through the shikimate pathway and the *qsuABD* genes encoding enzymes involved in the quinate/shikimate degradation pathway have been deleted to block protocatechuate synthesis. Protocatechuate, the major degradation product of shikimate, might receive special attention since the branching to its synthesis is prior to the formation of aromatic amino acids. Therefore, a flux shift towards protocatechuate will presumably lower the final aromatic amino acid yield.

Unlike in shikimate (Kogure et al., 2016) and 4-hydroxybenzoate overproduction (Purwanto et al., 2018), neither of the performed modifications had a significant effect on L-tyrosine titer when compared to AROM2. One reason for this could be that AroE requires NADPH as a cofactor and NADPH availability was not sufficient. With the point mutation (Ser361Phe) in 6-phosphogluconate dehydrogenase gene (*gnd*; cg1643), this bottleneck can be relieved (Ohnishi et al., 2005). Shikimate titer in a strain with this mutation was 40 % higher (Sato et al., 2020).

The synthesis of aromatic compounds is a metabolically costly process that consumes the precursors PEP and E4P in addition to ATP and NADPH; thus, initial efforts to increase flux

towards the synthesis of aromatic compounds has focused on increasing PEP and E4P pools. This has made the enzymes of glycolysis, gluconeogenesis, pentose phosphate and their connected pathways the common targets. In addition to its major uptake route via PTS, which consumes PEP, *C. glutamicum* has been shown to use the inositol permease for glucose uptake, which does not consume PEP (Lindner et al., 2011). Thus, rerouting glucose to the permease should increase PEP availability. However, efficient glucose uptake by the permease necessitates overexpression of a glucokinase gene in addition to either *iolT1* or *iolT2* (Lindner et al., 2011). Therefore, in this study, the glucokinase from *B. subtilis* and *iolT2* from *C. glutamicum* (Pérez-García et al., 2016) were integrated together into *ptsG* locus to inactivate the PTS. Contrary to expectations, L-tyrosine titer obtained with the constructed AROM23 strain was 1.3-fold lower than that obtained with its parent strain AROM2, despite the effort to increase PEP availability. However, retaining the PTS system for overproduction of shikimate was reported to be favorable (Sato et al., 2020), which is compatible with the results of this study. Another possibility to increase the PEP pool for L-tyrosine production in AROM31, could be to inactivate the PEP carboxylase gene, *ppc*, to inhibit the conversion of PEP to oxaloacetate (Walter et al., 2020). The overexpression of *aroB* in AROM31 can also be considered to increase carbon flux towards shikimate for L-tyrosine production since Sato et al. (Sato et al., 2020) reported a 1.5-fold increase in shikimate production with this modification.

As the final step, AROM3, the strain with the highest L-tyrosine titer on glucose, was considered for utilization of glucose, xylose, and their mixtures, in order to evaluate its potential for sustainable production from lignocellulosic feedstocks. This production was expected to be not only environmentally friendly but also to increase PEP and E4P availabilities for shikimate pathway. Lignocellulosic hydrolysates contain high amounts of xylose, which internalization is independent of PEP, upon the activities of xylose isomerase and xylulokinase, encoded by *xylA* and *xylB*, respectively. Here, it is demonstrated that xylose could be metabolized by AROM31 and when a glucose:xylose mixture of 1:3 was used, a statistically significant improvement of 12.5 % ($p=0.01$) in L-tyrosine titer was observed as compared to AROM3. This strain has a high potential for the production of value-added chemicals derived from L-tyrosine such as tyramine, L-DOPA, and flavonoids (Wu et al., 2018). Additionally, the renewable carbon sources with high xylose content (Narisetty et al., 2022) could serve as suitable sources for sustainable and bio-friendly production of L-tyrosine and L-tyrosine-derived compounds using AROM31 strain.

4.2.2 Analysis of L-tyrosine overproducer mutant *C. glutamicum* ATCC 21573

Classical breeding has long been used to obtain industrially useful *C. glutamicum* mutants for amino acid production. Unfortunately, these strains obtained through undirected mutagenesis commonly possess a large number of mutations that are not beneficial for a stable process. Indeed, the titer obtained with this strain in this work was much lower than that of reported. This poses a serious disadvantage for industrial production. Here, the genome sequence of the L-tyrosine overproducer *C. glutamicum* ATCC 21573 (Hagino et al., 1974) was comparatively examined compared to the wild-type strain of *C. glutamicum* for the pathways of central carbon and aromatic amino acid metabolism and their regulations in order to get an insight into L-tyrosine overproduction for our metabolic engineering efforts.

One important common between the constructed strain and *C. glutamicum* ATCC 21573 point that contributes to overproduction could be the mutation in the promoter region of *pheA* in *C. glutamicum* ATCC 21573 and the translational codon exchange in AROM3. This change in both strains reduced *pheA* gene expression, enhancing L-tyrosine production. The L-tyrosine overproducer *C. glutamicum* ATCC 21573 has been documented to be L-phenylalanine auxotroph; nevertheless, though slower and less, cells were growing in its absence in CGXII minimal media. Furthermore, L-phenylalanine supplementation did not completely restore growth, and its presence had an adverse effect on L-tyrosine titer, which is compatible with the results presented in this study. In conclusion, partly L-phenylalanine bradytrophy and partly carbon flux redistribution upstream from prephenate could explain L-tyrosine overproduction.

4.2.3 L-DOPA production using *C. glutamicum* AROM3

The rationally designed *C. glutamicum* AROM3 was then used for L-DOPA production. The final L-DOPA titer in the strain expressing the tyrosinase, AROM3D, was 185 ± 9 mg/L, which was 39 % higher than the titer obtained when L-tyrosine was externally added as the substrate for L-DOPA production (133 ± 35 mg/L L-DOPA) under the same conditions, as explained recently (Kurpejović et al., 2021).

Since the majority of processes developed for L-DOPA synthesis using tyrosinase were based on whole-cell biotransformation using pre-grown cells, the *C. glutamicum* CgEKV-I cells grown on glucose for L-DOPA synthesis were also exploited for L-tyrosine biotransformation. L-DOPA titer of 0.40 ± 0.01 g/L with 4 mM ascorbic acid was comparable to the values reported for *Brevundimonas* sp. SGJ, 0.402 g/L (Surwase et al., 2012) or for

Bacillus sp. JPJ, 0.497 g/L (Surwase & Jadhav, 2011). On the other hand, L-DOPA yield was 0.61 ± 0.02 g/g DCW with *C. glutamicum* CgEKV-I while it was ~ 0.42 and ~ 0.50 g/gDCW with *Brevundimonas* sp. SGJ and *Bacillus* sp. JPJ, respectively (Surwase et al., 2012; Surwase & Jadhav, 2011). Only after reaction parameters of biotransformation with *Brevundimonas* sp. SGJ were optimized and cell recycling was adopted, titer increased by almost sevenfold. Considering that from a liter of cultivation as much as 26.4 ± 1.9 g DCW *C. glutamicum* is obtained while only ~ 0.5 g DCW *Brevundimonas* sp. SGJ and ~ 5.5 g DCW *Bacillus* sp. JPJ could be obtained, many batches of biotransformation can be achieved with *C. glutamicum* just from a single cultivation.

In order to make a production process sustainable and biofriendly, cells should be grown on a renewable carbon source. To this end, different studies have evaluated the potential of the production of value-added chemicals by *C. glutamicum* using lignocellulosic materials as the sole carbon source. Gopinath et al. (2011) have reported that *C. glutamicum* grown in sulfuric acid hydrolysates of rice straw and wheat bran yielded 93 mM L-glutamate from either lignocellulosics hydrolysate. In another study, *C. glutamicum* GJ04, produced 61.7 g/L L-glutamate from acid pretreated wheat straw hydrolysate (Jin et al., 2020). Becker et al. (2018) was able to engineer *C. glutamicum* cells to efficiently consume not only carbohydrates but also the aromatics obtained from hydrothermal conversion of lignin from pine to produce 12.5 mM cis, cis-muconic acid. Later, Mhatre et al. (2022) demonstrated that corn stover biomass hydrolysates for simultaneous utilization of sugars and aromatics can be used for mixed-acid fermentation of lactate, succinate, and acetate. In another recent study, brown seaweed extract and brown seaweed hydrolysate from Laminaria hyperborean were used as green substrates to produce riboflavin with a titer of 1291.2 mg/L in cells engineered to consume mannitol and glucose (Pérez-García et al., 2022). In this work as a renewable carbon source hazelnut husk hydrolysate was used. To this end the CgEKV-II strain, capable of growing on glucose/xylose mixtures and producing L-DOPA, was evaluated for L-DOPA production from hazelnut husk. Incubation of CgEKV-II cells for 72 hours led to an L-DOPA titer of 20 ± 0.4 mg/L. This data is a firm basis for L-DOPA production from a renewable carbon source, however there is still space for further optimization.

CgEKV-II cells grown on husk were also collected and utilized to synthesize L-DOPA from commercially available L-tyrosine via whole-cell biotransformation. Via this method, L-DOPA titer increased significantly. In the first 72 hours of whole-cell biotransformation, in the absence of copper ions, titer was 31 mg/L, while with copper ions it was 82 mg/L. Both samples were supplemented with 4 mM of ascorbic acid. Further incubation increased the titer

slightly, however adversely affecting the productivity. Furthermore, when the L-tyrosine obtained from AROM3 strain was used for the biotransformation with the CgEKV-II cells grown on husk, the presence of copper ions reduced the final L-DOPA titer, while the presence of 4 mM of ascorbic acid as an L-DOPA antioxidant in the absence of copper ions led to a final L-DOPA titer of 202 ± 43 mg/L. This data have led to hypothesis that the whole-cell biotransformation process can be further improved by increasing the activity of tyrosinase enzyme, as reported by Molloy et al. (2013).

5. CONCLUSION

In this study, the main objective was to produce L-DOPA in *C. glutamicum* cells. To this end, firstly wild-type *C. glutamicum* ATCC 13032 grown on glucose and glucose/xylose mixtures was used for L-DOPA production with externally added L-tyrosine. Among the L-DOPA antioxidants tested were thymol, evaluated for the first time, and ascorbic acid. Next, in order to reduce the cost of L-DOPA production, L-tyrosine addition was circumvented by constructing an L-tyrosine overproducer strain. Then, for sustainable L-DOPA production, hazelnut husk hydrolysate was evaluated as a carbon source for this production. Finally, tyrosinase expressing cells were used for whole-cell biotransformation of L-tyrosine to L-DOPA.

When *R. solanacearum* tyrosinase was heterologously expressed in *C. glutamicum*, the highest titer with externally added L-tyrosine was 133 ± 35 mg/L L-DOPA on glucose and 255 ± 20 mg/L L-DOPA on glucose/xylose during fermentative production, with 0.4 and 0.2 mM thymol, respectively. During whole-cell biotransformation using these cells, ascorbic acid was proved to be more effective and led to the highest titer of 400 ± 10 mg/L with 6.6 mgDCW in the presence of 4 mM ascorbic acid. When hydrolysate from hazelnut husk was used as the sole carbon source, only 20 ± 1 mg/L of L-DOPA was produced with CgEKV-II strain during growth with 0.2 mM thymol. With the utilization of these cells for whole-cell biotransformation, a titer of 82 ± 1 mg/L of L-DOPA was obtained with 4 mM ascorbic acid.

The rationally designed *C. glutamicum* strains constructed to circumvent external L-tyrosine addition have demonstrated that coupling of the feedback resistant form of DAHP synthase with reduced expression of prephenate dehydratase for lower activity were adequate to enhance L-tyrosine production. Deletion of genes involved in branching pathway of protochuteate, *qsuABD*, and overexpression of shikimate pathway genes, *aroE* and *qsuC*, displayed no major effect on final L-tyrosine titer. The strain obtained with the most favorable modifications, AROM3 yielded 3.1 g L-tyrosine/L on glucose and 3.6 g L-tyrosine/L on a mixture of glucose and xylose. For this production, the L-phenylalanine was shown to be essential, since low L-phenylalanine concentrations led to reduced growth. Simultaneously, its high concentration led to a significant decrease in L-tyrosine titer, probably by acting as a feedback inhibitor. Unfortunately, AROM3 cells were unable to produced L-tyrosine when grown on husk hydrolysate.

With an attempt to further increase L-tyrosine titer, the unidentified aminotransferase of L-tyrosine biosynthesis was predicted and overexpressed. However, the expression of this gene, *dapC*, had no effect on L-tyrosine overproduction under the conditions tested in this study. As a final endeavor, the genome of the L-tyrosine producer strain, *C. glutamicum* ATCC 21573, was sequenced to get clues for possible genetic modifications to improve L-tyrosine titer, but no significant finding was obtained at this stage either. Overall, strains constructed in this study may serve as platform for the production of L-tyrosine and L-tyrosine-derived molecules not only from the most abundant carbon source glucose but also from renewable carbon sources with high glucose and xylose contents. With AROM3 strain expressing the tyrosinase, named as AROM3D, a titer of 185 ± 9 mg/L L-DOPA was obtained in the presence of 0.4 mM thymol. When the cells with the ability to utilize xylose were grown on husk hydrolysate as the carbon source and then used to convert L-tyrosine synthesized by AROM3 strain, a titer of 202 ± 43 mg/L of L-DOPA was obtained using 6 mg DCW in this biotransformation process.

In summary, this work evaluated the potential of *C. glutamicum* for production of two valuable compounds L-tyrosine and L-DOPA. The presented work suggested that for L-DOPA production whole-cell biotransformation was more favorable over fermentative production. The results also indicated that L-DOPA could be produced by *C. glutamicum* using a renewable carbon source.

As for future work, *aroB*, *aroK*, and *aroA* of the shikimate pathway could be overexpressed to evaluate their contribution to increase L-tyrosine titer and subsequent L-DOPA production. Additionally, alternative pretreatment methods to release fermentable sugars from hazelnut husk, such as steam explosion, could be evaluated to increase the sugar content in the hydrolysate.

REFERENCES

Ali, S., Ikram-ul-Haq, Qadeer, M. A., & Rajoka, M. I. (2005). Double mutant of Aspergillus oryzae for improved production of L-dopa (3,4-dihydroxyphenyl-L-alanine) from L-tyrosine. *Biotechnology and Applied Biochemistry*, *42*, 143–149. https://doi.org/10.1042/BA20040180

Ali, S., Shultz, J. L., & Ikram-ul-Haq. (2007). High performance microbiological transformation of L-tyrosine to L-dopa by Yarrowia lipolytica NRRL-143. *BMC Biotechnology*, *7*, 50. https://doi.org/10.1186/1472-6750-7-50

Arnow, L. E. (1937). Colorimetric Determination of the Components of 3,4-Dihydroxyphenylalanine-Tyrosine Mutants. *Journal of Biological Chemistry*, 531–538.

Averesch, N. J. H., & Krömer, J. O. (2018). Metabolic engineering of the shikimate pathway for production of aromatics and derived compounds-Present and future strain construction strategies. *Frontiers in Bioengineering and Biotechnology*, *6*(MAR). https://doi.org/10.3389/fbioe.2018.00032

Baumgart, M., Unthan, S., Rückert, C., Sivalingam, J., Grünberger, A., Kalinowski, J., Bott, M., Noack, S., & Frunzke, J. (2013). Construction of a Prophage-Free Variant of Corynebacterium glutamicum ATCC 13032 for Use as a Platform Strain for Basic Research and Industrial Biotechnology. *Applied and Environmental Microbiology*, *79*(19), 6006–6015. https://doi.org/10.1128/AEM.01634-13

Becker, J., Kuhl, M., Kohlstedt, M., Starck, S., & Wittmann, C. (2018). Metabolic engineering of Corynebacterium glutamicum for the production of cis , cis ‐ muconic acid from lignin. *Microbial Cell Factories*, *17*(115), 1–14. https://doi.org/10.1186/s12934-018-0963-2

Becker, J., Rohles, C. M., & Wittmann, C. (2018). Metabolically engineered Corynebacterium glutamicum for bio-based production of chemicals, fuels, materials, and healthcare products. *Metabolic Engineering*, *50*, 122–141. https://doi.org/10.1016/j.ymben.2018.07.008

Becker, J., & Wittmann, C. (2012). Systems and synthetic metabolic engineering for amino acid production - the heartbeat of industrial strain development. In *Current Opinion in Biotechnology*. https://doi.org/10.1016/j.copbio.2011.12.025

Becker, J., & Wittmann, C. (2015). Advanced biotechnology: Metabolically engineered cells for the bio-based production of chemicals and fuels, materials, and health-care products.

Angewandte Chemie - International Edition, *54*(11), 3328–3350. https://doi.org/10.1002/anie.201409033

Brocker, M., Schaffer, S., Mack, C., & Bott, M. (2009). Citrate utilization by Corynebacterium glutamicum is controlled by the CitAB two-component system through positive regulation of the citrate transport genes citH and tctCBA. *Journal of Bacteriology*, *191*(12), 3869–3880. https://doi.org/10.1128/JB.00113-09

Brüsseler, C., Radek, A., Tenhaef, N., Krumbach, K., Noack, S., & Marienhagen, J. (2018). The myo-inositol/proton symporter IolT1 contributes to D-xylose uptake in Corynebacterium glutamicum. *Bioresource Technology*, *249*(November 2017), 953–961. https://doi.org/10.1016/j.biortech.2017.10.098

Buchholz, J., Schwentner, A., Brunnenkan, B., Gabris, C., Grimm, S., Gerstmeir, R., Takors, R., Eikmanns, B. J., & Blombach, B. (2013). Platform Engineering of Corynebacterium glutamicum with Reduced Pyruvate Dehydrogenase Complex Activity for Improved Production of L -Lysine , L -Valine , and 2-Ketoisovalerate. *Applied and Environmental Microbiology*, *79*(18), 5566–5575. https://doi.org/10.1128/AEM.01741-13

Burschowsky, D., Thorbjørnsrud, H. V., Heim, J. B., Fahrig-Kamarauskaite, J., Würth-Roderer, K., Kast, P., & Krengel, U. (2018). Inter-Enzyme Allosteric Regulation of Chorismate Mutase in Corynebacterium glutamicum: Structural Basis of Feedback Activation by Trp. *Biochemistry*, *57*(5), 557–573. https://doi.org/10.1021/acs.biochem.7b01018

Buschke, N., Becker, J., Schäfer, R., Kiefer, P., Biedendieck, R., & Wittmann, C. (2013). Systems metabolic engineering of xylose-utilizing Corynebacterium glutamicum for production of 1,5-diaminopentane. *Biotechnology Journal*, *8*(5), 557–570. https://doi.org/10.1002/biot.201200367

Chávez-Béjar, M. I., Báez-Viveros, J. L., Martínez, A., Bolívar, F., & Gosset, G. (2012). Biotechnological production of l-tyrosine and derived compounds. *Process Biochemistry*, *47*(7), 1017–1026. https://doi.org/10.1016/j.procbio.2012.04.005

Da Silva, A. P., De Silva, N. F., Andrade, E. H. A., Gratieri, T., Setzer, W. N., Maia, J. G. S., & Da Silva, J. K. R. (2017). Tyrosinase inhibitory activity, molecular docking studies and antioxidant potential of chemotypes of Lippia origanoides (Verbenaceae) essential oils. *PLoS ONE*, *12*(5), 1–17. https://doi.org/10.1371/journal.pone.0175598

Darling, A. C. E., Mau, B., Blattner, F. R., & Perna, N. T. (2004). Mauve: Multiple alignment of conserved genomic sequence with rearrangements. *Genome Research*, *14*(7), 1394–1403. https://doi.org/10.1101/gr.2289704

Eggeling, L., & Bott, M. (Eds.). (2005). *Handbook of Corynebacterium glutamicum*. CRC Press, Boca Raton, Fla, USA.

Eikmanns, B. J., Kleinertz, E., Liehl, W., & Sahm, H. (1991). A family of Corynebacterium glutamicum/ Escerichia coli shuttle vectors for cloning, controlled gene expression, and promoter probing. *Gene*, *102*, 93–98.

Enei, H., Matsui, H., Nakazawa, H., Okumura, S., & Yamada, H. (1973). Synthesis of L-tyrosine or 3,4-dihydroxyphenyl-l-alanine from dl-serine and phenol or pyrocathechol. *Agricultural and Biological Chemistry*, *37*(3), 493–499. https://doi.org/10.1080/00021369.1973.10860717

Erdogan, V. (2018). Hazelnut production in Turkey: Current situation, problems and future prospects. *Acta Horticulturae*, *1226*, 13–23. https://doi.org/10.17660/ActaHortic.2018.1226.2

Fazel, A. M., & Jensen, R. (1979). Obligatory Biosynthesis of L-Tyrosine via the Pretyrosine Branchlet in Coryneform Bacteria. *Journal of Bacteriology*, *138*(3), 805–815.

Floras, N., Xiao, J., Berry, A., Bolivar, F., & Valle, F. (1996). Pathway engineering for the production of aromatic compounds in Escherichia coli. *Nature Biotechnology*, *14*, 620–623.

Foor, F., Morin, N., & Bostian, K. A. (1993). Production of L-dihydroxyphenylalanine in Escherichia coli with the tyrosine phenol-lyase gene cloned from Erwinia herbicola. *Applied and Environmental Microbiology*, *59*(9), 3070–3075.

Fordjour, E., Adipah, F. K., Zhou, S., Du, G., & Zhou, J. (2019). Metabolic engineering of Escherichia coli BL21 (DE3) for de novo production of l‐ DOPA from d‐ glucose. *Microbial Cell Factories*, 1–10. https://doi.org/10.1186/s12934-019-1122-0

Gibson, D. G., Young, L., Chuang, R. Y., Venter, J. C., Hutchison, C. A., & Smith, H. O. (2009). Enzymatic assembly of DNA molecules up to several hundred kilobases. *Nature Methods*, *6*(5), 343–345. https://doi.org/10.1038/nmeth.1318

Gopinath, V., Meiswinkel, T. M., Wendisch, V. F., & Nampoothiri, K. M. (2011). Amino acid production from rice straw and wheat bran hydrolysates by recombinant pentose-utilizing Corynebacterium glutamicum. *Applied Microbiology and Biotechnology*, *92*(5), 985–996. https://doi.org/10.1007/s00253-011-3478-x

Graindorge, M., Giustini, C., Kraut, A., Moyet, L., Curien, G., & Matringe, M. (2014). Three different classes of Aminotransferases Evolved Prephenate Aminotransferase functionality in Arogenate-competent Microorganisms. *Journal of Biological Chemistry*, *289*(6), 3198–3208. https://doi.org/10.1074/jbc.M113.486480

Gu, P., Yang, F., Li, F., Liang, Q., & Qi, Q. (2013). Knocking out analysis of tryptophan permeases in Escherichia coli for improving L-tryptophan production. *Applied Microbiology and Biotechnology*, *97*, 6677–6683. https://doi.org/10.1007/s00253-013-4988-5

Hagino, H, Nakayama, K., & Yoshida, H. (1974). *Process for the production of L-tyrosine. US Patent 3787287* (Patent No. US Patent 3787287).

Hagino, Hiroshi, & Nakayama, K. (1973a). L-Tyrosine Production by Analog-resistant Mutants Derived from a Phenylalanine Auxotroph of Corynebacterium glutamicum. *Agricultural and Biological Chemistry*, *37*(9), 2013–1023.

Hagino, Hiroshi, & Nakayama, K. (1973b). L-Tyrosine Production by Analog-resistant Prototrophic Mutants of Glutamic Acid Producing Bacteria. *Agricultural and Biological Chemistry*, *37*(9), 2007–2011. https://doi.org/10.1080/00021369.1973.10860957

Hagino, Hiroshi, & Nakayama, K. (1974). L-Phenylalanine Production by Analog-resistant Mutants of Corynebacterium glutamicum. *Agr. BioI. Chem.*, *38*(1), 157–161. https://doi.org/10.1080/00021369.1974.10861130

Hagino, Hiroshi, & Nakayama, K. (1975). L-Tryptophan Production by Analog-resistant Mutants Derived from a Phenylalanine and Tyrosine Double Auxotroph of Corynebacterium. *Agr. Biol. Chem*, *39*(2), 343–349. https://doi.org/10.1080/00021369.1975.10861621

Hagino, Hiroshi, Yoshida, H., Kato, F., Arai, Y., Katsumata, R., & Nakayama, K. (1973). L-Tyrosine production by Polyauxotrophic Mutants of Corynebacterium glutamicum. *Agricultural and Biological Chemistry*, *37*(9), 2001–2005.

Hanahan, D. (1983). Studies on transformation of Escherichia coli with plasmids. *Journal of Molecular Biology*, *166*(4), 557–580. https://doi.org/10.1016/S0022-2836(83)80284-8

Harisha, S. (2007). Biotechnology Procedures and Experiments Handbook. In *Infinity Science Press Llc*.

Harmsen, P., Bermudez, L., & Bakker, R. (2010). Literature Review of Physical and Chemical Pretreatment Processes for Lignocellulosic Biomass. In *Biomass* (Issue September).

Hartmann, M., Tauch, A., Eggeling, L., Bathe, B., Möckel, B., Pühler, A., & Kalinowski, J. (2003). Identification and characterization of the last two unknown genes, dapC and dapF, in the succinylase branch of the L-lysine biosynthesis of Corynebacterium glutamicum. *Journal of Biotechnology*, *104*(1–3), 199–211. https://doi.org/10.1016/S0168-1656(03)00156-1

Heider, S. A. E., & Wendisch, V. F. (2015). Engineering microbial cell factories: Metabolic engineering of Corynebacterium glutamicum with a focus on non-natural products. *Biotechnology Journal*, *10*(8), 1170–1184. https://doi.org/10.1002/biot.201400590

Henke, N. A., Heider, S. A. E., Peters-Wendisch, P., & Wendisch, V. F. (2016). Production of the marine carotenoid astaxanthin by metabolically engineered Corynebacterium glutamicum. *Marine Drugs*, *14*(7), 1–21. https://doi.org/10.3390/md14070124

Hernández-Chávez, G., Martinez, A., & Gosset, G. (2019). Metabolic engineering strategies for caffeic acid production in Escherichia coli. *Electronic Journal of Biotechnology*, *38*, 19–26. https://doi.org/10.1016/j.ejbt.2018.12.004

Hernández-Romero, D., Sanchez-Amat, A., & Solano, F. (2006). A tyrosinase with an abnormally high tyrosine hydroxylase/dopa oxidase ratio: Role of the seventh histidine and accessibility to the active site. *FEBS Journal*, *273*(2), 257–270. https://doi.org/10.1111/j.1742-4658.2005.05038.x

Ikeda, M., & Nakagawa, S. (2003). The Corynebacterium glutamicum genome: Features and impacts on biotechnological processes. *Applied Microbiology and Biotechnology*, *62*(2–3), 99–109. https://doi.org/10.1007/s00253-003-1328-1

Ikeda, M., Okamoto, K., & Katsumata, R. (1999). Cloning of the transketolase gene and the effect of its dosage on aromatic amino acid production in Corynebacterium glutamicum. *Applied Microbiology and Biotechnology*, *51*(2), 201–206. https://doi.org/10.1007/s002530051382

Ikeda, Masato. (2006). Towards bacterial strains overproducing L-tryptophan and other aromatics by metabolic engineering. *Applied Microbiology and Biotechnology*, *69*(6), 615–626. https://doi.org/10.1007/s00253-005-0252-y

Ikeda, Masato. (2012). Sugar transport systems in Corynebacterium glutamicum: Features and applications to strain development. *Applied Microbiology and Biotechnology*, *96*(5), 1191–1200. https://doi.org/10.1007/s00253-012-4488-z

Ikeda, Masato, & Katsumata, R. (1992). Metabolic Engineering To Produce Tyrosine or Phenylalanine in Tryptophan-Producing Corynebacterium glutamicum Strain. *Applied and Environmental Microbiology*, *58*(3), 781–785.

Ikeda, Masato, & Katsumata, R. (1999). Hyperproduction of tryptophan by Corynebacterium glutamicum with the modified pentose phosphate pathway. *Applied and Environmental Microbiology*, *65*(6), 2497–2502. https://doi.org/10.1128/aem.70.12.7277-7287.2004

Ikram-ul-Haq, Ali, S., & Qadeer, M. A. (2002). Biosynthesis of L-DOPA by Aspergillus oryzae. *Bioresource Technology*, *85*(1), 25–29. https://doi.org/10.1016/S0960-

8524(02)00060-3

Jakoby, M., Carole-Estelle, Ngouoto-Nkili, & Burkovski, A. (1999). Construction and application of new Corynebacterium glutamicum vectors. *Biotechnology Techniques*, *13*(6), 437–441. https://doi.org/10.1023/A:1008968419217

Jin, C., Huang, Z., & Bao, J. (2020). High-Titer Glutamic Acid Production from Lignocellulose Using an Engineered Corynebacterium glutamicum with Simultaneous Co-utilization of Xylose and Glucose. *ACS Sustainable Chemistry & Engineering*, *8*(16), 6315–6322. https://doi.org/https://doi.org/10.1021/acssuschemeng.9b07839

Juminaga, D., Baidoo, E. E. K., Redding-Johanson, A. M., Batth, T. S., Burd, H., Mukhopadhyay, A., Petzold, C. J., & Keasling, J. D. (2012). Modular engineering of L-tyrosine production in Escherichia coli. *Applied and Environmental Microbiology*, *78*(1), 89–98. https://doi.org/10.1128/AEM.06017-11

Kalinowski, J., Bathe, B., Bartels, D., Bischoff, N., Bott, M., Burkovski, A., Dusch, N., Eggeling, L., Eikmanns, B. J., Gaigalat, L., Goesmann, A., Hartmann, M., Huthmacher, K., Krämer, R., Linke, B., McHardy, A. C., Meyer, F., Möckel, B., Pfefferle, W., … Tauch, A. (2003). The complete Corynebacterium glutamicum ATCC 13032 genome sequence and its impact on the production of L-aspartate-derived amino acids and vitamins. *Journal of Biotechnology*, *104*(1–3), 5–25. https://doi.org/10.1016/S0168-1656(03)00154-8

Kallscheuer, N., & Marienhagen, J. (2018). Corynebacterium glutamicum as platform for the production of hydroxybenzoic acids. *Microb Cell Fact*, *17*(70), 1–13.

Kawaguchi, H., Vertes, A. A., Okino, S., Inui, M., & Yukawa, H. (2006). Engineering of a xylose metabolic pathway in Corynebacterium glutamicum. *Applied and Environmental Microbiology*, *72*(5). https://doi.org/10.1128/AEM.72.5.3418-3428.2006

Kermasha, S., & Tse, M. (2000). Biocatalysis of tyrosinase in chloroform medium, using selected phenolic substrates. *Journal of Chemical Technology and Biotechnology*, *75*(6), 475–483. https://doi.org/10.1002/1097-4660(200006)75:6<475::AID-JCTB237>3.0.CO;2-2

Kim, Y. J., & Uyama, H. (2005). Tyrosinase inhibitors from natural and synthetic sources: Structure, inhibition mechanism and perspective for the future. *Cellular and Molecular Life Sciences*, *62*(15), 1707–1723. https://doi.org/10.1007/s00018-005-5054-y

Kinoshita, S., Udaka, S., & Shimono, M. (1957). Studies on the amino acid fermentation. Part I. Production of L-glutamic acid by various microorganisms. *Journal of General and Applied Microbiology*, *3*, 193–205. https://doi.org/10.2323/jgam.3.193

Klaffl, S., Brocker, M., Eikmanns, B. J., & Bott, M. (2013). Complex Regulation of the Phosphoenolpyruvate Carboxykinase Gene pck and Characterization of Its GntR-Type Regulator IolR as a Repressor of myo -Inositol Utilization Genes in Corynebacterium glutamicum. *Journal of Bacteriology*, *195*(18), 4283–4296. https://doi.org/10.1128/JB.00265-13

Knowles, W. S. (2004). *Asymmetric Catalysis on Industrial Scale: Challenges, Approaches and Solutions* (H.-U. Blaser & E. Schmidt (Eds.); pp. 21–38). Wiley-VCH Verlag GmbH & Co. KGaA, Weinheim.

Kogure, T., Kubota, T., Suda, M., Hiraga, K., & Inui, M. (2016). Metabolic engineering of Corynebacterium glutamicum for shikimate overproduction by growth-arrested cell reaction. *Metabolic Engineering*, *38*, 204–216. https://doi.org/10.1016/j.ymben.2016.08.005

Kortmann, M., Kuhl, V., Klaffl, S., & Bott, M. (2015). A chromosomally encoded T7 RNA polymerase-dependent gene expression system for Corynebacterium glutamicum: Construction and comparative evaluation at the single-cell level. *Microbial Biotechnology*, *8*(2), 253–265. https://doi.org/10.1111/1751-7915.12236

Koyanagi, T., Katayama, T., Suzuki, H., Nakazawa, H., Yokozeki, K., & Kumagai, H. (2005). Effective production of 3,4-dihydroxyphenyl-L-alanine (L-DOPA) with Erwinia herbicola cells carrying a mutant transcriptional regulator TyrR. *Journal of Biotechnology*, *115*, 303–306. https://doi.org/10.1016/j.jbiotec.2004.08.016

Kremling, A., Kremling, S., & Bettenbrock, K. (2009). Catabolite repression in Escherichia coli - A comparison of modelling approaches. *FEBS Journal*, *276*(2), 594–602. https://doi.org/10.1111/j.1742-4658.2008.06810.x

Krishnaveni, R., Rathod, V., Thakur, M. S., & Neelgund, Y. F. (2009). Transformation of L-tyrosine to L-dopa by a novel fungus, acremonium rutilum, under submerged fermentation. *Current Microbiology*, *58*(2), 122–128. https://doi.org/10.1007/s00284-008-9287-5

Kurpejović, E., Wendisch, V. F., & Sariyar Akbulut, B. (2021). Tyrosinase-based production of l-DOPA by Corynebacterium glutamicum. *Applied Microbiology and Biotechnology*, *0123456789*. https://doi.org/10.1007/s00253-021-11681-5

Lee, J. W., Kim, H. U., Choi, S., Yi, J., & Lee, S. Y. (2011). Microbial production of building block chemicals and polymers. *Current Opinion in Biotechnology*, *22*(6), 758–767. https://doi.org/10.1016/j.copbio.2011.02.011

Lee, Jang Young, & Xun, L. (1998). Novel biological process for L-DOPA production from

L-tyrosine by p-hydroxyphenylacetate 3-hydroxylase. *Biotechnology Letters*, *20*, 479–482. https://doi.org/10.1023/A:1005440229420

Lee, Joo Young, Na, Y. A., Kim, E., Lee, H. S., & Kim, P. (2016). The actinobacterium Corynebacterium glutamicum, an industrial workhorse. In *Journal of Microbiology and Biotechnology* (pp. 807–822). https://doi.org/10.4014/jmb.1601.01053

Lee, S. G., Ro, H. S., Hong, S. P., Kim, E. H., & Sung, M. H. (1996). Production of L-DOPA by thermostable tyrosine phenol-lyase of a thermophilic Symbiobacterium species overexpressed in recombinant Escherichia coli. *Journal of Microbiology and Biotechnology*, *6*(2), 98–102. https://doi.org/10.1016/j.algal.2016.08.014

Limayem, A., & Ricke, S. C. (2012). Lignocellulosic biomass for bioethanol production: Current perspectives, potential issues and future prospects. *Progress in Energy and Combustion Science*, *38*(4), 449–467. https://doi.org/10.1016/j.pecs.2012.03.002

Lindner, S. N., Seibold, G. M., Henrich, A., Krämer, R., & Wendisch, V. F. (2011). Phosphotransferase system-independent glucose utilization in Corynebacterium glutamicum by inositol permeases and glucokinases. *Applied and Environmental Microbiology*, *77*(11), 3571–3581. https://doi.org/10.1128/AEM.02713-10

Liu, G., Wu, J., Yang, H., & Bao, Q. (2010). Codon usage patterns in corynebacterium glutamicum: Mutational bias, natural selection and amino acid conservation. *Comparative and Functional Genomics*, *2010*. https://doi.org/10.1155/2010/343569

Liu, J., Wu, X., Yao, M., Xiao, W., & Zha, J. (2020). Chassis engineering for microbial production of chemicals: from natural microbes to synthetic organisms. *Current Opinion in Biotechnology*, *66*, 105–112. https://doi.org/10.1016/j.copbio.2020.06.013

Liu, L., Duan, X., & Wu, J. (2016). L-Tryptophan Production in Escherichia coli Improved by Weakening the Pta-AckA Pathway. *PLOS One*, *0158200*, 1–16. https://doi.org/10.1371/journal.pone.0158200

Lütke-Eversloh, T., Santos, C. N. S., & Stephanopoulos, G. (2007). Perspectives of biotechnological production of L-tyrosine and its applications. *Applied Microbiology and Biotechnology*, *77*(4), 751–762. https://doi.org/10.1007/s00253-007-1243-y

Lütke-Eversloh, T., & Stephanopoulos, G. (2007). L-Tyrosine production by deregulated strains of Escherichia coli. *Applied Microbiology and Biotechnology*, *75*, 103–110. https://doi.org/10.1007/s00253-006-0792-9

Mao, Y., Li, G., Chang, Z., Tao, R., Cui, Z., Wang, Z., Tang, Y. J., Chen, T., & Zhao, X. (2018). Metabolic engineering of Corynebacterium glutamicum for efficient production of succinate from lignocellulosic hydrolysate. *Biotechnology for Biofuels*, *11*(1), 1–17.

https://doi.org/10.1186/s13068-018-1094-z

Marienhagen, J., Kennerknecht, N., Sahm, H., & Eggeling, L. (2005). Functional analysis of all aminotransferase proteins inferred from the genome sequence of Corynebacterium glutamicum. *Journal of Bacteriology*, *187*(22), 7639–7646. https://doi.org/10.1128/JB.187.22.7639-7646.2005

Matsumura, E., Nakagawa, A., Tomabechi, Y., Ikushiro, S., Sakaki, T., Katayama, T., Yamamoto, K., Kumagai, H., Sato, F., & Minami, H. (2018). Microbial production of novel sulphated alkaloids for drug discovery. *Scientific Reports*, *8*(1), 1–10. https://doi.org/10.1038/s41598-018-26306-7

Matsumura, E., Nakagawa, A., Tomabechi, Y., Koyanagi, T., Kumagai, H., Yamamoto, K., Katayama, T., Sato, F., & Minami, H. (2017). Laboratory-scale production of (S)-reticuline, an important intermediate of benzylisoquinoline alkaloids, using a bacterial-based method. *Bioscience, Biotechnology and Biochemistry*, *81*(2), 396–402. https://doi.org/10.1080/09168451.2016.1243985

Meiswinkel, T. M., Gopinath, V., Lindner, S. N., Nampoothiri, K. M., & Wendisch, V. F. (2013). Accelerated pentose utilization by Corynebacterium glutamicum for accelerated production of lysine, glutamate, ornithine and putrescine. *Microbial Biotechnology*, *6*(2). https://doi.org/10.1111/1751-7915.12001

Mhatre, A., Shinde, S., Jha, A. K., Rodriguez, A., Wardak, Z., Jansen, A., Gladden, J. M., George, A., Davis, R. W., & Varman, A. M. (2022). Corynebacterium glutamicum as an Efficient Omnivorous Microbial Host for the Bioconversion of Lignocellulosic Biomass. *Frontiers in Bioengineering and Biotechnology*, *10*(April), 1–14. https://doi.org/10.3389/fbioe.2022.827386

Min, K., Park, D.-H., & Yoo, Y. J. (2010). Electroenzymatic synthesis of l -DOPA. *Journal of Biotechnology*, *146*(1–2), 40–44. https://doi.org/10.1016/j.jbiotec.2010.01.002

Min, K., Park, K., & Park, D. (2015). Overview on the biotechnological production of L -DOPA. *Applied Microbiology and Biotechnology*, *99*, 575–584. https://doi.org/10.1007/s00253-014-6215-4

Molloy, S., Nikodinovic-Runic, J., Martin, L. B., Hartmann, H., Solano, F., Decker, H., & O'Connor, K. E. (2013). Engineering of a bacterial tyrosinase for improved catalytic efficiency towards D-tyrosine using random and site directed mutagenesis approaches. *Biotechnology and Bioengineering*, *110*(7), 1849–1857. https://doi.org/10.1002/bit.24859

Nagatsua, T., & Sawadab, M. (2009). l-dopa therapy for Parkinson's disease: Past, present,

and future. *Parkinsonism and Related Disorders*, *15*(1), 3–8. https://doi.org/10.1016/S1353-8020(09)70004-5

Nakagawa, A., Minami, H., Kim, J. S., Koyanagi, T., Katayama, T., Sato, F., & Kumagai, H. (2011). A bacterial platform for fermentative production of plant alkaloids. *Nature Communications*, *2*(1), 326–328. https://doi.org/10.1038/ncomms1327

Narisetty, V., Cox, R., Bommareddy, R., Agrawal, D., Ahmad, E., Pant, K. K., Chandel, A. K., Bhatia, S. K., Kumar, D., Binod, P., Gupta, V. K., & Kumar, V. (2022). Valorisation of xylose to renewable fuels and chemicals, an essential step in augmenting the commercial viability of lignocellulosic biorefineries. *Sustainable Energy and Fuels*, *6*(1), 29–65. https://doi.org/10.1039/d1se00927c

Nikolova, G., Karamalakova, Y., & Gadjeva, V. (2019). Reducing oxidative toxicity of L-dopa in combination with two different antioxidants: an essential oil isolated from Rosa Damascena Mill., and vitamin C. *Toxicology Reports*, *6*(March), 267–271. https://doi.org/10.1016/j.toxrep.2019.03.006

Ohnishi, J., Katahira, R., Mitsuhashi, S., Kakita, S., & Ikeda, M. (2005). A novel gnd mutation leading to increased L-lysine production in Corynebacterium glutamicum. *FEMS Microbiology Letters*, *242*(2), 265–274. https://doi.org/10.1016/j.femsle.2004.11.014

Para, G., Lucciardi, P., & Baratti, J. (1985). *Synthesis of L-tyrosine by immobilized*. 273–279.

Park, H. S., Lee, J. Y., & Kim, H. S. (1998). Production of L-DOPA(3,4-dihydroxyphenyl-L-alanine) from benzene by using a hybrid pathway. *Biotechnology and Bioengineering*, *58*(2–3), 339–343. https://doi.org/10.1002/(SICI)1097-0290(19980420)58:2/3<339::AID-BIT36>3.0.CO;2-4

Pátek, M., Nešvera, J., Guyonvarch, A., Reyes, O., & Leblon, G. (2003). Promoters of Corynebacterium glutamicum. *Journal of Biotechnology*, *104*(1–3), 311–323. https://doi.org/10.1016/S0168-1656(03)00155-X

Pavan, M. E., López, N. I., & Pettinari, M. J. (2020). Melanin biosynthesis in bacteria, regulation and production perspectives. *Applied Microbiology and Biotechnology*, *104*(4), 1357–1370. https://doi.org/10.1007/s00253-019-10245-y

Pérez-García, F., Burgardt, A., Kallman, D. R., Wendisch, V. F., & Bar, N. (2021). Dynamic co-cultivation process of corynebacterium glutamicum strains for the fermentative production of riboflavin. *Fermentation*, *7*(1). https://doi.org/10.3390/fermentation7010011

Pérez-García, F., Klein, V. J., Brito, L. F., & Brautaset, T. (2022). From Brown Seaweed to a

Sustainable Microbial Feedstock for the Production of Riboflavin. *Frontiers in Bioengineering and Biotechnology*, *10*(April), 1–15. https://doi.org/10.3389/fbioe.2022.863690

Pérez-García, F., Peters-Wendisch, P., & Wendisch, V. F. (2016). Engineering Corynebacterium glutamicum for fast production of l-lysine and l-pipecolic acid. *Applied Microbiology and Biotechnology*, *100*(18), 8075–8090. https://doi.org/10.1007/s00253-016-7682-6

Peters-Wendisch, P. G., Schiel, B., Wendisch, V. F., Katsoulidis, E., Möckel, B., Sahm, H., & Eikmanns, B. J. (2001). Pyruvate carboxylase is a major bottleneck for glutamate and lysine production by Corynebacterium glutamicum. *Journal of Molecular Microbiology and Biotechnology*, *3*, 295–300. https://doi.org/10.1097/00004647-199703000-00009

Pfeifenschneider, J., Brautaset, T., & Wendisch, V. F. (2012). Perspective: Jatropha cultivation in southern India: Assessing farmers' experiences. *Biofuels, Bioproducts and Biorefining*, *6*(3), 246–256. https://doi.org/10.1002/bbb

Pühler, A., & Schwarzer, A. (1991). Manipulation of Corynebacterium glutamicum by gene disruption and replacement. *Nature Biotechnology*, *9*, 1067–1071. https://doi.org/10.1038/nbt0191-84

Purwanto, H. S., Kang, M.-S., Ferrer, L., Han, S.-S., Lee, J.-Y., Kim, H.-S., & Lee, J.-H. (2018). Rational engineering of the shikimate and related pathways in Corynebacterium glutamicum for 4-hydroxybenzoate production. *Journal of Biotechnology*, *282*(April), 92–100. https://doi.org/10.1016/j.jbiotec.2018.07.016

Ros, J. R., Rodriguez-lopez, J. N., & Garcia-Canovas, F. (1993). Effect of L-ascorbic acid on the monophenolase activity of tyrosinase. *Biochem J*, *295*, 309–312. https://doi.org/10.1042/bj2950309

Sasaki, Y., Eng, T., Herbert, R. A., Trinh, J., Chen, Y., Rodriguez, A., Gladden, J., Simmons, B. A., Petzold, C. J., & Mukhopadhyay, A. (2019). Engineering Corynebacterium glutamicum to produce the biogasoline isopentenol from plant biomass hydrolysates. *Biotechnology for Biofuels*, *12*(1), 1–15. https://doi.org/10.1186/s13068-019-1381-3

Sasikumar, K., Hannibal, S., Wendisch, V. F., & Nampoothiri, K. M. (2021). Production of Biopolyamide Precursors 5-Amino Valeric Acid and Putrescine From Rice Straw Hydrolysate by Engineered Corynebacterium glutamicum. *Frontiers in Bioengineering and Biotechnology*, *9*(March), 1–9. https://doi.org/10.3389/fbioe.2021.635509

Sato, N., Kishida, M., Nakano, M., Hirata, Y., & Tanaka, T. (2020). Metabolic Engineering of Shikimic Acid-Producing Corynebacterium glutamicum From Glucose and Cellobiose

Retaining Its Phosphotransferase System Function and Pyruvate Kinase Activities. *Frontiers in Bioengineering and Biotechnology*, *8*(September), 1–14. https://doi.org/10.3389/fbioe.2020.569406

Satooka, H., & Kubo, I. (2011). Effects of thymol on mushroom tyrosinase-catalyzed melanin formation. *Journal of Agricultural and Food Chemistry*, *59*(16), 8908–8914. https://doi.org/10.1021/jf2014149

Schäfer, A., Tauch, A., Jsger, W., Kalinowski, J., Thierbachb, G., & Piihler, A. (1994). pK18mobsacB. *Gene*, *145*, 49–5201.

Schenck, C. A., & Maeda, H. A. (2018). Phytochemistry Tyrosine biosynthesis , metabolism , and catabolism in plants. *Phytochemistry*, *149*, 82–102. https://doi.org/10.1016/j.phytochem.2018.02.003

Shen, T., Liu, Q., Xie, X., Xu, Q., & Chen, N. (2012). Improved Production of Tryptophan in Genetically Engineered Escherichia coli with TktA and PpsA Overexpression. *Journal of Biomedicine and Biotechnology*, *605219*, 1–8. https://doi.org/10.1155/2012/605219

Simon, R., Priefer, U. & Pühler, A. (1983). A Broad Host Range Mobilization System for In Vivo Genetic Engineering: Transposon Mutagenesis in Gram Negative Bacteria. *Nature*, *1*(1), 784–791. https://doi.org/doi.org/10.1038/nbt1183-784

Singh, K. D., Schmalisch, M. H., Stülke, J., & Görke, B. (2008). Carbon catabolite repression in Bacillus subtilis: Quantitative analysis of repression exerted by different carbon sources. *Journal of Bacteriology*, *190*(21), 7275–7284. https://doi.org/10.1128/JB.00848-08

Singh, S., Cheng, G., Sathitsuksanoh, N., Wu, D., Varanasi, P., George, A., Balan, V., Gao, X., Kumar, R., Dale, B. E., Wyman, C. E., & Simmons, B. A. (2015). Comparison of different biomass pretreatment techniques and their impact on chemistry and structure. *Frontiers in Energy Research*, *3*(FEB), 1–12. https://doi.org/10.3389/fenrg.2014.00062

Singh, V., Haque, S., Niwas, R., Srivastava, A., Pasupuleti, M., & Tripathi, C. K. M. (2017). Strategies for fermentation medium optimization: An in-depth review. *Frontiers in Microbiology*, *7*, 2087. https://doi.org/10.3389/fmicb.2016.02087

Stansen, C., Uy, D., Delaunay, S., Eggeling, L., Goergen, J. L., & Wendisch, V. F. (2005). Characterization of a Corynebacterium glutamicum lactate utilization operon induced during temperature-triggered glutamate production. *Applied and Environmental Microbiology*. https://doi.org/10.1128/AEM.71.10.5920-5928.2005

Surek, E., & Buyukkileci, A. O. (2017). Production of xylooligosaccharides by autohydrolysis of hazelnut (Corylus avellana L.) shell. *Carbohydrate Polymers*, *174*, 565–571.

https://doi.org/10.1016/j.carbpol.2017.06.109

Surwase, S. N., & Jadhav, J. P. (2011). Bioconversion of l-tyrosine to l-DOPA by a novel bacterium Bacillus sp. JPJ. *Amino Acids*, *41*(2), 495–506. https://doi.org/10.1007/s00726-010-0768-z

Surwase, S. N., Patil, S. A., Apine, O. A., & Jadhav, J. P. (2012). Efficient microbial conversion of L-Tyrosine to L-DOPA by brevundimonas sp. SGJ. *Applied Biochemistry and Biotechnology*, *167*(5), 1015–1028. https://doi.org/10.1007/s12010-012-9564-4

Tang, S., Zheng, Y., Zhao, N. N., Lin, Y., Han, S., & Zheng, S. (2021). Synthesis of l-Tyrosine by Pichia pastoris Displaying Tyrosine Phenol Lyase. *ACS Food Science and Technology*, *1*(2), 186–192. https://doi.org/10.1021/acsfoodscitech.0c00019

Tanji, Y., Hattori, K., Suzuki, K., & Miyanaga, K. (2008). Spontaneous deletion of a 209-kilobase-pair fragment from the Escherichia coli genome occurs with acquisition of resistance to an assortment of infectious phages. *Applied and Environmental Microbiology*, *74*(14), 4256–4263. https://doi.org/10.1128/AEM.00243-08

Taylor, P. P., Pantaleone, D. P., Senkpeil, R. F., & Fotheringham, I. G. (1998). Novel biosynthetic approaches to the production of unnatural amino acids using transaminases. *Trends Biotechnol*, *16*, 412–418.

Torres, V., & Voit, E. O. (2002). *Pathway Analysis and Optimization in Metabolic Engineering*. Cambridge University Press, UK. https://doi.org/10.1017/CBO9780511546334

Tuncagil, S., Kayahan, S. K., Bayramoglu, G., Arica, M. Y., & Toppare, L. (2009). l-Dopa synthesis using tyrosinase immobilized on magnetic beads. *Journal of Molecular Catalysis B: Enzymatic*, *58*(1–4), 187–193. https://doi.org/10.1016/j.molcatb.2008.12.014

Veldmann, K. H., Dachwitz, S., Risse, J. M., Lee, J., Sewald, N., & Wendisch, V. F. (2019). Bromination of L -tryptophan in a Fermentative Process With Corynebacterium glutamicum. *Frontiers in Bioengineering and Biotechnology*, *7*(September), 1–13. https://doi.org/10.3389/fbioe.2019.00219

Walter, T., Al Medani, N., Burgardt, A., Cankar, K., Ferrer, L., Kerbs, A., Lee, J. H., Mindt, M., Risse, J. M., & Wendisch, V. F. (2020). Fermentative n-methylanthranilate production by engineered corynebacterium glutamicum. *Microorganisms*, *8*(6), 1–20. https://doi.org/10.3390/microorganisms8060866

Wei, T., Cheng, B. Y., & Liu, J. Z. (2016a). Genome engineering Escherichia coli for L-DOPA overproduction from glucose. *Scientific Reports*, *6*(July), 1–9.

https://doi.org/10.1038/srep30080

Wendisch, V. F., Bott, M., & Eikmanns, B. J. (2006). Metabolic engineering of Escherichia coli and Corynebacterium glutamicum for biotechnological production of organic acids and amino acids. *Current Opinion in Microbiology*, *9*, 268–274. https://doi.org/10.1016/j.mib.2006.03.001

Wendisch, V. F., Brito, L. F., Gil Lopez, M., Hennig, G., Pfeifenschneider, J., Sgobba, E., & Veldmann, K. H. (2016). The flexible feedstock concept in Industrial Biotechnology: Metabolic engineering of Escherichia coli, Corynebacterium glutamicum, Pseudomonas, Bacillus and yeast strains for access to alternative carbon sources. *Journal of Biotechnology*, *234*, 139–157. https://doi.org/10.1016/j.jbiotec.2016.07.022

Wendisch, V. F., Graaf, A. A. D. E., & Sahm, H. (2000). Quantitative Determination of Metabolic Fluxes during Coutilization of Two Carbon Sources: Comparative Analyses with. *Microbiology*, *182*(11), 3088–3096.

Wibberg, D., Andersson, L., Tzelepis, G., Rupp, O., Blom, J., Jelonek, L., Pühler, A., Fogelqvist, J., Varrelmann, M., Schlüter, A., & Dixelius, C. (2016). Genome analysis of the sugar beet pathogen Rhizoctonia solani AG2-2IIIB revealed high numbers in secreted proteins and cell wall degrading enzymes. *BMC Genomics*, *17*(1), 1–12. https://doi.org/10.1186/s12864-016-2561-1

Wichers, H., Malingre, T. M., & Huizing, H. J. (1983). Planta 9. *New York*, *158*, 482–486. https://doi.org/10.1007/BF00397239

Wu, F., Cao, P., Song, G., Chen, W., & Wang, Q. (2018). Expanding the repertoire of aromatic chemicals by microbial production. *Journal of Chemical Technology and Biotechnology*, *93*(10), 2804–2816. https://doi.org/10.1002/jctb.5690

Yakandawala, N., Romeo, T., Friesen, A. D., & Madhyastha, S. (2008). Metabolic engineering of Escherichia coli to enhance phenylalanine production. *Applied Microbiology and Biotechnology*, *78*(2), 283–291.

Yang, X., Zhang, X., & Zhou, R. (2001). Determination of l-Dopa Content and Other Significant Nitrogenous Compounds in the Seeds of Seven Mucuna and Stizolobium Species in China. *Pharmaceutical Biology*, *39*(4), 312–316. https://doi.org/10.1076/phbi.39.4.312.5905

Yildiz, H. B., Caliskan, S., Kamaci, M., Caliskan, A., & Yilmaz, H. (2013). L-Dopa synthesis catalyzed by tyrosinase immobilized in poly(ethyleneoxide) conducting polymers. *International Journal of Biological Macromolecules*, *56*, 34–40. https://doi.org/10.1016/j.ijbiomac.2013.01.031

Zahoor, A., Lindner, S. N., & Wendisch, V. F. (2012). Metabolic engineering of Corynebacterium glutamicum aimed at alternative carbon sources and new products. *Computational and Structural Biotechnology Journal*, *3*(4), e201210004. https://doi.org/10.5936/csbj.201210004

Zhang, C., Zhang, J., Kang, Z., Du, G., & Chen, J. (2015). Rational engineering of multiple module pathways for the production of l-phenylalanine in Corynebacterium glutamicum. *Journal of Industrial Microbiology and Biotechnology*, *42*, 787–797. https://doi.org/10.1007/s10295-015-1593-x

Zhang, C., Zhang, J., Kang, Z., Du, G., Yu, X., Wang, T., & Chen, J. (2013). Enhanced production of L-phenylalanine in Corynebacterium glutamicum due to the introduction of Escherichia coli wild-type gene aroH. *Journal of Industrial Microbiology and Biotechnology*, *40*(6), 643–651. https://doi.org/10.1007/s10295-013-1262-x

Zhou, H., Liao, X., Liu, L., Wang, T., Du, G., & Chen, J. (2011). Enhanced l-phenylalanine production by recombinant Escherichia coli BR-42 (pAP-B03) resistant to bacteriophage BP-1 via a two-stage feeding approach. *Journal of Industrial Microbiology and Biotechnology*, *38*(9), 1219–1227. https://doi.org/10.1007/s10295-010-0900-9

Zolghadri, S., Bahrami, A., Hassan Khan, M. T., Munoz-Munoz, J., Garcia-Molina, F., Garcia-Canovas, F., & Saboury, A. A. (2019). A comprehensive review on tyrosinase inhibitors. *Journal of Enzyme Inhibition and Medicinal Chemistry*, *34*(1), 279–309. https://doi.org/10.1080/14756366.2018.1545767

APPENDIX A

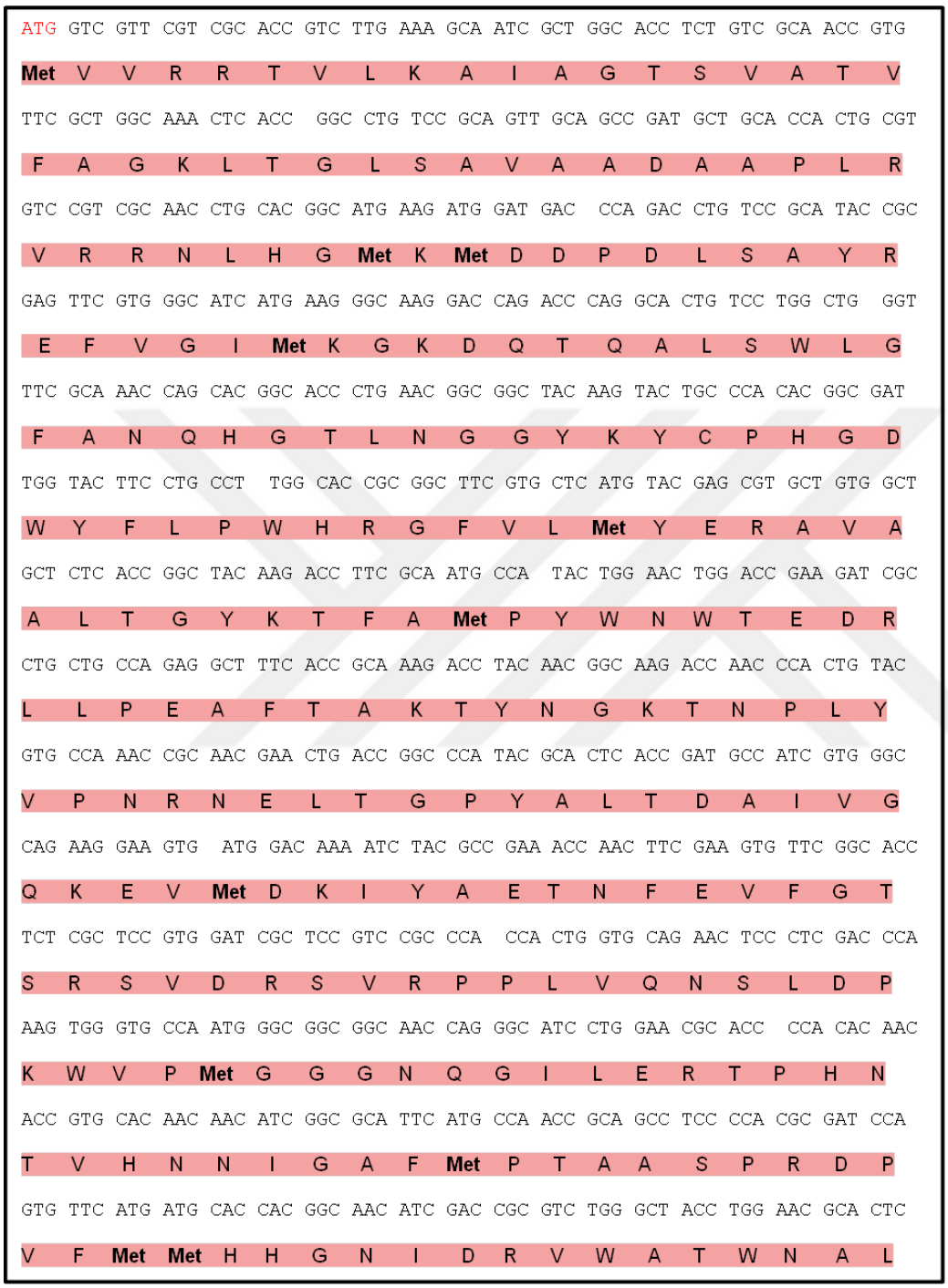

Figure A.1. The first tyrosinase gene synthesized by GenScript for expression in *C. glutamicum*.

AA	Codon	High		Low		AA	Codon	High		Low	
		N	RSCU	*N*	RSCU			*N*	RSCU	*N*	RSCU
Phe	UUU	149	0.17	1058	1.37	Ser	UCU	371	0.77	539	1.22
	UUC*	1608	1.83	481	0.63		**UCC***	1972	4.11	284	0.64
Leu	UUA	19	0.03	486	0.78		UCA	175	0.36	360	0.82
	UUG	239	0.33	1284	2.06		UCG	59	0.12	676	1.53
	CUU	656	0.91	707	1.13	Pro	CCU	527	0.92	492	1.11
	CUC*	1583	2.21	341	0.55		CCC	185	0.32	205	0.46
	CUA	140	0.2	274	0.44		**CCA***	1454	2.55	371	0.84
	CUG*	1666	2.32	651	1.04		CCG	119	0.21	705	1.59
Ile	AUU	412	0.43	1207	1.71	Thr	ACU	304	0.38	605	1.2
	AUC*	2477	2.57	654	0.93		**ACC***	2758	3.45	427	0.85
	AUA	7	0.01	257	0.36		ACA	74	0.09	378	0.75
Met	AUG	1143	1	863	1		ACG	61	0.08	601	1.2
Val	**GUU***	1495	1.45	883	1.11	Ala	**GCU***	1707	1.18	957	1.08
	GUC*	1631	1.59	452	0.57		**GCC***	1138	0.79	512	0.58
	GUA	336	0.33	396	0.5		**GCA***	2529	1.75	789	0.89
	GUG	650	0.63	1443	1.82		GCG	411	0.28	1300	1.46
Tyr	UAU	47	0.07	632	1.41	Cys	UGU	64	0.44	213	1.3
	UAC*	1311	1.93	262	0.59		**UGC***	230	1.56	114	0.7
TER	UAA	100	2.19	39	0.85	TER	UGA	4	0.09	47	1.03
	UAG	33	0.72	51	1.12	Trp	UGG	577	1	661	1
His	CAU	47	0.09	560	1.35	Arg	CGU	744	1.62	557	1.45
	CAC*	981	1.91	271	0.65		**CGC***	1887	4.11	362	0.94
Gln	CAA	284	0.34	539	0.79		CGA	89	0.19	317	0.83
	CAG*	1385	1.66	830	1.21		CGG	16	0.03	489	1.27
Asn	AAU	141	0.13	795	1.37	Ser	AGU	19	0.04	483	1.09
	AAC*	1955	1.87	369	0.63		AGC	284	0.59	305	0.69
Lys	AAA	298	0.26	664	0.91	Arg	AGA	5	0.01	236	0.62
	AAG*	2014	1.74	800	1.09		AGG	13	0.03	341	0.89
Asp	GAU	959	0.55	1537	1.53	Gly	GGU	1026	0.93	1069	1.46
	GAC*	2559	1.45	468	0.47		**GGC***	2830	2.55	562	0.77
Glu	**GAA***	2117	1.04	1095	0.91		GGA	549	0.5	568	0.78
	GAG	1941	0.96	1313	1.09		GGG	26	0.02	724	0.99

Figure A.2. The codon usage and preference in *C. glutamicum* (G. Liu et al., 2010).

N: number of codons

* Statistically excess codons in genes with high expression

High: Codons in highly expressed genes; Low: Codons in under-expressed genes.

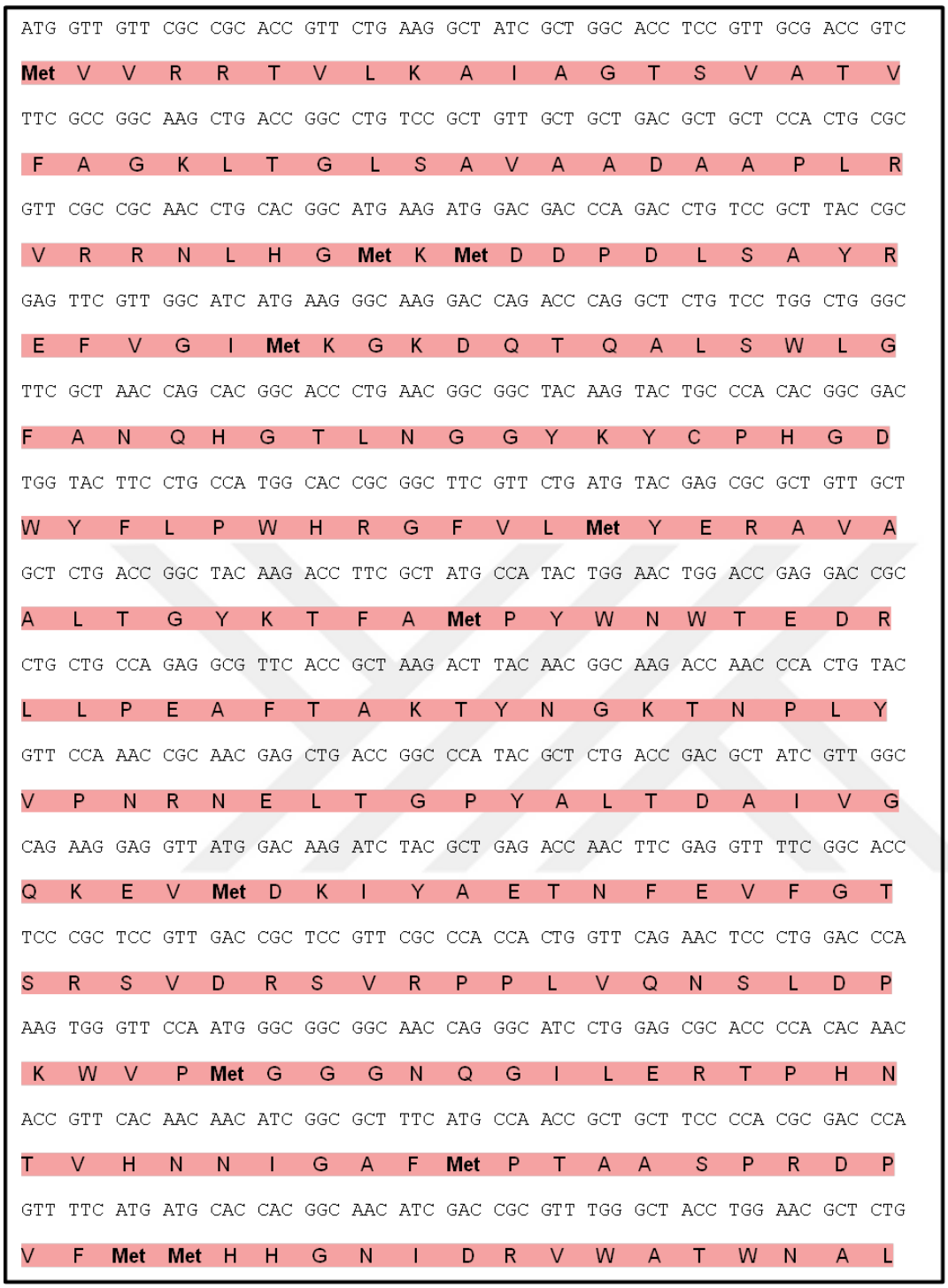

Figure A.3. The second, manually codon optimized gene synthesized by GenScript.

APPENDIX B

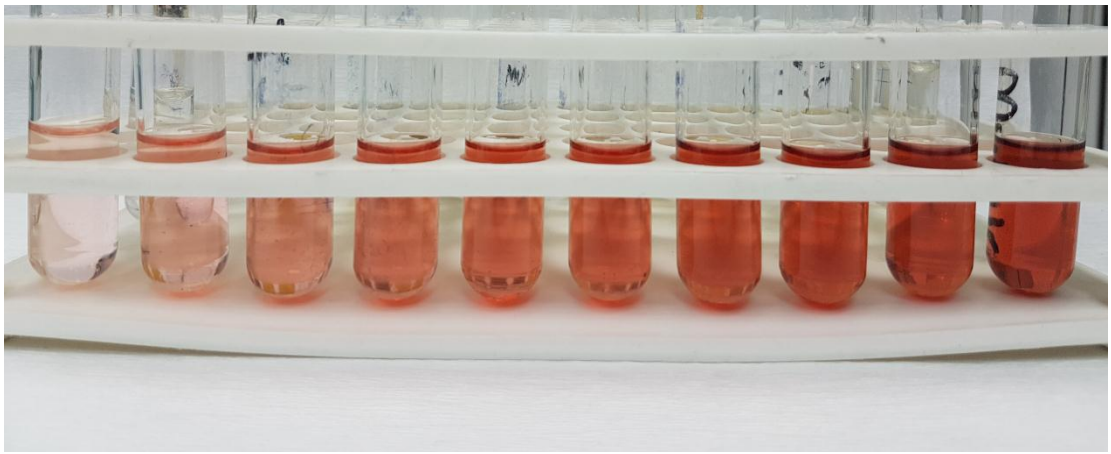

Figure B.1. Samples for standard calibration curve for L-DOPA with Arnow's method.

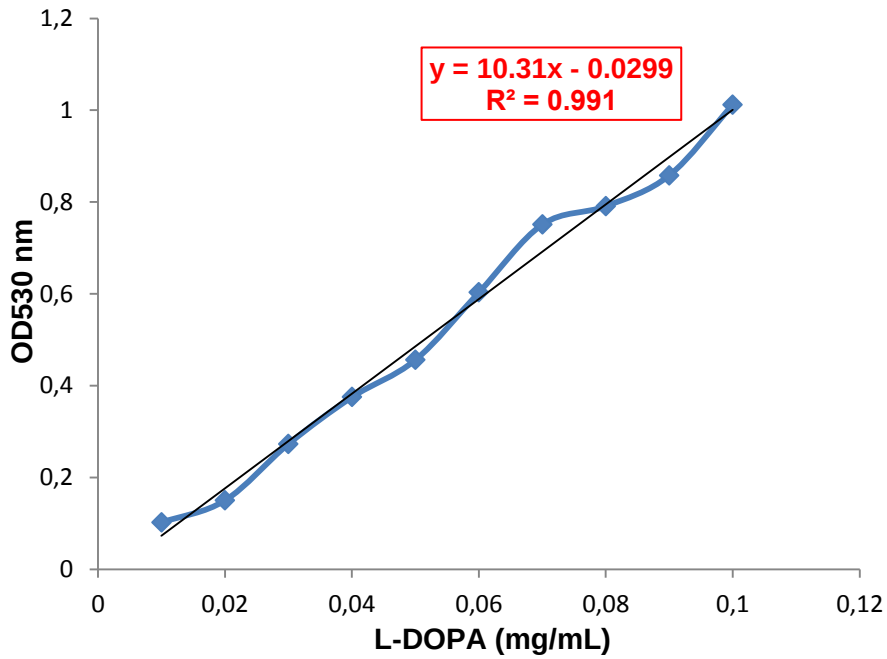

Figure B.2. Standard calibration curve for L-DOPA measument with Arnow's method.

Table B.1. Data for standard calibration curve for L-DOPA with HPLC.

L-DOPA mg/mL	Height	Retention time
0.1	304.62543	2.739
0.2	626.60583	2.798
0.3	854.83215	2.700
0.5	1299.48438	2.679
0.7	1689.69568	2.665
0.85	1909.64087	2.655
0.9	2024.57324	2.815
1	2098.52026	2.647

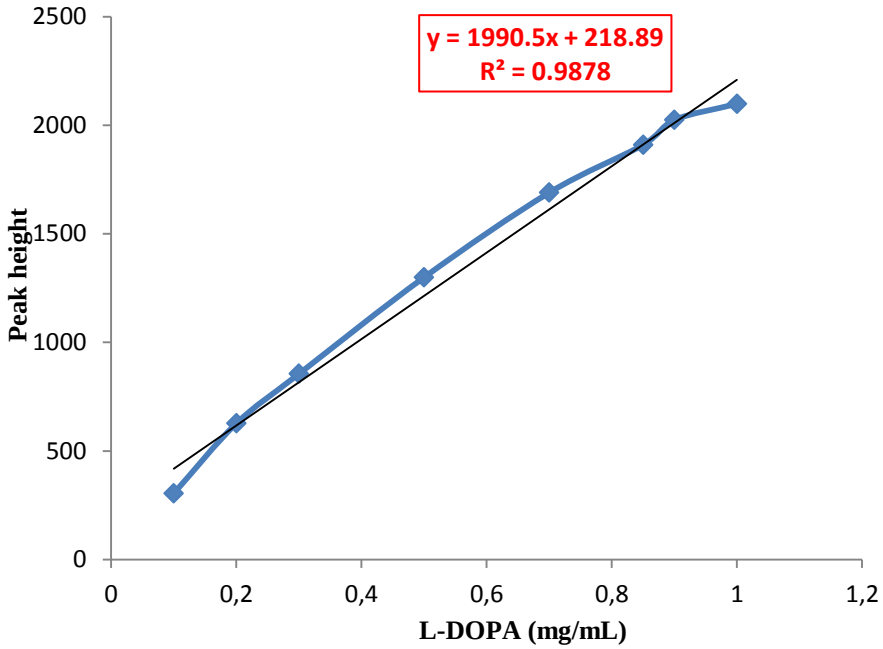

Figure B.3. Standard calibration curve for L-DOPA measument with HPLC.

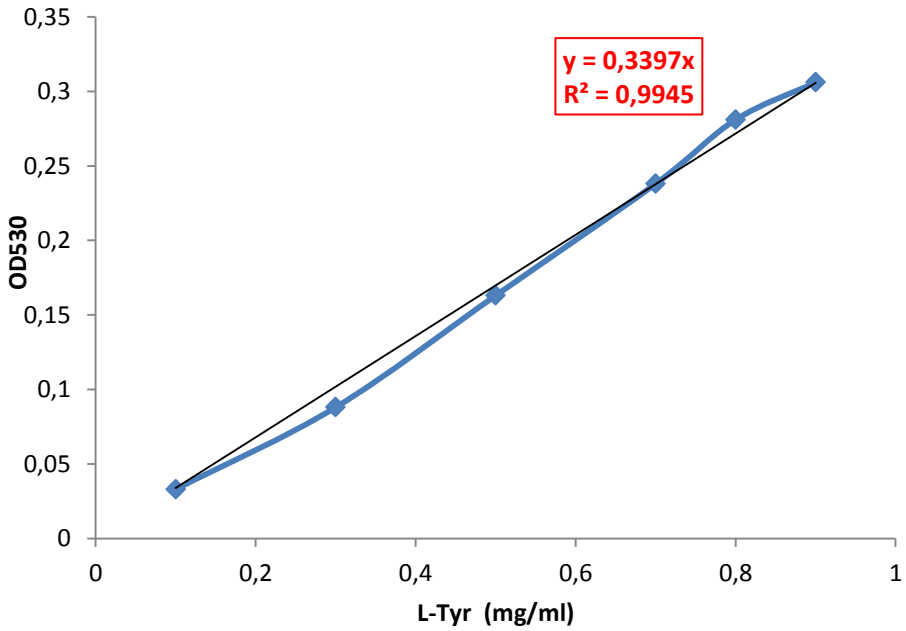

Figure B.4. Standard calibration curve for L-tyrosine measument with Arnow's method.

Table B.3. Data for standard calibration curve for L-tyrosine with HPLC.

L-Tyr mg/mL	Height	Retention time
0.1	131.1944	3.424
0.2	233.3083	3.363
0.3	316.2896	3.334
0.5	484.8277	3.282
0.7	642.0183	3.250
0.85	758.2651	3.228
0.9	800.4035	3.328
1	879.0899	3.218

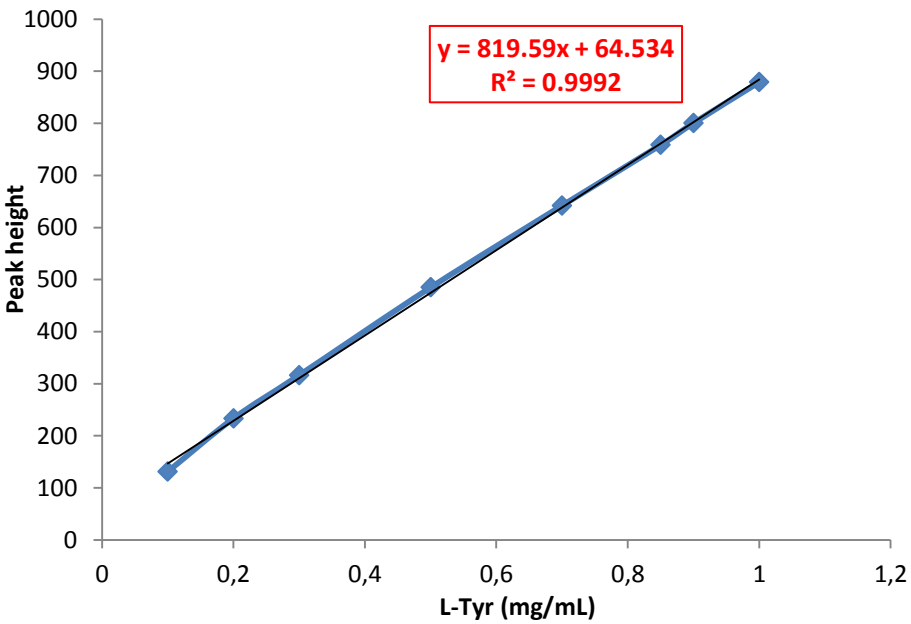

Figure B.5. Standard calibration curve for L-tyrosine measument with HPLC.

APPENDIX C

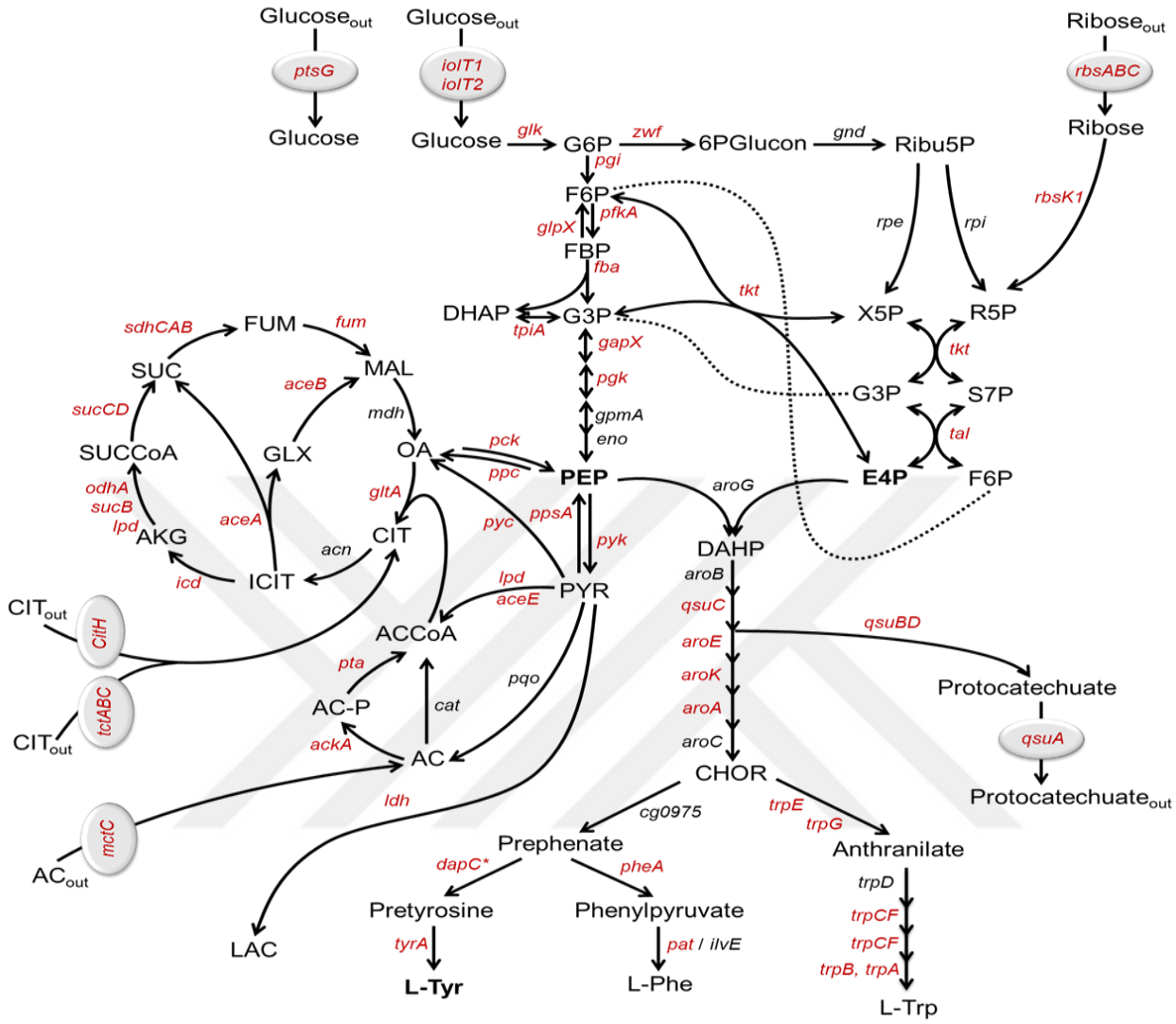

Figure C.1. Pathways critical for carbon flux during L-Tyr overproduction. The genes with mutations causing amino acid replacements have been designated in red. Abbreviations: *ptsG*, glucose-specific enzyme II component of PTS; *iolT1* and *iolT2*, inositol transporters; *glk*, glucokinase; *zwf*, glucose-6- phosphate 1-dehydrogenase; *pgi*, glucose-6-phosphate isomerase; *pfkA*, 6-phosphofructokinase; *glpX*, fructose-1,6-bisphosphatase; *fba*, fructose-bisphosphate aldolase; *gapX*, glyceraldehyde-3-phosphate dehydrogenase; *tpiA*, triosephosphate isomerase; *pgk*, phosphoglycerate kinase; *gpmA*, phosphoglyceromutase; *eno*, enolase; *pck*, PEP carboxykinase; *ppc*, PEP carboxylase; *ppsA*, PEP synthase; *pyk*, pyruvate kinase; *pyc*, pyruvate carboxylase; *lpd*, dihydrolipoyl dehydrogenase; *aceE*, pyruvate dehydrogenase E1 component; *pqo*, pyruvate:quinone oxidoreductase; *cat*, CoA transferase; *ackA*, acetate kinase; *pta* phosphate acetyltransferase; *dapC*, N-succinyldiaminopimelate aminotransferase; *ldh*, lactate dehydrogenase; *mctC*, monocarboxylic acid transporter; *tctABC* and *citH*, citrate uptake proteins; *gnd* , 6-phosphogluconate dehydrogenase;

tkt, transketolase; *tal*, transaldolase; *rpe*, ribulose-phosphate 3-epimerase; *rpi*, ribose 5-phosphate isomerase; *rbsABC*, ribose transport complex; *rbsK1*, ribokinase; *aroG*, 3-deoxy-7-phosphoheptulonate synthase; *aroB*, 3-dehydroquinate synthase; *qsuC*, dehydroquinate dehydratase; *aroE*, shikimate 5-dehydrogenase; *aroK*, shikimate kinase; *aroA*, 3-phosphoshikimate 1-carboxyvinyltransferase; *aroC*, chorismate synthase; *trpE*, anthranilate synthase component 1; *trpG*, anthranilate synthase component 2; *trpD*, anthranilate phosphoribosyltransferase; *trpCF*, indole-3-glycerol-phosphate synthase/phosphoribosylanthranilate isomerase; *trpB*, tryptophan synthase beta chain; *trpA*, tryptophan synthase alpha chain; *cg0975*, chorismate mutase; *pheA*, prephenate dehydratase; *pat*, phenylalanine aminotransferase; *ilvE*, branched-chain amino acid aminotransferase; *tyrA*, prephenate dehydrogenase; *mdh*, malate dehydrogenase; *fum*, fumarate hydratase; *aceB*, malate synthase; *sdhCAB*, succinate dehydrogenases; *sucB*, dihydrolipoamide succinyltransferase; *sucC*, succinate-CoA ligase subunit beta, *sucD*, succinate-CoA ligase subunit alpha; *odhA*, 2-oxoglutarate dehydrogenase; *icd*, isocitrate dehydrogenase; *aceA*, isocitrate lyase; *acn*, aconitate hydratase; *gltA*, citrate synthase; *qsuA*, integral transport membrane protein; *qsuB*, 3-dehydroshikimate dehydratase; *qsuD*, shikimate dehydrogenase. *Predicted function.

Table C1. Mutational changes in enzymes of glycolysis, gluconeogenesis, and feeder pathways for glycolysis.*Silent mutations.

Gene ID	Gene name	Enzyme name	Nucleotide mutations	Nucleotide position	Amino acid replacements
cg2558	***cg2558****	glucose-6-phosphate 1-epimerase	GTT → **A**TT	481–483	V161I
			AAT → **G**AT	456–458	N152D
cg1111	***eno***	enolase	silent mutations only		
cg3068	***fba****	fructose-bisphosphate aldolase, class II	GAA → G**C**A	778–780	E260A
			TCT → **G**CT	1027–1029	S343A
cg1069	***gapX****	glyceraldehyde 3-phosphate dehydrogenase	GA**A** → GA**C**	49-51	E17D
			AGC → **C**GC	295–297	S99R
			GAC → **A**AC	811–813	D271N
cg2399	***glk****	glucokinase	TTT → TT**G**	34–36	F12L
			GGT → G**A**T	187–189	G63D
			GGG → G**A**G	616–618	G206E
cg1157	***glpX (fbp)****	fructose-1,6-bisphosphatase	**G**CA → **T**CA	917-919	A306S
cg0482	***gpmA***	phosphoglyceromutase 1	silent mutations only		
cg1409	***pfkA****	ATP-dependent phosphofructokinase	GGC → G**C**C	136–138	G46A
cg0973	***pgi****	glucose-6-phosphate isomerase	GTT → G**C**T	25–27	V9A
			GAT → **A**AT	1561–1563	D521N
cg1790	***pgk****	phosphoglycerate kinase	GCT → **C**AA	763–765	A255E
			AGC → **C**GC	946–948	S316R
			GAC → G**G**C	1060–1062	D354G
cg2091	***ppgK***	polyphosphate glucokinase	silent mutations only		
cg0644	***ppsA****	phosphoenolpyruvate synthase	GTT → **A**TT	229–231	V77I
			GAC → GA**A**	283–285	D95E
			CTC → **T**TC	769–771	L257P
			ATA → A**CC**	1042–1044	I348T
cg2291	***pyk****	pyruvate kinase	TCT → **G**CT	985–987	S329A
cg1789	***tpiA****	triosephosphate isomerase	CAG → C**C**G	217–219	Q73P

Table C2. Mutational changes in enzymes of pentose phosphate pathway. *Silent mutations.

Gene ID	Gene name	Enzyme name	Nucleotide mutations	Nucleotide position	Amino acid replacements
cg0458	***deoC****	deoxyribose-phosphate aldolase	TCC → **G**CC	16–18	S6A
			ACC → A**G**C	43–45	T15S
			GCA → G**T**A	154–156	A52V
			AAA → AA**C**	574–576	K192N
			GCA → **A**C**G**	595–597	A199T
cg1643	***gnd***	6-phosphogluconate dehydrogenase	no mutation		
cg1780	***pgl***	6-phosphogluconolactonase	ACT → **T**CT	28–30	T10S
cg2800	***pgm***	phosphoglucomutase	silent mutations only		
cg1075	***prsA***	ribose-phosphate pyrophosphokinase	silent mutations only		
cg1546	***rbsK1****	ribokinase	ACA → **G**CA	115–117	T39A
			GGT → G**AC**	280-282	G94D
			GAT → **A**AT	379–381	D127N
			AAA → **C**AA	382–384	K128Q
			AAC → **G**A**T**	403–405	N135D
			GAC → G**C**C	520–522	D174V
			GAC → G**C**C	610–612	D204N
			AGT → G**G**T	619–621	S207G
			ACT → **G**CT	652-654	T218A
			AGG → A**A**G	862–864	R288K
			GAC → GA**A**	901–903	D301E
cg1801	***rpe***	ribulose-phosphate 3-epimerase	silent mutations only		
cg2753	***rph***	ribonuclease PH	silent mutations only		
cg2658	***rpi***	ribose 5-phosphate isomerase	no mutation		
cg1776	***tal****	transaldolase	TTC → T**A**C	532–534	F178Y
cg1774	***tkt****	transketolase	GTT → **A**TT	1666–1668	V556I
cg1778	***zwf****	glucose-6-phosphate 1-dehydrogenase	ACA → **G**CA	448–450	T150A

Table C3. Mutational changes in enzymes of pyruvate dehydrogenase complex, TCA and glyoxylate cycles, and anaplerotic reactions. *Silent mutations.

Gene ID	Gene name	Enzyme name	Nucleotide mutations	Nucleotide position	Amino acid replacements
cg2560	***aceA****	isocitrate lyase	GCA → **T**C**T**	652–654	A218S
			ACC → **GTT**	667–669	T223V
			ACT → **T**C**C**	673–675	T225S
			CTC → **A**TC	799–801	L267I
			CTC → CT**G**	880-882	E294A
			AAG → **C**AG	892–894	K298Q
			GAAGGC–GTTCGCTCT → GA**–**GGC**T**GT**C**C**A**C**GAA**	901–915	301 EGVRS 305 → EAVHE
cg2559	***aceB****	malate synthase	GAG → GA**C**	286–288	E96D
			GAA → GA**C**	571–573	E191D
cg2466	***aceE****	pyruvate dehydrogenase E1 component	AAG → **G**AG	1609-1611	K537E
			GTG → **A**TG	1807–1809	V603M
cg3047	***ackA****	acetate kinase	ATA → **G**TA	145–147	I49V
			GCA → **A**CA	181–183	A61T
cg1737	***acn***	aconitate hydratase	silent mutations only		
cg2840	***actA****	succinyl-CoA:acetate CoA-transferase	GGC → G**A**C	1180–1182	G394D
cg1145	***fum****	fumarate hydratase, class II	GAG → **A**AG	442–444	T148I
			ACC → A**T**C	490–492	E164K
			GAT → **A**AT	1324–1326	D442N
cg0949	***gltA****	citrate synthase	GAC → **A**AC	340–342	D114N
			AGC → A**A**C	865–867	S289N
			GGC → **A**GC	1147–1149	G383S
			GCA → **C**CA	1234–1236	A412P
			AAC → AA**G**	1276–1278	N426K
			TTG → TT**T**	1291–1293	L431F
cg0766	***icd****	isocitrate dehydrogenase	AAC → **G**AC	184–186	N62D
			GAA → GA**C**	319–321	E107D
			ATC → A**C**C	358–360	I120T
			ACA → **G**C**T**	2065–2067	T689A
			ACC → **T**CC	2158–2160	T720S
cg0441	***lpd****	dihydrolipoyl dehydrogenase	AAG → A**G**G	199–201	K67R
			ATC → A**CT**	322–324	I108T

		(E3 component)	CAT → **G**AT	331–333	H111D
			CTT → **T**TT	337-339	L113F
			GAC → GA**A**	376–378	D126E
			GAC → GA**A**	460–462	D154E
			TTT → T**A**T	484–486	F162Y
			TTT → T**C**T	733–735	F245S
			GAG → GA**C**	883–885	E295D
			GAT → **CC**T	913–915	D305P
			ACT → **GCC**	1021–1023	T341A
			TCT → **G**CT	1075–1077	S359A
			GAG → **C**AG	1108–1110	E370Q
			GCA → G**G**A	1240–1242	A414G
cg3335	***malE****	malic enzyme	GCC → **A**C**A**	844–846	A282T
			GAC → **C**AC	850–852	E284Q
cg2613	***mdh***	malate dehydrogenase	silent mutations only		
cg2192	***mqo***	malate dehydrogenase (quinone)	silent mutations only		
cg1280	***odhA****	2-oxoglutarate dehydrogenase E1 component	AAC → A**G**C	40–42	N14S
			AGG → A**A**G	430–432	R144K
			CGC → **A**GC	2788–2790	R930K
			ATC → **G**TC	3007–3009	I1003V
cg3169	***pck* (*pckG*)***	phosphoenolpyruvate carboxykinase (GTP)	CCA → **T**CA	1192–1194	P398S
cg1787	***ppc****	phosphoenolpyruvate carboxylase	GCC → G**T**C	598–600	A200V
			GGT → G**AA**	721–723	G241E
			GAA → **A**AA	2335–2337	E779K
			ACG → A**G**G	2485–2487	T829R
cg0798	***prpC1****	citrate synthase	ACC → **T**CC	196–198	T66S
			GCC → **A**CC	235–237	A79T
			TCC → **C**CC	730–732	P244S
cg3048	***pta****	phosphate acetyltransferase	GTC → **A**TC	229–231	V77I
cg0791	***pyc****	pyruvate carboxylase	CAC → **A**AC	10–12	H4N
			CCA → **T**CA	417–420	P140S
			GA**G** → GA**C**	457–459	E153D
			AGC → A**C**C	1915–1917	S639T
			GTA → G**CC**	2170–2172	V724A
			GAG → G**C**C	2854–2856	E952A
			GCG → G**T**G	2866–2868	A956V

cg0446	***sdhA****	succinate dehydrogenase	ACC → **C**CC	22–24	T8P
			GAACCGAAC → G**TTAA**G**GGG**	982–990	328 EPN 330 → VKG
			AAC → **G**A**T**	994–996	N332D
			– –C–AGGCAG–CGATTG CGCGTGCACAGGCT → **GTC**AGGCA**AT**CGA**AC**GCGC–T–CA–A–GC**A**	1519–1545	507 QAAIARAQA 515 → VQAIERAQA
			GAA → G**GC**	1723–1725	K575A
			CAGCAC → CA**C**C**C**C	1744–1749	S582T,T583P
cg0447	***sdhB****	succinate dehydrogenase	AAG → AA**C**	274–276	K92N
cg0445	***sdhCD***	succinate dehydrogenase	silent mutations only		
cg2421	***sucB* (*aceF*)***	dihydrolipoamide succinyltransferase	GAA → GA**C**	616–618	E206D
			GAAGCA → G**C**A**C**CA	622–627	E208A,A209P
		(2-oxoglutarate dehydrogenase E2 component)	GAA → **A**AA	970–972	E324K
			AAGGAAGAGCC → – & AAGA → –	1018–1028 & 1030–1033	(340 KEEPK 344 → – & K345Q)
			TTC → T**A**C	1555–1557	F519Y
cg2837	***sucC****	succinate--CoA ligase subunit beta	GCG → **A**CG	100–102	A34T
			ACT → **G**CT	462–464	T88A
cg2836	***sucD***	succinyl-CoA synthetase alpha subunit	silent mutations only		

Table C4. Mutational changes in enzymes of pyruvate degradation. *Silent mutations.

Gene ID	Gene name	Enzyme name	Nucleotide mutations	Nucleotide position	Amino acid replacements
cg3107	***adhA****	Zn-dependent alcohol dehydrogenase	GAT → GA**G**	616–618	D206E
			TCA → **C**CA	682–684	S228P
cg0400	***adhC****	alcohol deyhrogenase, class C	GAC → GA**G**	76–78	D26E
			GTC → **A**TC	208–210	V70I
			AAC → **G**AC	358–360	N120D
			AAC → **G**AC	448–450	N150D
			TCT → **G**CT	679–681	S227A
			ACC → A**AA**	697–699	T233K
			AGC → **A**G**A**	769–771	S257G

			CAC → CA**A**	784–786	H262Q
			GTT → G**C**T	1048–1050	V350A
cg0637	***betB****	putative betaine aldehyde dehydrogenase (BADH), oxidoreductase	GAC → **A**AC	172–174	D58N
			GGA → **A**GA	340–342	G114R
			AGC → **G**GC	433–435	S145G
			ACG → **G**CG	844–846	T282A
			AGA → **GC**A	970–972	R324A
			GAA → G**C**A	994–995	E332A
			TCT → **GCC**	1024–1026	S342A
			TCA → **G**CA	1033–1035	S345A
			ACC → A**A**C	1096–1098	T366N
			ATCAGC → A**CCG**GC	1105–1110	I369T,S370G
			GAC → **A**AC	1231–1233	D411N
			AAA → **G**AA	1279–1281	K427E
cg0642	***cg0642****	pyruvate phosphate dikinase	CAA → **G**AA	118–120	Q40E
			ATT → A**CA**	724–726	I242T
			GCT → **A**CT	799–801	A267T
			ATG → **C**TG	1231–1233	M411L
			GCC → **A**CC	1498–1500	A500T
			GAT → **A**AT	1792–1794	D598N
			AAG → A**G**G	1807–1809	K603R
			TCA → **GG**A	1873–1875	S625G
cg1027	***dld***	quinone-dependent D-lactate dehydrogenase	Not found in OP		
cg3219	***ldh****	L-lactate dehydrogenase	TCT → T**T**T	772–774	S258F
cg2891	***pqo***	pyruvate dehydrogenase	silent mutations		

Table C5. Mutational changes in the transporter proteins of selected carbon sources. *Silent mutations.

Gene ID	Gene name	Protein name	Nucleotide mutations	Nucleotide position	Amino acid replacements
cg2120	***ptsF****	fructose-PTS fructose-specific EIIABC component	AAT → A**T**T	13–15	N5I
			AGC → **C**GC	247–249	S83R
			GTT → G**G**T	496–498	V166G
			CAACAA → **GCTGCG**	2044–2049	Q682A,Q683A
			AAC → **GC**C	2059–2061	N687A
cg1537	***ptsG***	PTS system glucose-specific	GGC → G**A**C	565–567	G189D

(*ptsM*)*	EIIBC component		
	GGA → G**CT**	745–747	G249A
	AAC → A**G**C	874–876	N292S
	ATT → **G**T**C**	889–891	I297V
	ATC → **C**T**G**	997-999	I333L
	CTCTCCATT → **A**TC**G**CT**T**T**G**	1084–1092	L362I,S363A,I364L
	CGA → **AAG**	1099–1101	R367K
	AAG → **CGC**	1105–1107	K369R
	GCA → G**TT**	1234–1236	A412V
	ATT → **G**T**C**	1336–1338	I446V
	GTT → G**CA**	1348–1350	V450A
	GTT → **ACC**	1360–1362	V454T
	TTC → **C**TC	1369–1371	F457L
	GCACTG → **TTCT**T**C**	1381–1386	A461F,L462F
	GAA → G**C**A	1402–1404	E468A
	CGT → **AAG**	1420–1422	R474K
	AAGGTT → **CAAA**T**G**	1426–1431	K476Q,V477M
	GCTGAAAAG → G**GA**G**CTG**AG	1435–1443	A479G,D480A,K481E
		1450–1551	484 EEDLKAEANA 493 → N – – – – – – – – – N 499 VAAAGAG 505 → AAPVAPA 509 GAGAAAGAA 517 → AVAGGAAAT
	GCT → **A**C**C**	1564–1566	A522T
	AAG → **CGT**	1573–1575	K525R
	GAA → **C**A**G**	1588–1590	E530Q
	GA**C** → GA**A**	1597–1599	D533E
	GTT → **ACC**	1603–1605	V535T
	AAG → **C**A**C**	1621–1623	K541H
	ATT → **G**TT	1627–1629	I543V
	CAA → **G**AA	1693–1695	Q565E
	GAT → GA**G**	1780–1782	D594E
	GTT → **A**TT	1787–1789	V597I
	GTC → **A**TC	1801–1803	V601I
	GTT → **A**TT	1807–1809	V603I
	ACC → **GA**C	1846–1848	T616D
	AGG → A**A**G	1864–1866	R622K

			GCTGAC → **C**C**A**GA**G**	1906–1911	A636P,D637E
			GAT → **A**A**C**	1927–1929	D643N
			GCG → **AAT**	1966–1968	A656N
			GAA → **C**A**G**	1978–1980	E660Q
			GAA → G**TC**	1984–1986	E662V
			CCT → **GAA**	1993–1995	P665E
			GAT → G**CA**	1999–2001	D667A
			AATTCTTCC → **G**A**CG**C**CA**CC	2008–2016	670 NSS 672 → DAT
			AAGAACGAG → A**CT – – –** GA**A**	2041–2049	681 KNE 683 → T– E
cg2121	***ptsH***	PTS HPr component	Silent mutations		
cg2117	***ptsI****	PTS EI component	**A**GC → **C**GC	1147–1149	S383R
cg2925	***ptsS****	sucrose-PTS sucrose-specific EIIABC component	AGC → A**C**C	598–600	S200T
			GTG → **T**TG	871–873	V291L
			GCA → **A**CA	1066–1068	A356T
			TTC → T**A**C	1201–1203	
			AAT → **G**AT	1252–1254	
			CCG → **T**CG	1768–1770	
cg1411	***rbsA****	ABC-type sugar (aldose) transport system, ATPase component	GAG → G**G**G	1564–1566	E522G
cg1413	***rbsB***	secreted sugar-binding protein	GCG → G**T**G	691–693	A231V
cg1412	***rbsC***	ribose/xylose/arabinose/galactoside ABC-type transport system, permease component	silent Mutations		
cg1414	***rbsD***	uncharacterized component of ribose/xylose transport systems	no mutation		
Acetate transport					
cg0953	***mctC****	Na+/panthothenate symporter or related permease	GAC → **A**AC	146–148	D49N
			GTT → TTA	520–522	V174L
			TGA → T**A**A	691–693	K235T
			GAA → GA**C**	703–705	D231K
			TAA → T**C**A	900–902	K301Q
Citrate transport					
cg0088	***citH***	citrate transporter	GTC → G**C**C	988–990	V330A
cg3125	***tctA***	putative membrane protein	GCG → G**G**G	511–513	A171G
			GCA → **A**CA	691–693	A231T
			GTC → **A**TC	1468–1470	V490I
			ATC → **G**CT	1480–1482	
cg3126	***tctB***	putative membrane protein	TCC → **G**CC	412–414	S138A
cg3127	***tctC***	putative membrane protein	GAT → GA**G**	832–834	D278E
			AAC → A**G**C	919–921	N307S

			TCA → **C**CA	925–927	S309P
Myo-inositol transport					
cg0206	***iolP***	efflux carrier	CTT → **A**TT	484–486	L162I
			AAC → **CAC**	577–579	N193H
			AAT → **G**A**A**	589–591	N197E
			GCG→ G**G**G	643–645	A215G
			TCG → **C**CG	682–684	S228P
			ACT → **GT**T	694–696	T232V
			ATC → **GTT**	697–699	I233V
			GTC → **AT**T	712–714	V238I
			TTA → TT**C**	715–717	L239F
			GTG → **AT**C	727–729	V243I
			ATC→ **G**TC	832–834	I278V
			TTA → TT**T**	910–912	L304F
			ACT → **TCA**	1045–1047	T349S
			GCA → G**T**A	1063–1065	A355V
			GTG → **GC**G	1087–1089	V363A
cg0223	***iolT1****	metabolite Transport Protein	AGA →A**A**A	751–753	R251K
			GTT → **A**TT	766–768	V256I
			GCA →**A**CA	1087–1089	A363T
cg3387	***iolT2****	permease of the major facilitator superfamily	CCT →C**T**T	634–636	L212F

Table C6. Mutational changes in the enzymes of aromatic compounds metabolism and transport. *Silent mutations.

Gene ID	Gene name	Enzyme name	Nucleotide mutations	Nucleotide position	Amino acid replacements
cg0873	***aroA****	3-phosphoshikimate 1-carboxyvinyltransferase	GGT → G**A**T	880–882	G294D
cg1827	***aroB***	3-Dehydroquinate synthase	silent mutations		
cg1829	***aroC***	Chorismate synthase	silent mutations		
cg1835	***aroE****	Shikimate 5-dehydrogenase	GAG → **A**AG	127–129	E43K
			TGC → **C**GC	181–183	C61R
			TGC → **C**GC	253–255	C85R
			CAC → **A**AC	289–291	A97E
			GGC → G**T**C	370–372	A124S
			CAC → CA**T**	613–615	T205I

			CAC → C**G**C	679–681	T227A
cg1129	***aroF****	DAHP synthase	ATC → A**C**C	325–327	I109T
			GAA → G**C**A	790–792	E264A
cg2391	***aroG***	DAHP synthase	silent mutations		
cg1828	***aroK****	Shikimate kinase	CAG → CA**C**	331–333	Q111H
			GCC → **A**CC	415–417	A139T
cg0503	***qsuC*** **(*aroD*)**	dehydroquinate dehydratase	AAA → **C**AA	430–432	K144Q
cg0975	***cg0975***	chorismate mutase	silent mutations		
cg1253	***dapC***	N-succinyldiaminopimelate aminotransferase	TTG → **A**T**G**	412-414	L138M
cg2418	***ilvE***	branched-chain amino acid aminotransferase	silent mutations		
cg0267	***pat**** **(*aroT*)**	phenylalanine aminotransferase	TGG → **CA**G	136–138	W46Q
			GTG → G**C**G	121–123	V41A
			GTT → G**C**T	511–513	V171A
			CAC → **T**AC	598–600	H200Y
cg3207	***pheA****	prephenate dehydratase	ACC → A**T**C	52–54	T18I
			CCC → **T**CC	208–210	P70S
cg3364	***trpA****	tryptophan synthase alpha chain	ATC → **G**TC	109–111	I37V
			CGA → C**C**A	769–771	R257P
cg3363	***trpB****	tryptophan synthase beta chain	ACC → **G**CC	1210–1212	T404A
cg3362	***trpCF****	indole-3-glycerol-phosphate synthase/phosphoribosylanthranilate isomerase	GTC → **A**TC	379–381	V127I
			GCA → **A**CA	637–639	A213T
			TTG → T**C**G	904–906	L302S
cg3361	***trpD***	anthranilate phosphoribosyltransferase	silent mutations		
cg3359	***trpE****	anthranilate synthase component 1	GGC → **TC**C	259–261	G87S
			GCC → **A**CC	553–555	A185T
cg3360	***trpG****	anthranilate synthase component 2	ATG → AT**A**	190–192	M64I
cg0279	***tyrA****	prephenate dehydrogenase	GTC → **A**TC	277–279	V93I
cg2637	***benA****	benzoate 1,2-dioxygenase alpha subunit (aromatic ring hydroxylation dioxygenase A)	GCA → GAA	25–27	A9E
			GAA → GAT	70–72	E24D
			GAA → AAA	1135–1137	E379K
			GGC → GAC	1246–1248	G416D
			GAG → GAC	1336–1338	E446D
cg2638	***benB****	benzoate dioxygenase small subunit	GTC → ATC	214–216	V72I
			AGC → AAC	277–279	S93N
cg2639	***benC****	benzoate dioxygenase reductase	GAG → GGG	1531–1533	E511G
cg2640	***benD****	benzoate diol dioxygenase bend	CAG → CGG	286–288	Q96R

cg2636	***catA****	catechol 1,2-dioxygrnase	TAC → TTC	496–498	Y166F
cg2635	***catB****	chloromuconate cycloisomerase	GCG → ACG	646–648	A216T
cg2634	***catC***	muconolactone isomerase	no mutation		
cg2966	***cg2966****	2-polyprenyl-6-methoxyphenol hydroxylase or related FAD-dependent oxidoreductase	C**G**C → C**A**C	553-555	R185H
			GCA → **T**CA	1543-1545	A515S
			AAC → **C**AC	1561-1563	N521H
			A**C**C → A**T**C	1624-1626	T542I
			GCA → **AAG**	1654-1656	A552K
			ACG → **TCA**	1705-1707	T569S
			CAA → **G**AC	1810-1812	Q604E
			AA**A** → AA**C**	1846-1848	K616N
cg1462	***menF*** **(*entC*)***	isochorismate synthase	GAC → **A**AC	505–507	D169N
			–CCAACAGTT → **T**CC**CC**CA**–**T**C**	739–747	247PTV249 → SPI
			GTA → **AG**A	811–813	Y271D
			ACA → A**A**A	817–819	H273K
cg2629	***pcaB****	3-carboxy-cis,cis-muconate cycloisomerase	G**C**G → G**T**G	580-582	A194V
cg2628	***pcaC****	3-oxoadipate enol-lactone hydrolase/ 4-carboxymuconolactonedecarboxylase	**T**AT → **C**AT	10-12	Y4H
cg2626	***pcaD***	3-oxoadipate enol-lactone hydrolase/ 4-carboxymuconolactonedecarboxylase	silent mutations		
cg2625	***pcaF***	putative acetyl-coa:acetyltransferase	silent mutations		
cg2630	***pcaG****	protocatechuate dioxygenase alpha subunit	**A**TC → **G**TC	52-54	I18V
cg2631	***pcaH***	protocatechuate dioxygenase beta subunit	silent mutations		
cg2623	***pcaI***	probable fesuccinyl-coa:3-ketoacid-coenzyme a transferase subunit	no mutations		
cg2622	***pcaJ***	probable succinyl-coa:3-ketoacid-coenzyme a transferase subunit	silent mutations		
cg1226	***pobA***	4-hydroxybenzoate 3-monooxygenase	**C**TT → **T**TT	361-363	L121F
			CCC → **T**CC	706-708	P236S
			TGC → **C**GC	805-807	C269R
cg0502	***qsuB***	4-hydroxyphenylpyruvate dioxygenase	GCG → GC**A**	811–813	N271D
			GTC → G**C**C	1036–1038	V346A
cg1283	***qsuD*** **(*aroE1*)***	shikimate dehydrogenase	GAA → **A**AA	343–345	E115K
			AAC → **G**AC	358–360	N120D
cg3385	***rhcD2****	catechol 1,2-dioxygenase	AAT → **G**AT	58–60	N20D
			GAT → **AG**A	178–180	D60E
			GCA → **C**CA	412–414	A138P

			AAG → A**G**G	799–801	K267R
cg3386	***rhcM2****	maleylacetate reductase	ATA → A**C**A	298–300	I100T
			GTG → G**C**G	574–576	V192A
			AAC → **G**AC	631–633	N211D
			GCA → **A**CA	847–849	A283T
			TTGTCA → T**CAG**CA	895–900	L299, S300A
			AAA → **C**A**G**	913–915	K305Q
			GTC → **A**TC	967–969	V323I
Aromatic compound transporters					
cg1257	***aroP***	aromatic amino acid transport protein	no mutation		
cg2643	***benE****	benzoate membrane transport protein	ATG → **T**TG	250–252	M84L
			GAC → **A**AC	484–486	D162N
			TTG → **A**T**A**	559–561	L187I
			TCC → **C**CC	637–639	S213P
			CAC → **G**AC	919–921	H307D
			CTC → **T**TC	1192–1194	L398F
cg2642	***benK****	putative benzoate transport protein	GAA → G**C**A	706–708	E236A
			ATG → **C**TG	1024–1026	M342L
			GCA → **A**CA	1243–1245	A415T
cg3353	***genK****	gentisate transport protein	**G**TT → **A**TT	595–597	V199I
			GA**C** → GA**A**	658–660	D220E
			ACC → **G**CC	1210–1212	T404A
cg1225	***pcaK****	4-hydroxybenzoate and protocatechuate transport protein	ATC → **C**TC	547–549	I183L
			TCC → **A**CC	604–606	S202T
			GAT → **A**AT	616–618	D206N
			TAT → T**T**T	898–900	Y300F
			insertion with stop codon	953–972	318 → 323
Cg1305	***pheP****	L-Phe uptake	A**A**A → A**G**A	34–36	K12R
			G**T**C → G**C**C	1318–1320	V440A
cg0501	***qsuA***	integral transport membrane protein	TCA → **A**CA	37–39	S13T
			GCT → C**AC**	676–678	R226H
			GGT → **C**GT	1339–1341	G447R
			AGC → **G**GC	1369–1371	S457G
			GCCTCC → **T**CC**G**C**A**	1375–1380	A459S,S460A
			GAGGCCCAAC → G**GCAAAACCA**	1381–1390	461 GKTTGKAS
			– → CAGGCAAAGCCTCCGAGGCCCAAC	1391	
cg2618	**vanK***	vanillate transporter VANK	**GC**C → **A**C**T**	529-531	A177T

GGC → **A**GC		1198-1200	G400S

APPENDIX D

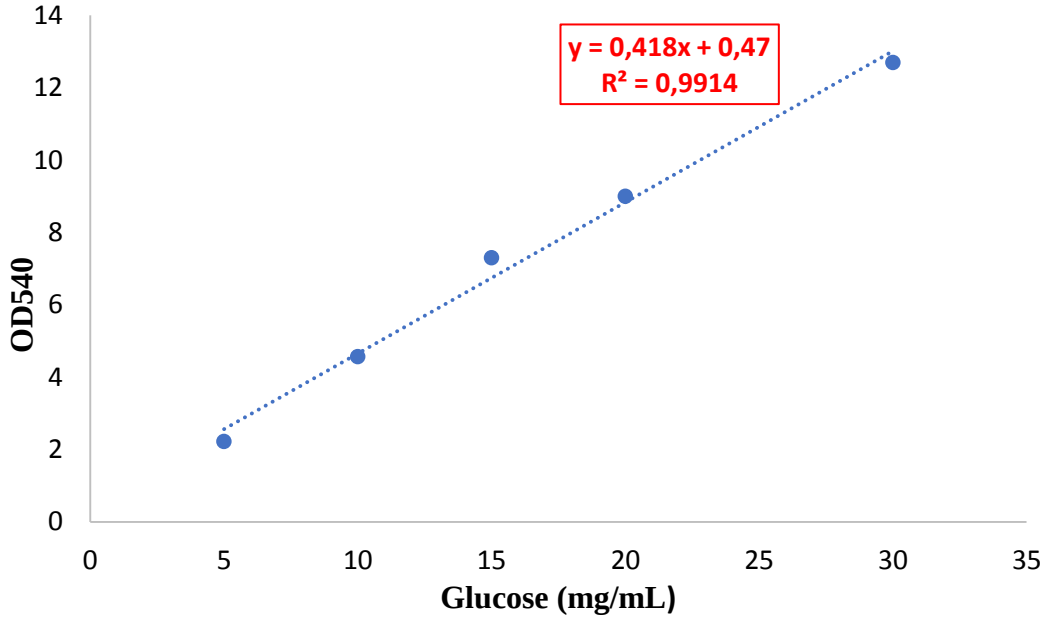

Figure D.1: Standard curve for DNS method.

APPENDIX E

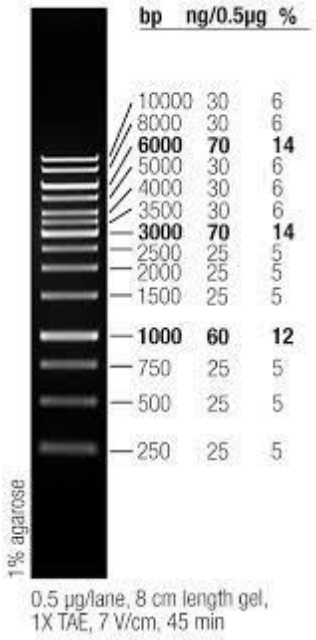

Figure E.1: 1 Kb gene ladder (Thermo Fisher, SM0313).

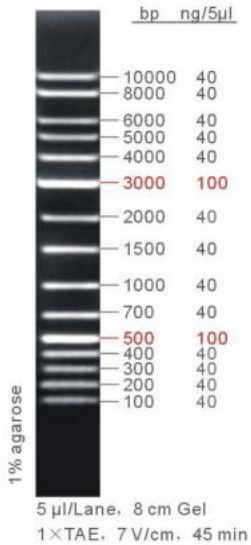

Figure E.2: 1 Kb gene ladder (Biomatik, M7113).

CURRICULUM VITAE /ÖZGEÇMİŞ

Eldin Kurpejović

Professional summary & Skills

Driven to learn quickly, advanced molecular cloning proficiency and training in biochemical engineering. Advanced background in strain development via metabolic engineering, bioprocess engineering, microbial genetics, enzyme kinetics, anti-microbial research, and synthetic biology supporting team needs. Flexible and hardworking team player focused on boosting efficiency and performance with conscientious and detail-oriented approaches.

Laboratory skills proficiency: Bioreactors, Fermentation, HPLC-GC, and Affinity Chormatography, Molecular cloning, Agarose electrophoresis, SDS-PAGE, ELISA, Bacterial transformation and conjugation, Bacterial genome-wide comparison and analysis. Solid knowledge of MS Word/Excel and Mauve.

Education

Integrated Masters with PhD — 2016-present
Department of Bioengineering, Institute of Pure and Applied Sciences, Marmara University, Istanbul/Turkey

Undergraduate studies — 2012-2016
Department of Bioengineering, Faculty of Engineering, Marmara University, Istanbul/Turkey

Experience

Visiting Researcher FEMS awardee (Grant number: FEMS-GO-2019-509) | Department of Genetics of Prokaryotes, at Prof. V.F. Wendisch's laboratory, Bielefeld University, Germany — Jan-April 2021

Mentorship of undergraduate and graduate students|2017-present

Intern | Biochemical hematology laboratory, General Hospital Rozaje, Montenegro — Jun-Sep 2013-14-15

Publications

Kurpejović, E., Wendisch, V. F., & Sariyar Akbulut, B. (2021). Tyrosinase-based production of L-DOPA by *Corynebacterium glutamicum*. Applied microbiology and biotechnology, 10.1007/s00253-021-11681-5. https://doi.org/10.1007/s00253-021-11681-5.

Avci, F. G., Atas, B., Aksoy, C. S., **Kurpejović, E.**, Gulsoy Toplan, G., Gurer, C., Guillerminet, M., Orelle, C., Jault, J. M., & Sariyar Akbulut, B. (2019). Repurposing bioactive aporphine alkaloids as efflux pump inhibitors. Fitoterapia, 139(October), 104371. https://doi.org/10.1016/j.fitote.2019.104371.

Conference Presentations

Kurpejovic, E., Wibberg, D., Burgardt, A., Bastem, G.M., Busche, T., Wendisch, V.F., Akbulut, B.S. (2022). "Genome-wide mutational analysis of the L-tyrosine overproducer *Corynebacterium glutamicum* ATCC 21573" FEMS conference on Microbiology, 30.6-2.7.2022, Serbia.

Kurpejovic, E., Bastem, G.M., Wibberg, D., Burgardt, A., Busche, T., Wendisch, V.F., Akbulut, B.S. (2021). "Comparative growth of *Corynebacterium glutamicum* ATCC 21573 and ATCC 13032 in different carbon sources and evaluation of L-tyrosine synthesis" 4th International EURASIAN conference on biological and chemical sciences, EURASIANBIOCHEM 24-26 November 2021.

Kurpejović, E., Pakalin, B., Sayar, A.N., Sariyar Akbulut B.(2019). "Optimization of pretreatment conditions for the saccharification of hazelnut husk towards its utilization for microbial growth" 9th Internatinal CeBiTec Research Conference, September 2019, Bielefeld.

Akbulut, B.S., Atas, B., Aksoy, C.S., **Kurpejovic, E.**, Avci, F.G., Sayar, A.A., (2017). "Evaluation of Active Natural Products as Bacterial Efflux Pump Inhibitors", EpiChemBio and MuTaLig COST joint meeting (CM1406-CA15135), University of Porto, 22-24th September 2017, Portugal.

Languages

Native in Montenegrin/Serbian

Fluent in English and Turkish

Familiar with German and Spanish